Signals Controlling Peripheral B Cell Development, Selection, and Activation

Marc Andre Schwartz

A dissertation

submitted in partial fulfillment of the

requirements for the degree of

Doctor of Philosophy

University of Washington

2013

Reading Committee:

David J Rawlings, Chair

Daniel Campbell

Michael J Bevan

Program Authorized to Offer Degree:

Department of Immunology

University of Washington

Abstract

Signals Controlling Peripheral B Cell Development, Selection, and Activation

Marc Andre Schwartz

Chair of the Supervisory Committee:

Professor David J Rawlings

Department of Immunology

Control of B cell development through transitional stages in the periphery is critical for the proper maintenance and selection of mature, functional B cell subsets capable of mediating humoral immunity. We have established an important role for T cells and CD40 in supporting development and selection of transitional B cells. T cells and CD40 are required for optimal B cell homeostatic proliferation in response to lymphopenia, and expression of CD40 provides a competitive advantage to B cells developing in a mixed BM chimera environment. Further, transgenic BCR models demonstrate altered BCR-specificity based selection in the absence of CD40. The combination of single-cell BCR cloning and high throughput BCR sequencing was used to determine the role of CD40 on B cell selection in a non-transgenic setting with

unrestricted clonal diversity. We found altered specificity profiles of cloned BCRs and reduced BCR diversity in high throughput sequence data sets from CD40-deficient mice. In addition, a critical, B cell-intrinsic role was demonstrated for Wiskott-Aldrich syndrome protein (WASp). In the setting of B cell-specific deficiency of WASp, mice develop spontaneous autoimmune disease dependent on B cell expression of the Toll-like receptor signaling adapter MyD88. Collectively, the data presented here expand our understanding of the control of B cell development, selection, and activation in peripheral lymphoid compartments, and suggest novel methods for modulating B cell subsets in the settings of immunodeficiency and autoimmunity.

Table of Contents

Chapter I: Introduction

1.1 **Adaptive Immunity**

Defense against infection depends critically on the recognition and response to an ever-changing spectrum of pathogens. Molecular evolution of the vast majority of infectious organisms occurs frequently within the human lifespan, precluding the ability to rely solely on static recognition elements[1]. To overcome this challenge, the vertebrate immune system employs a set of germline-encoded receptors intended to recognize conserved pathogen-associated molecular patterns (PAMPs) and a separate set of receptors capable of adapting to any current infectious agent; the cells expressing these two groups of surface molecules are grouped into innate and adaptive components of the immune system, respectively. T and B lymphocytes comprise the adaptive arm of the immune system, and their respective antigen receptors represent the elegant means by which adaptation to infection is acquired. Instead of a multitude of receptors recognizing various molecular patterns, each lymphocyte expresses a single specificity antigen receptor. The presence of billions of lymphocytes, each with a unique specificity, permits an enormous potential to recognize foreign material. As first proposed by Macfarlane Burnet over 50 years ago, only lymphocytes that manage to bind antigenic material during an immune response are activated, allowing their clonal selection and expansion[2]. Consequentially, the total available antigen receptor repertoire is a key determinant of the ability to mount effective adaptive immune responses.

A major obstacle to establishing this specificity repertoire is the possibility of self-recognition leading to autoimmune responses. Tolerance refers to conditioning of the adaptive

immune system to avoid autoimmunity, and its mechanisms, while not completely understood, include the removal and suppression of lymphocytes possessing autoreactive antigen receptors. Proper functioning of the immune system relies on striking a balance between expanding the diversity of antigen receptors (which improves the ability to respond to a wide range of pathogens) and prevention of autoreactive immune responses.

1.2 **B Cell Development**

Formation of a functional, diverse antigen receptor repertoire is the primary goal of lymphocyte development, which occurs in the thymus for T cells and generally the bone marrow for B cells. After differentiation from hematopoietic stem cells into B-lineage committed precursors, developing B cells begin to sequentially rearrange B cell receptor (BCR) gene segments[1]. Immediately following successful surface expression of a BCR, B cells are unable to participate in immune responses and are thus designated as immature. Censoring of autoreactive BCRs begins at this stage, and operates primarily by inducing either receptor editing or clonal deletion of B cells with sufficient affinity for ubiquitous self-antigen. A formative demonstration of this process was accomplished by cloning expressed BCR transcripts from BM B cell precursors just prior to their expression on the B cell surface[3]. The majority of recombinant antibodies made from these cloned BCRs possessed self-specificity (75%), whereas antibodies made from immature B cells post surface-BCR expression displayed far less autoreactivity (43%). Cells that pass this first tolerance checkpoint eventually leave the BM and enter the periphery.

To enter a mature, functional compartment, B cells must further progress through multiple transitional stages of development in the periphery; a process thought to occur primarily in the spleen[4]. There are three major mature B cell subsets: B1 B cells found in the peritoneal and pleural spaces, marginal zone (MZ) B cells found in the splenic marginal sinus, and follicular mature (FM) B cells which recirculate through B cell follicles in most secondary lymphoid tissues[5]. The majority of B cells entering all of these mature compartments have progressed through transitional stages in the spleen[4], although there is some evidence of concomitant transitional cell development in the BM[6]. The hallmark functional characteristic of immature, transitional B cells is the induction of apoptosis in response to BCR cross-linking[7]. This is in stark contrast to the proliferation and upregulation of activation markers seen in mature B cells following BCR cross-linking, and appears to be due in part to a BCR-specific nuclear defect in transcription of key NF-kappaB target genes[8]. In addition, calculation of turnover rates by continuous BrdU labeling revealed that transitional B cells are characterized by significantly shorter half-lives as compared to mature B cells[9]. Transitional subsets can also be identified by their predominance during early B cell reconstitution. Functional assays that distinguish the immature B cell state have led to precise definitions of surface phenotypes for transitional B cell subsets. The earliest transitional stage is termed T1 and defined by the surface phenotype AA4hi, CD21low, CD24hi, CD23low, IgMhi, and IgDlow[9]. T2 cells have been defined by various groups with slight variations in surface phenotype, but have been generally distinguished from T1 cells by increased expression of CD23, CD21, and IgD while maintaining AA4 expression[5,10]. Finally, some groups define a third transitional population with reduced surface IgM expression, which may contain anergic B cells[9].

In addition to the BCR, developing peripheral B cells also depend critically on the cytokine B cell activation factor of the TNF family (BAFF). BAFF is produced predominantly by neutrophils, monocytes, and macrophages, and is initially membrane-bound until released by protease cleavage as a soluble trimer[11]. When BAFF is absent in mice, B cell development arrests at the early transitional stage and almost no mature FM or MZ cells are produced, although B1 cells appear to develop normally[12]. Alternatively, when BAFF is overexpressed the peripheral B cell compartment is expanded, eventually leading to severe autoimmune disease[13]. BAFF can bind to three TNF family receptors: B cell maturation antigen (BCMA), transmembrane activator and calcium modulator and cyclophilin ligand interactor (TACI), and BAFF receptor (BAFFR)[11]. During peripheral B cell development, BAFFR appears to be the primary receptor responsible for mediating the effects of BAFF as deficiency of BAFFR results in a phenotype virtually identical to that found in BAFF-deficient mice[14]. Engagement of BAFFR by BAFF results in activation of the alternative NF-kappaB pathway, which in turn upregulates pro-survival genes including MCL1, Bcl-XL and A1[11,15]. BCR signals are thought to act in concert with BAFFR stimulation to promote peripheral B cell survival. This cooperation may simply be an additive effect of BCR-generated classical NF-kappaB activation, as both classical and alternative NF-kappaB components are required for normal development and maintenance of peripheral B cells[15]. Alternatively, one study proposed that BCR signals are critical to maintain adequate quantities of p100, a substrate required for alternative NF-kappaB activation[16]. In addition, BCR signals have been shown to increase surface expression of BAFFR, which occurs in concert with developmental progression of transitional cells[17].

Under normal physiologic conditions, the rate of B cell production far exceeds the rate of removal from the peripheral B cell population, and as a result most transitional B cells do not

survive the competition for entry into mature subsets[18,19]. Those B cells that do survive appear to be selected in part based on the specificity of their antigen receptor. Negative selection by clonal deletion, which begins in the bone marrow immediately following BCR expression, continues in the periphery as transitional cells that receive a BCR stimulus of sufficient strength undergo apoptosis[20,21]. In addition, although still somewhat controversial, multiple lines of evidence indicate positive selection by clonal expansion of transitional B cells occurs via BCR engagement of self-ligand[22]. First, conditional BCR ablation results in the rapid loss of mature B cells implying that BCR signaling is required for survival of B cells in the periphery[23]. This finding may be explained by the need for a tonic, or antigen-independent, BCR signal, but comparisons of V_H and V_L chain variable segment usage between transitional and mature compartments indicate that a minority of available heavy/light chain pairs are enhanced in the mature population, implicating ligand-mediated positive selection[24]. In addition, transgenic models have suggested that self-reactive B cells with low BCR density are positively selected[25], and at least two models show enrichment of transgenic B cells specific for an endogenous epitope: anti-Thy-1 B cells appear to be selected into the B1 compartment[26], and mice carrying only the heavy chain M167 transgene show expansion of phosphorylcholine (PC)-reactive M167-idiotype$^+$ cells in the MZ compartment[10,27]. However, in an unmanipulated, endogenous B cell repertoire, the importance of ligand-mediated positive selection and the antigens responsible remain unclear.

Identification of positively selected transitional B cells is complicated by the low steady-state proportion of cycling peripheral B cells. However, recent work in our laboratory has identified a late transitional B cell subset (termed CD21-intermediate transitional 2 or CD21intT2 cells) enriched for cycling cells[10]. These cells can serve as direct precursors to both

FM and MZ B cell subsets and, in the M167-heavy chain transgenic model, expansion of PC-specific B cells occurs first in the T2 population followed by further expansion in the MZ subset. In addition, an assay was developed recently that measures the proliferation history of a population of B cells (the KREC assay)[28]. Use of KREC analysis in both mice and humans has demonstrated that mature B cells have proliferated several times since light chain rearrangement, more so in MZ cells than in the FM subset. Together, these results suggest that induction of proliferation in transitional B cells, whether induced by BCR engagement or other signals, may affect both naïve B cell numbers and the mature B cell repertoire. It is therefore imperative to identify the molecular signals involved in transitional B cell proliferation, as any perturbation of these signaling pathways may disrupt selection of the BCR repertoire.

Initial efforts in our lab to determine the signals controlling proliferation of T2 cells implicated T cell help through CD40. As a result, a thorough analysis of the contribution of T cells and CD40 to transitional cell cycling and selection into mature compartments was conducted. Additionally, the effect of CD40 on the mature BCR repertoire was analyzed using a combination of transgenic BCR models, single-cell cloning, and high-throughput sequencing. These studies are described in detail in Chapter 2.

1.3 **Mature B Cell Functions**

After entering a mature subset, B cells are able to participate in immune responses. Most mature peripheral B cells are part of the recirculating FM population, and are predominantly thought to participate in T-dependent (TD) immune responses. The classic TD response involves initial acquisition of pathogen material by innate immune cells, such as dendritic cells and

macrophages, which present processed peptide in MHC complexes to naïve T cells. B cells with specificity for native pathogen material can also acquire and internalize antigen via BCR engagement. B cells can acquire antigen in multiple forms, including opsonized particulate antigen on the surface of subcapsular sinus macrophages, small soluble antigens transported through conduits into follicles, and larger antigens recycled to the surface of DCs[29]. Processed peptides can then be presented along with MHCII on the surface of B cells, and if a cognate CD4+ T cell is encountered, activating signals from the T cell can drive B cell activation resulting in proliferation, germinal center formation, and eventual differentiation into memory or antibody-secreting plasma cells. In addition, there is mounting evidence that B cells can modulate TD immune responses via cytokine production during interaction with T cells[30]. Production of IFN-gamma and IL-12 can follow B cell priming by Th1 cells, whereas IL-2, IL-13, and IL-4 can be produced following Th2 cell priming[31]. B cells have also been described to secrete IL-10 and thereby mediate regulatory properties; the identification of specific contexts and B cell subsets responsible for IL-10 production is currently an active area of research[32].

The specialized MZ and B1 B cell subsets mediate a distinct set of functions. Both of these subsets are more rapidly activated and thought to mediate predominantly T-independent (TI) immune responses, although more recently MZ cells have demonstrated the ability to participate in TD responses as well[33,34]. Rapid responses by MZ B cells result from a combination of robust antigen-presenting ability as well as the expression of germline-encoded pathogen recognition receptors, most notably Toll-like receptors (TLRs)[34]. As a result MZ B cells with BCR specificity for nucleic acids, or complexes containing nucleic acids, are particularly adept at responding to nucleic acid-containing antigen via BCR/TLR co-engagement. In addition, these innate-like subsets are responsible for basal IgM production, or

natural IgM. This secreted IgM antibody contains conserved specificities, including phosphorylcholine (PC) and malondialehyde (MDA) among others[35]. Natural IgM provides rapid protection of blood-borne infections, particularly of polysaccharide capsule-containing microbes such as *S. pneumoniae*. In addition, these antibodies are thought to mediate homeostatic functions including the non-inflammatory clearance of apoptotic cell debris[36]. Apoptotic debris has been postulated, by our group and others, to serve as positively selecting antigen for developing B cells, but this has not been definitively demonstrated experimentally.

Although MZ B cells exhibit stronger responses to TLR ligands in vitro[37], FM B cells also express TLRs, and TLR engagement appears to regulate a wide range of B cell functions[38]. TLRs are involved in localization as well as modulation of antibody production during TI immune responses. In addition, TLR engagement during TD responses has been shown to drive class switching to IgG2a/c, differentiation to antibody-secreting plasma cells, and B cell cytokine production. In the context of TD responses, B cell TLRs appear to be particularly important for anti-viral immunity[39]. Because they can receive PAMP signals through TLRs, B cells are uniquely capable of modulating immune responses without instruction from activated innate immune cells. As such, B cells have been increasingly appreciated as capable of initiating naïve T cell activation and driving TD responses without necessarily needing prior T cell activation[40]. While this may promote robust responses to certain pathogens, when not properly regulated this property can also promote the production of pathogenic autoantibodies that result in host damage[41]. For example, AM14-transgenic B cells require TLRs but not T cells to produce rheumatoid factor autoantibodies on a lupus-prone background[42]. These data highlight a potential dominant role for B cells in driving autoantibody production and resulting autoimmune disease, particularly when autoantigens capable of stimulating TLRs are involved.

A driving role for B cells in autoimmunity is further supported by recent studies on autoimmune risk variants. Genome-wide association studies (GWAS) have identified many genetic variants associated with a variety of autoimmune diseases in humans[43]. The molecules affected by these variants are therefore of great interest to understanding the etiology of autoimmunity. Allelic variants affecting protein tyrosine phosphatase nonreceptor 22 (PTPN22), for example, are strongly associated with type 1 diabetes, lupus, rheumatoid arthritis, and Graves disease, among others[44,45]. Functional studies with cell lines and murine models demonstrate an effect of this variant on antigen receptor signaling in both T and B cells. In addition to PTPN22, several other molecules involved in antigen receptor signaling have been associated with autoimmune risk, including CSK, Lyn, FCgammaRIIB, BLK, BANK1, and Wiskott-Aldirch syndrome protein (WASp)[46,47]. A more complete understanding of how modulation of these signaling pathways induces autoimmunity requires determination of the cell subset(s) responsible and more precise characterization of the functional effects on antigen receptors as well as other immune receptors, such as TLRs, that could contribute to autoimmune disease.

Mutations in the gene encoding WASp result in a primary immunodeficiency with associated autoimmunity[48]. Data from our lab and others indicates a competitive advantage for the expression of WASp in peripheral B cells, especially MZ cells[49]. The effect of WASp-deficiency on B cell functional responses, however, remains undefined. Further, the B-cell specific contribution to autoimmunity in the setting of WASp-deficiency is unknown. Investigation of these unanswered questions is detailed in Chapter III.

Chapter II: The Role of T Cells and CD40 in Peripheral B Cell Development

2.1 Introduction

The notion of T cell involvement in B cell development is supported by a variety of studies from other labs. First, an analysis of B cell V_H family genes demonstrated reduced usage of the V_HJ558 family in spleen and lymph node B cells of athymic nude mice[50]. Reconstitution of athymic mice with CD4+ T cells enhanced V_HJ558 usage beginning 5 days and lasting up to one year after T cell transfer, suggesting that T cells can modulate the BCR repertoire. Analysis of the BCR repertoire in B cells taken from hyper-IgM patients with CD40L mutations revealed increased levels of autoreactive BCRs in mature B cells compared to normal controls, supporting the idea that the effect of T cells on B cell repertoire is mediated through CD40 signaling[51]. Modulation of BCR repertoire may result from the ability of CD40 engagement to promote survival of transitional B cells and their subsequent selection into mature subsets. This idea is supported by *in vitro* data demonstrating that early transitional B cells survive and proliferate following BCR and CD40 stimulation, whereas they undergo apoptosis if the BCR alone is engaged[20]. An effect of CD40 on B cell survival is contradicted by the presence of normal numbers of mature B cells in both T cell- and CD40-deficient mice. However, other signals may compensate for the lack of CD40 from T cells; for example, patients with CD40L mutations have increased levels of the survival factor BAFF[51]. Also, mice with defects in both Bruton's tyrosine kinase (Btk, a signaling protein important downstream of the BCR) and CD40 have a more severe reduction in peripheral B cell numbers than mice with Btk mutations alone[52,53]. These data indicate that the pro-survival role of CD40 is unmasked by a deficiency in BCR signaling. Consistent with the possible role of CD40 engagement during B cell development, CD40L was shown to be expressed on naïve CD4 T cells at low levels[54]. CD40L is traditionally thought to be

expressed only on activated T cells, but its availability on naïve CD4 T cells would provide an accessible source of CD40L to transitional B cells in the spleen.

Interestingly, recent data related to a model of chronic graft versus host (cGVH) disease have also implicated a role for CD4 T cells in B cell development[55]. In this model, CD4 T cells are isolated from mice with a mutant form of the MHC class II molecule I-A and injected into recipients with WT I-A. Donor CD4 T cells are reactive to unmutated I-A in recipients, causing their activation and subsequent interaction with host B cells, eventually leading to autoantibody production and a lupus-like disease. However, if the host B cells developed in the absence of host CD4 T cells, despite normal numbers of B cells present there is no autoantibody production or lupus-like disease following transfer of mutant I-A CD4 T cells. Additional studies have implicated IL4 and CD40 signals as possible mediators of this effect, which has been referred to as B cell nurturing. In short, these experiments demonstrate that when B cells develop without CD4 T cells present, they are functionally defective in their ability to mediate cGVH disease.

Another study provided evidence of a role for T cells during peripheral B cell maturation in the context of athymic rats[56]. These T cell deficient animals exhibited an increased ratio of transitional:mature B cells, indicating an impairment in B cell maturation in the absence of T cells. Further, mature B cells had decreased MHCII, ICAM-1, CD44, and L-selectin in the absence of T cells. Implantation of thymic tissue or adoptive transfer of T cells was sufficient to reverse these effects and restore normal B cell maturation. Similar results were described recently in a humanized mouse model[57]. Poor maturation of B cells beyond transitional stages was attributed to an initial lack of T cells, whereas B cell maturation was accelerated in older mice that possessed greater T cell frequencies. An autologous T cell transplant was capable of

increasing B cell maturation, while depletion of T cells reduced B cell maturation, indicating an important role for T cells in B cell development and in particular reconstitution following BM transplant. This finding was suggested to also play a role in the delayed B cell maturation observed in humans following cord blood transplants.

In summary, there is a developing body of literature indicating an important role for CD4 T cells and CD40 during the development of a functional B cell population. Here, we explore in detail how CD4 T cells, through CD40 signaling, contribute to B cell development and function both in a normal physiologic setting and in the context of reconstitution in a lymphopenic environment. T cells and CD40 are shown to drive proliferation of B cells in response to lymphopenia, and expression of CD40 provides a selective advantage during transitional cell development and, most notably, in MZ B cells. In addition, the effect of CD40 signals on the mature B cell repertoire were explored using transgenic BCR models, single-cell BCR cloning, and high throughput BCR sequencing. Regulation of B cell selection is critical to maintain a pool of lymphocytes sufficiently diverse to recognize foreign infectious material without allowing production of pathogenic autoreactive antibodies. We show a perturbation of normal BCR-specificity based selection in the absence of CD40. Collectively, our data provide further evidence of an important role for T cells and CD40 during peripheral B cell development and selection into mature compartments.

2.2 Results

CD4+ T Cells Contribute to B Cell Homeostatic Proliferation through CD40

To evaluate whether CD4+ T cells and CD40 play a role in peripheral B cell development we first assessed their effect on lymphopenia-induced homeostatic proliferation (Figure 1A) as we have shown previously that transitional cells are most sensitive to the signals driving this process[10]. Compared to B cells transferred alone, B cells transferred into RAG KO mice along with an equal number of CD4+ T cells, but not CD40L KO T cells, exhibited increased proliferation (Figure 2A). As T cells also undergo homeostatic proliferation when transferred to RAG KO mice, we further evaluated B cell HP using μMT recipient mice which have relatively normal splenic T cell subsets. In this system, depletion of CD4+ T cells, transfer of CD40-deficient B cells, and transfer of WT B cells into a CD40L-deficient μMT recipient resulted in a 50% reduction in proliferation one week-post transfer relative to WT B cells transferred into μMT recipients. (Figure 1B,D). In contrast, depletion of CD8+ T cells, inhibition of IL4, and deficiency of MyD88 or TRIF had no observed effect on B cell HP (Figure 1D and Figure 2B). Following transfer to lymphopenic recipients, recovered B cells consistently have a CD21hiCD24hi phenotype, similar to MZ cells in an unmanipulated WT spleen. Whenever CD4+ T cells or the CD40 pathway was inhibited during a HP experiment, a subset of recovered cells displayed lower CD21 and CD24 levels, and these cells had not proliferated (Figure 1C). These data suggest a major role for CD4+ T cells, through CD40 signaling, in replenishing B cell numbers during lymphopenia.

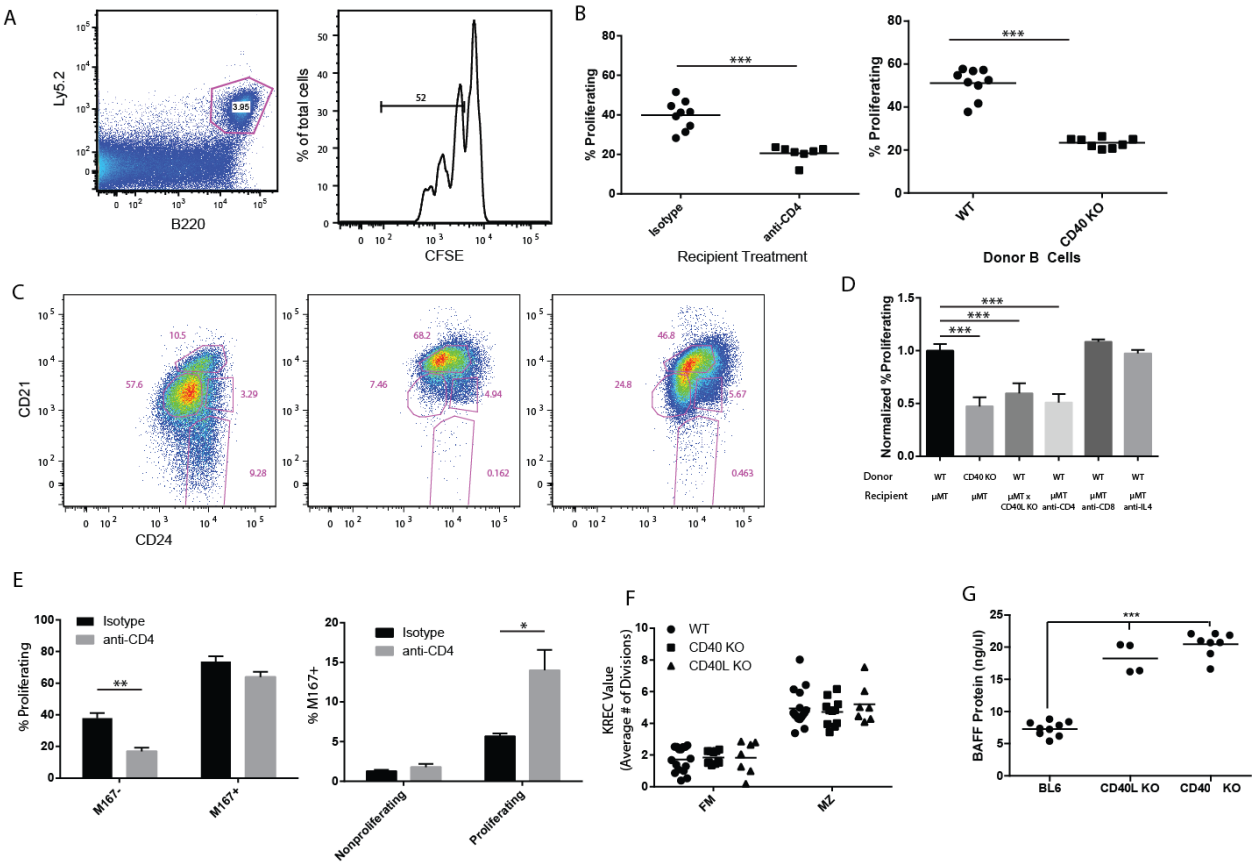

Figure 1. Effect of CD40 on B Cell Homeostasis. (A-E) B cell homeostatic proliferation (HP) measured by transfer of splenic B cells into B cell deficient host. (A) Gating on congenically marked donor B cells (left panel) and proliferating cells by CFSE dilution (right panel). (B) B cell HP measured after transfer of WT B cells to µMT mice treated with either isotype or CD4-depleting antibody (left panel) and transfer of WT or CD40 KO B cells to µMT recipients (right panel). (C) Surface phenotype of WT donor B cells prior to HP experiment (left panel), after HP (middle panel), and CD40 KO B cells after HP (right panel). (D) Summary of HP data from multiple experiments, data normalized to WT or isotype treated control for each individual experiment. (E) HP experiment using donor B cells from M167-transgenic mice, showing proliferation of Id- and Id+ cells (left panel) and the frequency of Id+ cells in non-proliferating or proliferating cells (right panel). (F) KRECs assay on sorted FM and MZ cells from WT, CD40 KO, and CD40L KO mice. (G) Serum BAFF levels measured by ELISA in WT, CD40 KO, and CD40L KO mice.

BCR signals have been proposed to contribute to B cell HP as well; this was addressed using M167-transgenic mice, in which a fraction of B cells contain a self-reactive phosphorylcholine (PC)-specific BCR recognizable by an idiotype (Id)-specific antibody[27].

Compared to Id-negative cells, Id+ B cells exhibited increased HP and, intriguingly, while HP levels were reduced in Id-negative cells when CD4 cells were depleted, HP of Id+ cells was unaffected, resulting in enrichment for Id+ cells in the proliferating subset of CD4-depleted mice (Figure 1E). Collectively, these data point to independent roles for both CD40- and BCR-induced signals during B cell HP.

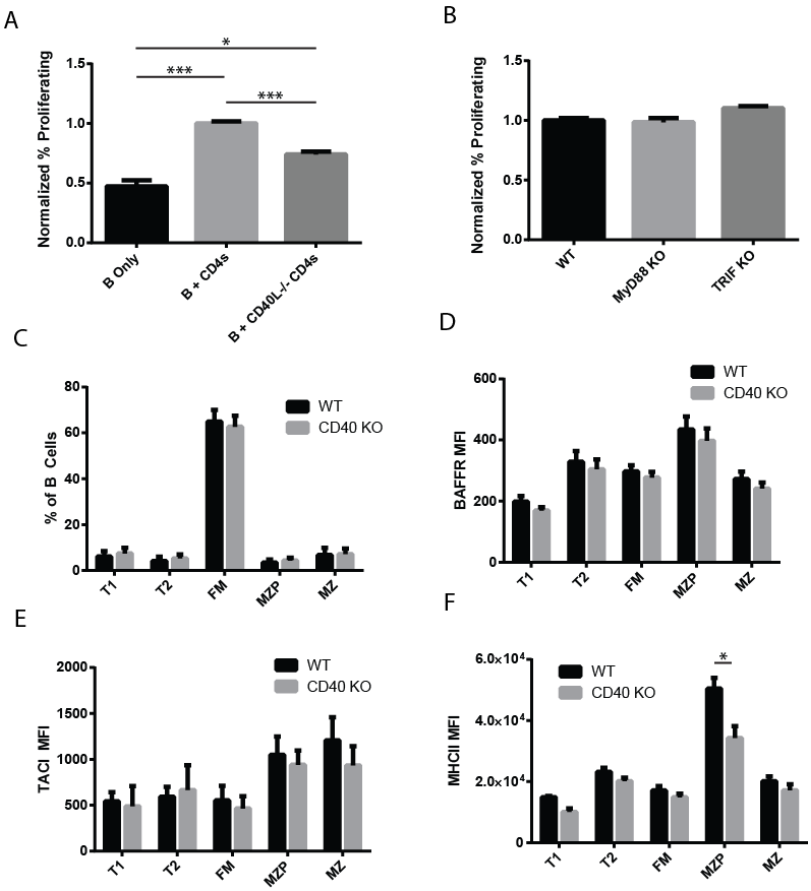

Figure 2. (A) Transfer of B cells and/or CD4+ T cells into RagKO recipients. (B) HP experiments with MyD88-/- and TRIF-/- donor B cells. (C) Peripheral B cell subsets in WT and CD40-/- mice. BAFFR (D), TACI (E), and MHCII (F) surface expression on B cell subsets in WT and CD40-/- mice.

Based on data from HP experiments, we further evaluated whether CD40 plays a role in physiologic B cell development and homeostasis. As expected from previous studies, no

difference was observed when quantifying peripheral B cell subsets in CD40 KO mice compared to WT controls (Figure 2C). Cumulative division of FM and MZ B cells was assessed using the kappa recombination excision circle (KREC) assay, revealing no detectable difference between WT, CD40 KO, and CD40L KO mice (Figure 1F). Surface marker expression was compared among B cell subsets, and while BAFFR and TACI levels were not different, the MZ-precursor (MZP) subset had lower levels of MHCII when CD40 was absent (Figure 2D-F). In regard to these mostly negative results, we wondered whether the relatively normal appearance of peripheral B cells in CD40-/- mice was due to an increase in other signals that promote B cell development and thereby compensate for lack of CD40. Consistent with data from CD40L-deficient hyper-IgM patients[51], both CD40L- and CD40-deficient mice display increased levels of serum BAFF (Figure 1G). Therefore, we propose that deficiency of CD40 results in a compensatory increase in circulating BAFF levels which helps maintain peripheral B cell numbers.

CD40 Promotes Peripheral B Cell Homeostasis in Mixed BM Chimeras

As increased BAFF levels may compensate for the lack of CD40, we created mixed BM chimeras to follow WT and CD40 KO B cell development in the same environment. Congenically marked WT and CD40-/- BM was transferred to irradiated μMT mice, allowing discrimination of WT, CD40-/-, and recipient-derived lymphocytes (Figure 3A). We tested several donor ratios to generate chimeras in which the early transitional stage was composed of equal quantities of WT and CD40-/- B cells; this was accomplished at a 65:35 CD40-/-:WT BM ratio. At 3 months post-transplant, we found a significant increase in CD40-expressing cells beginning at the late transitional stage and becoming most notable in the MZ subset (Figure 3B).

Depletion of CD4+ T cells throughout the duration of this experiment eliminated enrichment of WT B cells in transitional cells, but only partially reduced enrichment for WT cells in the MZ subset. A 90:10 CD40-/-:WT BM ratio was used to further test competitive selection of WT B cells; in these experiments enrichment for WT cells in transitional stages was not observed, but the competitive advantage of CD40-expression remained in the MZ subset, and was partially reduced by CD4-T cell depletion (Figure 3C). These data demonstrate that CD40 signals can promote transitional B cell development and population in particular of the MZ compartment.

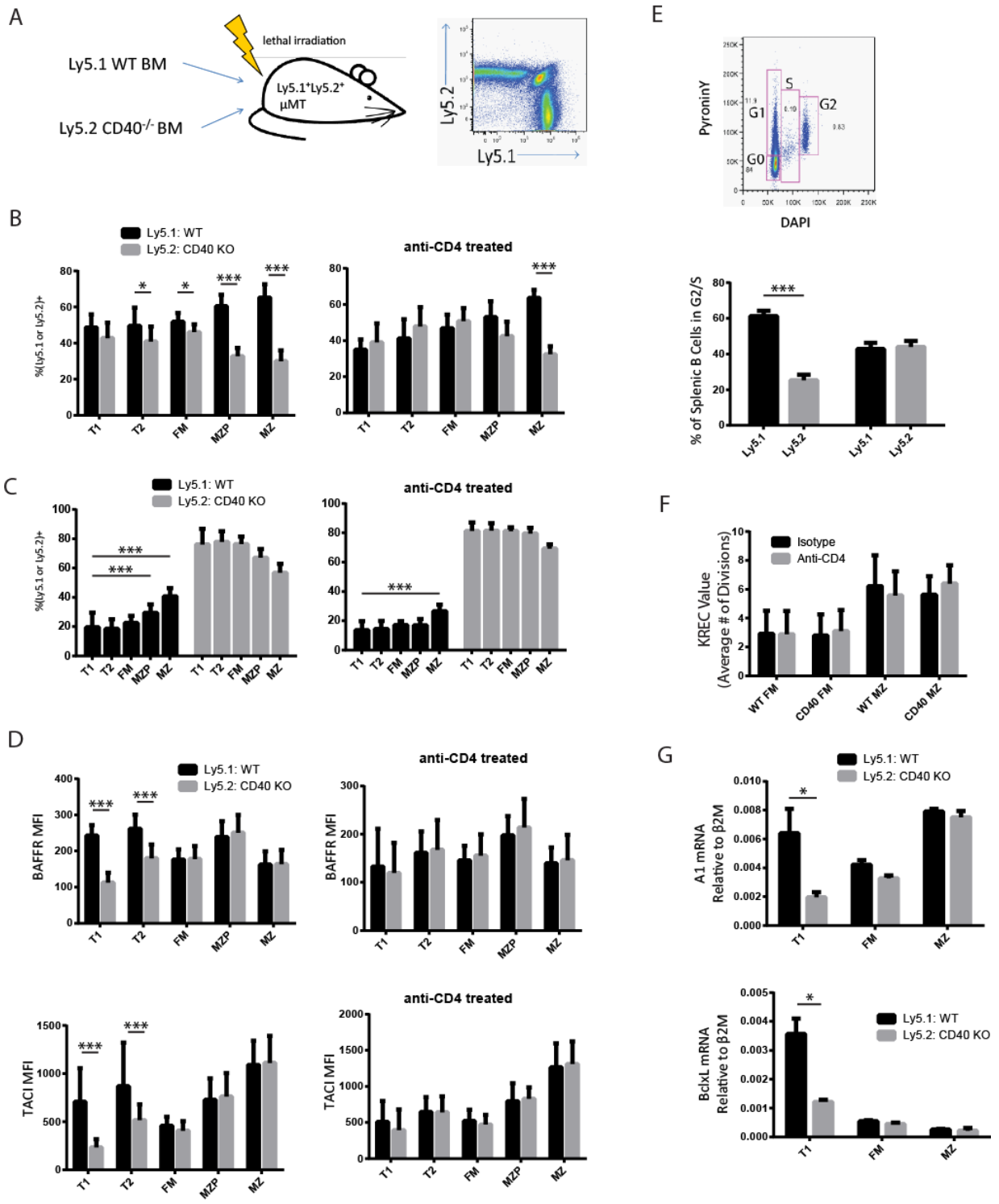

Figure 3. (A) WT/CD40 KO mixed BM chimeras created by transfer of congenically marked BM to µMT recipients. (B) Percentage of ly5.1+(WT) and ly5.2+(CD40 KO) cells in each B cell subset 3 months after creation of mixed BM chimeras created with a 65:35(CD40KO:WT) ratio

of donor BM, either untreated (left panel) or depleted of CD4 T cells throughout the experiment (right panel). (C) Analysis of BM chimeras created with a 90:10(CD40KO:WT) ratio of donor BM, untreated (left panel) or depleted of CD4 T cells (right panel). (D) BAFFR and TACI surface expression in T1 cells in BM chimeras created using all WT donors (left 2 panels) or WT and CD40 KO donors (right 2 panels). (E) Average BAFFR and TACI MFI values in untreated (left panels) and CD4-depleted (right panels) chimeras. (F) Cell cycle analysis by DAPI and PyroninY staining; percentage of ly5.1+ and ly5.2+ cells in a combined S and G2 gate (top panel) in WT/CD40 KO chimeras (middle panel) and WT/WT chimeras (bottom panel). (G) KRECs assay on FM and MZ cell subsets sorted by ly5.1/ly5.2 from mixed BM chimeras, untreated and CD4-depleted. (H) qPCR of subsets sorted from mixed BM chimeras,; mRNA levels of A1 (top panel) and BclxL (bottom panel) relative to β2-microglobulin.

To further evaluate how CD40 affects B cell development, surface levels of BAFF family receptors were analyzed as upregulation of BAFFR in particular coincides with developmental progression of transitional subsets[58]. Surprisingly, BAFFR and TACI levels, measured by flow cytometry and qPCR, were abnormally high in WT transitional cells *only* in the setting of a mixed BM chimera with CD40-deficient cells, and this difference was completely abolished by the depletion of CD4 cells (Figure 3E and Figure 4B,C). Consistent with these data, *in vitro* stimulation of B cells with CD40 increases surface levels of BAFFR and TACI (Figure 4D,E). We therefore propose that CD40 signals received through interaction with CD4+ T cells promote upregulation of BAFF family receptors in transitional B cells.

Finally, we asked whether CD40 promotes transitional B cell cycling in mixed chimeras, as previous data have suggested that a small subset of transitional cells is dividing[4,10]. Using DAPI and PyroninY to gate on cells in S and G2 phases, we found that the fraction of cycling cells was significantly enriched for WT over CD40-deficient cells (Figure 3F). However, no difference was observed in KREC values among WT and CD40-deficient FM and MZ subsets sorted from chimera recipients (Figure 3G). As KREC values reflect cumulative division, these

results demonstrate that the cells which made it into mature compartments have divided equally on average regardless of CD40 expression; however, CD40 appears to promote a greater frequency of transitional cells entering mature compartments, especially the MZ subset. Lastly, survival-associated genes A1 and BclxL were shown by qPCR to be increased in WT over CD40-deficient early transitional cells (Figure 3H).

Collectively, data from mixed BM chimeras demonstrates that transitional B cells can receive CD4+ T cell help through CD40, and this signal promotes the B cell developmental program by increasing expression of BAFF receptors and survival genes, leading to a competitive advantage in entering mature, functional B cell subsets, most notably the MZ compartment.

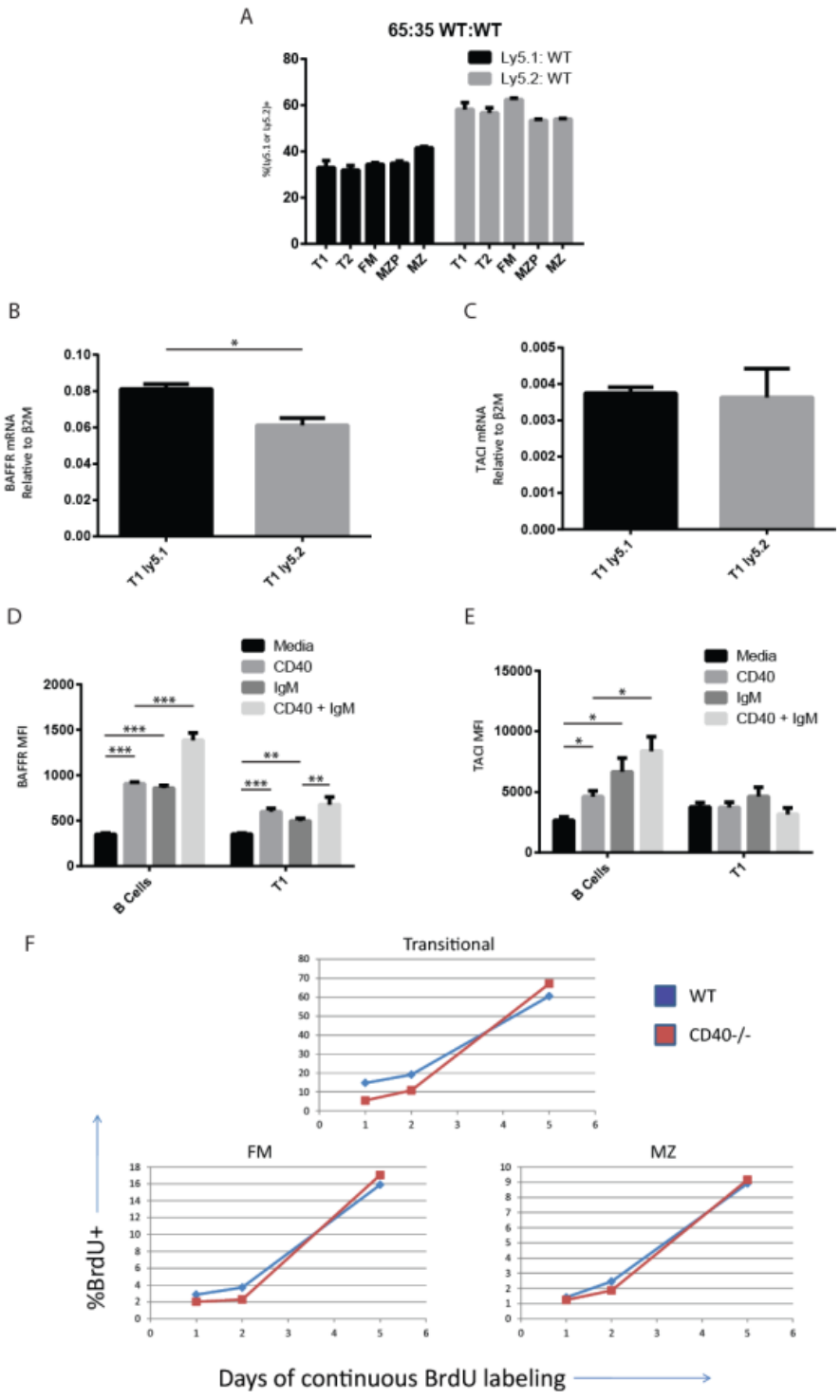

Figure 4. (A) Characterization of mixed BM chimeras generated from 2 WT, congenically marked donors. BAFFR (B) and TACI (C) qPCR in sorted T1 cells from WT/CD40-/- mixed BM chimeras. Surface expression of BAFFR (D) and TACI (E) after *in vitro* stimulation of B

cells with CD40 and IgM. (F) BrdU labeling by drinking water in WT/CD40-/- mixed BM chiemras.

CD40 Controls B Cell Development when BCR Signaling is Impaired

Next, we sought to expand upon prior observations that, while CD40-deficiency does not reduce peripheral B cell numbers compared to WT mice, removal of CD40 significantly reduces the B cell population in mice with mutations in btk[52,53]. Btk-deficient (XID) mice have impaired BCR signaling and a reduced, but not absent, mature B cell population compared to WT mice. We depleted CD4 T cells from XID mice and mice lacking both btk and tec to determine whether the effect of CD40 depends on T cells, as T cell depletion in WT mice does not affect peripheral B cell subsets (data not shown). In both of these models, depletion of T cells induced a block in development at the late transitional stage, resulting in an almost complete absence of both FM and MZ subsets (Figure 5A-D). As a separate model of reduced antigen-mediated BCR signaling, we made CD40-deficient HEL-specific MD4-transgenic mice to determine whether CD40 is required for peripheral development of a monoclonal B cell population unable to recognize self-antigen. We found a significant reduction in peripheral B cell numbers, but not subset percentages, in CD40-deficient MD4 mice, consistent with a role for CD40 in development of B cells with little or no self-specificity (Figure 5E). Together, these data indicate that if transitional B cells do not receive a sufficient signal through the BCR, they rely instead on interaction with CD4+ T cells through CD40 to enter mature subsets.

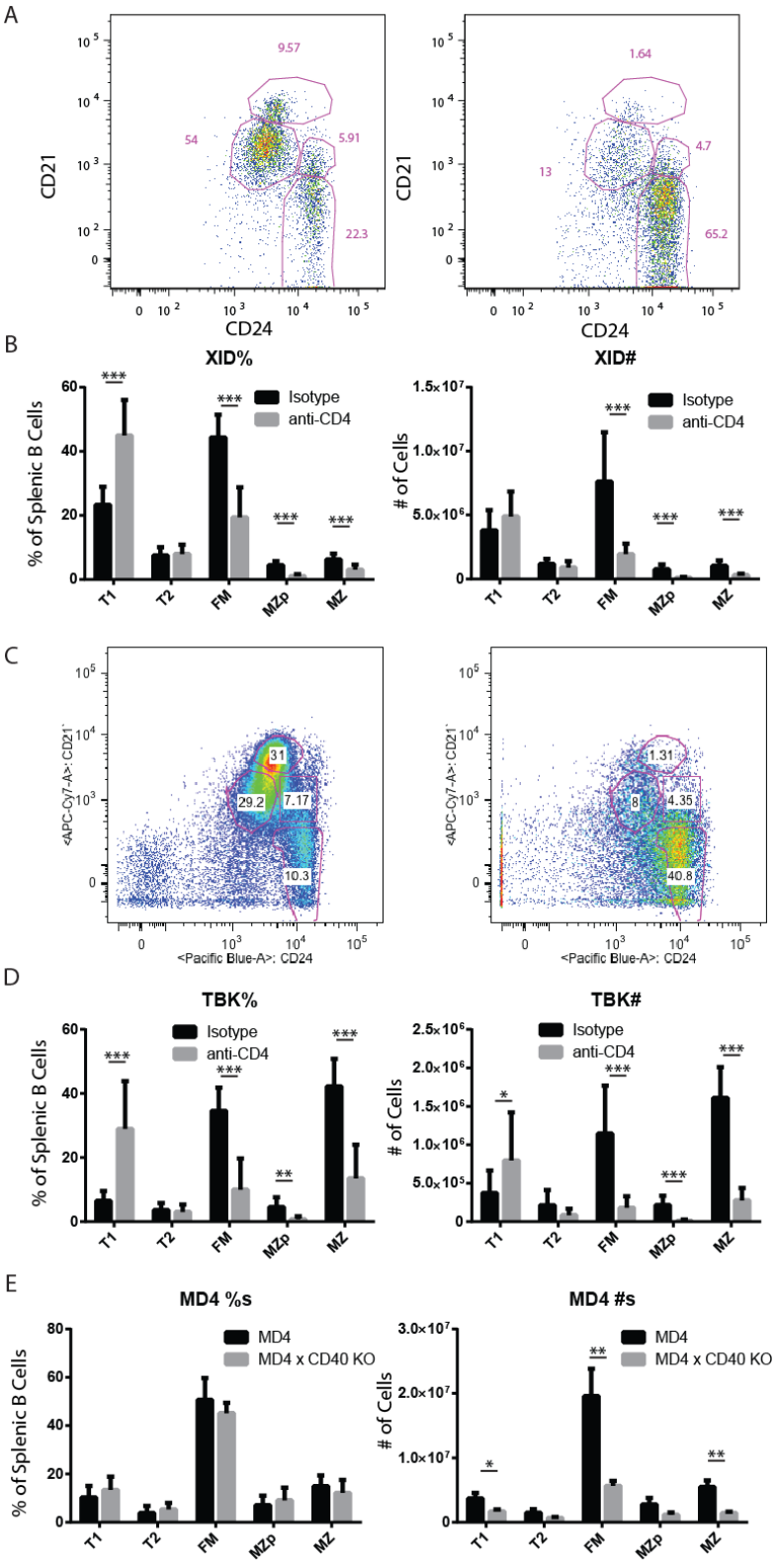
A
CD21
CD24
9.57
54
5.91
22.3
1.64
13
4.7
65.2
B
XID%
XID#
% of Splenic B Cells
# of Cells
Isotype
anti-CD4
T1
T2
FM
MZp
MZ
C
<APC-Cy7-A>: CD21
<Pacific Blue-A>: CD24
31
29.2
7.17
10.3
1.31
8
4.35
40.8
D
TBK%
TBK#
E
MD4 %s
MD4 #s
MD4
MD4 x CD40 KO

Figure 5. (A) B cell subset gating on XID mice (left panel) and XID mice depleted of CD4 T cells (right panel). (B) Average subset %s (left panel) and #s (right panel) in XID mice treated with isotype or CD4-depleting antibody. (C) B cell subset gating on tec/btk DKO mice treated with isotype (left panel) or CD4-depleting antibody (right panel). (D) Average subset %s (left panel) and #s (right panel) in tec/btk DKO mice treated with isotype or CD4-depleting antibody. (E) B cell subset %s (left panel) and #s (right panel) in MD4-transgenic mice and MD4 x CD40 KO mice.

Increased Self-Antigen Mediated Positive Selection of MZ B Cells in the absence of CD40

As CD40 appears to be of increased importance when BCR signaling is impaired, the corresponding notion that BCR signals are more important when CD40 is absent was addressed using the M167-transgenic model. PC-specific cells are enriched in the MZ subset of these mice, and we asked whether deficiency of CD40 affects this selective process. First, we found a reduction in the total number of FM cells and an associated increase in the percentage of MZ cells in M167-tg mice lacking CD40 (Figure 6A,B). Further, selection of Id+ PC-specific cells was significantly increased in the MZ subset of CD40 KO x M167-tg mice (Figure 6C,D). To account for the possible influence of variable BAFF levels, a new set of mixed BM chimeras was created using BM from M167-tg mice with and without CD40. Consistent with non-transgenic data, these chimeras exhibited a strong selective advantage for CD40 expressing cells at the late transitional stage and continuing into both FM and MZ subsets (Figure 6E). Additionally, both T2 and MZ CD40-deficient cells contained significantly more Id+ cells compared to CD40-expressing subsets (Figure 6F). These results suggest that in the absence of CD40, population of mature B cell compartments increasingly depends on antigen-mediated positive selection of transitional cells.

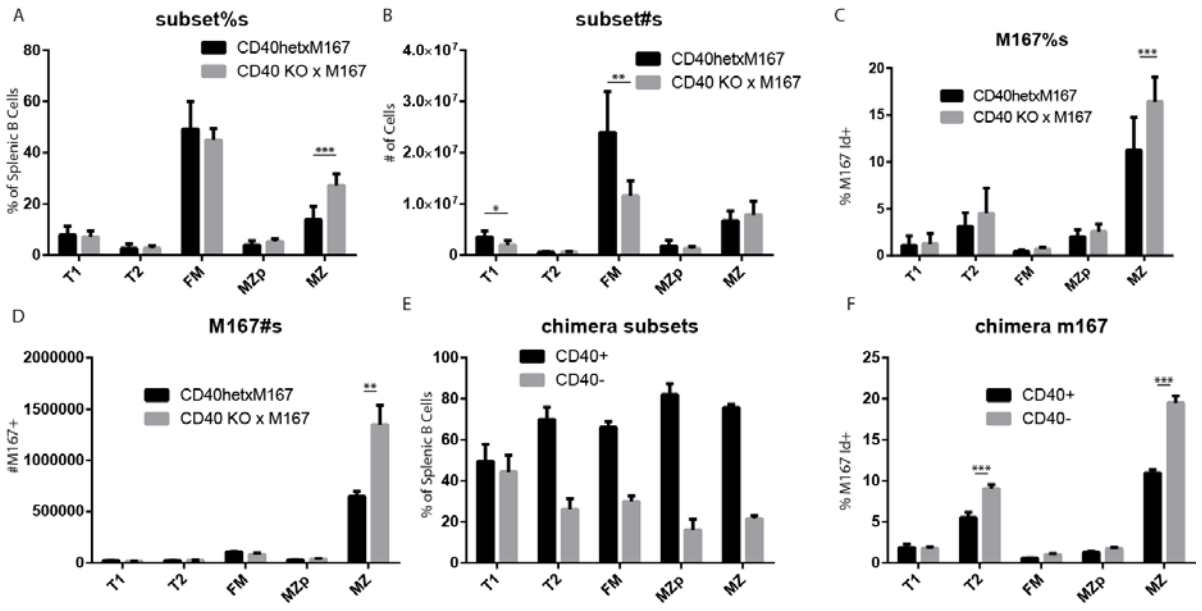

Figure 6. B cell subset %s (A) and #s (B) in CD40 KO/M167-transgenic mice. (C) Frequency of Id+ cells in CD40hetM167, CD40KOM167, and CD4-depleted M167 mice. (D) Total number of Id+ cells in CD40hetM167 and CD40KOM167 mice. (E-I) Analysis of mixed BM chimeras using CD40hetM167 and CD40KOM167 donor BM. (E) Frequency of CD40+ and CD40- cells in B cell subsets. (F) M167 Id+ % in CD40+ and CD40- B cell subsets. (G) KRECs assay on MZ cells sorted by CD40 and M167 Id. Average BAFFR (H) and TACI (I) MFIs in B cell subsets gated by CD40 and M167 Id.

To further evaluate selection in M167-tg WT/CD40 mixed BM chimeras, proliferation history was measured using the KREC assay in Id+ and Id- MZ cells sorted from both CD40+ and CD40-deficient subsets. While we did not detect a difference in KREC level based on CD40 expression alone, CD40-deficient Id+ cells had significantly higher KREC values than CD40-deficient Id- cells (Figure 7A), providing further evidence of an increase in the importance of antigen-mediated selection when CD40 is unavailable. BAFFR and TACI surface expression was also evaluated in B cell subsets categorized based on both CD40 expression and Id-binding (Figure 7B,C). Consistent with earlier data, CD40-expressing transitional cells had high levels of BAFFR and TACI expression. However, PC-specific transitional cells had divergent phenotypes

with regard to BAFFR and TACI; lower BAFFR and higher TACI levels were observed on PC-specific transitional cells compared to Id- cells. These data provide further evidence of a role for CD40 in driving expression of BAFF receptors in transitional cells, and suggest an independent role for antigen-mediated BCR signals in modulating expression of these receptors.

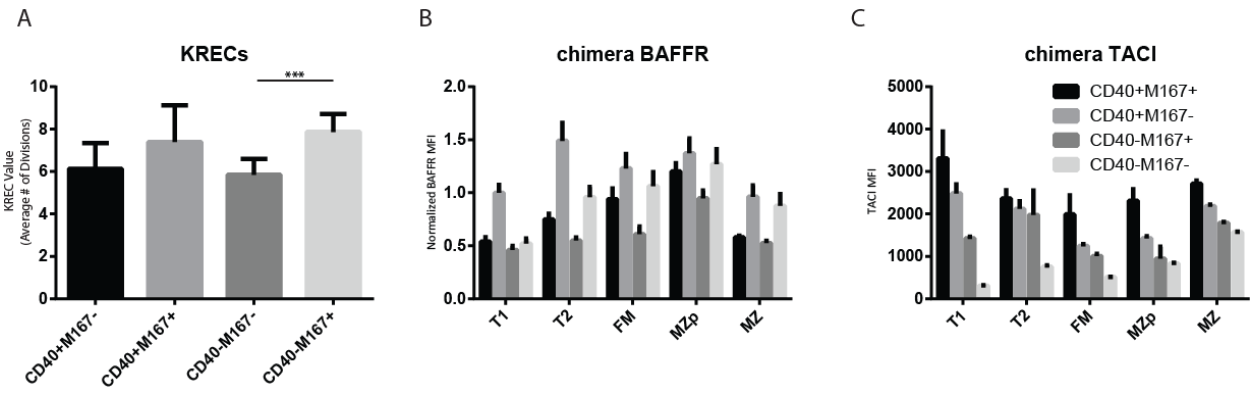

Figure 7. (A) KRECs assay in cells sorted from M167-tg WT/CD40-/- mixed BM chimeras based on both CD40 expression and Id-specific antibody binding. Surface expression of BAFFR (B) and TACI (C) in mixed BM chimeras, gated based on CD40 and Id-antibody.

Altered Specificity Profile of Mature B Cells in CD40-/- Mice

Based on the data from transgenic models, we sought to expand our analysis of B cell selection to the setting of an unrestricted BCR repertoire. Using established methods[3], single FM and MZ B cells from WT and CD40-/- mice were sorted by FACS, and their individual heavy and light chain BCR genes were cloned into expression vectors allowing production of recombinant antibodies in HEK293T cells. Out of 840 sorted single B cells, 303 full antibodies were produced (72 WT FM, 85 CD40-/- FM, 63 WT MZ, and 83 CD40-/- MZ). Following purification from culture supernatants, antibody specificity was first evaluated with a commercially available antinuclear antibody (ANA) ELISA kit. A low-positive control was used

on all plates to establish a threshold for positivity; based on this cutoff, 25% (18/72) of WT FM, 27% (23/85) of CD40-/- FM, 35% (22/63) of WT MZ, and 27% (22/83) of CD40-/- MZ antibodies displayed positive ANA reactivity (Figure 8A), suggesting a possible increase in autoreactive FM BCRs and decrease in autoreactive MZ BCRs in CD40-/- mice. Next, reactivity to dsDNA, insulin, and LPS (three structurally diverse antigens) was assessed by ELISA as others have done to evaluate polyreactivity[51,59]. Compared to WT controls, fewer CD40-/- antibodies from both FM and MZ subsets were positive for dsDNA, whereas there was little difference between FM and MZ subsets for both genotypes. A distinct pattern was observed for insulin and LPS ELISAs, whereby FM antibodies contained a higher proportion of reactive antibodies than MZ, while both FM and MZ antibodies from CD40-/- mice were less reactive than WT. Antibodies were classified as polyreactive if positive by ANA and at least two of the three individual antigens. Similar to previous data on polyreactivity in mature, naïve B cells[3], 4% (3/72) of WT FM antibodies were polyreactive (Figure 8B); in contrast, only 1% (1/85) of CD40-/- FM antibodies were polyreactive, an no polyreactive antibodies were found in either WT or CD40-/- MZ subsets.

Antibody specificity was further evaluated by ANA immunofluorescence assays (IFA), allowing identification of nuclear and cytoplasmic staining patterns (Figure 8C). Positive patterns were detected in 19% of WT FMs, 21% of CD40-/- FMs, 25% of WT MZs, and 17% of CD40-/- MZs; while slightly lower than the fractions of positive ANAs, IFAs displayed a similar relationship between WT and CD40-/- subsets. Additionally, nuclear staining patterns were more frequent in WT MZ (12.5%) antibodies compared to WT FM (5.41%), while CD40-/- FM (2.35%) and MZ (8.43%) subsets displayed lower rates of nuclear patterns compared to WT counterparts, a finding consistent with the dsDNA ELISA results.

Finally, we sought to develop specificity profiles by pooling all cloned antibodies for each subset and analyzing them on autoantigen arrays containing 88 endogenous antigens associated with various antibody-mediated autoimmune diseases. This assay was intended to evaluate average specificity patterns in each subset, as opposed to the antibody ELISAs and IFAs which identified individual antibody characteristics. As none of the recombinant antibodies being tested had undergone affinity maturation, reactivity levels on autoantigen arrays were generally low as they are intended for detecting high affinity antibodies in serum samples. However, a relative comparison among each subset of normalized, average signals for each antigen revealed a similar pattern in both WT and CD40-/- FM subsets (Figure 8D). In contrast, the WT MZ subset displayed a distinct reactivity pattern compared to FM subsets, with far fewer antigens generating a detectable signal. Lastly, the pattern displayed by the CD40-/- MZ subset could be described as intermediate between the WT MZ and FM patterns, along with a few unique antigen signals.

Taken together, these data reflect a divergent specificity profile in FM and MZ subsets in WT mice, and further suggest that the normal polarization of BCR specificities within the FM and MZ subsets may be altered in the absence of CD40.

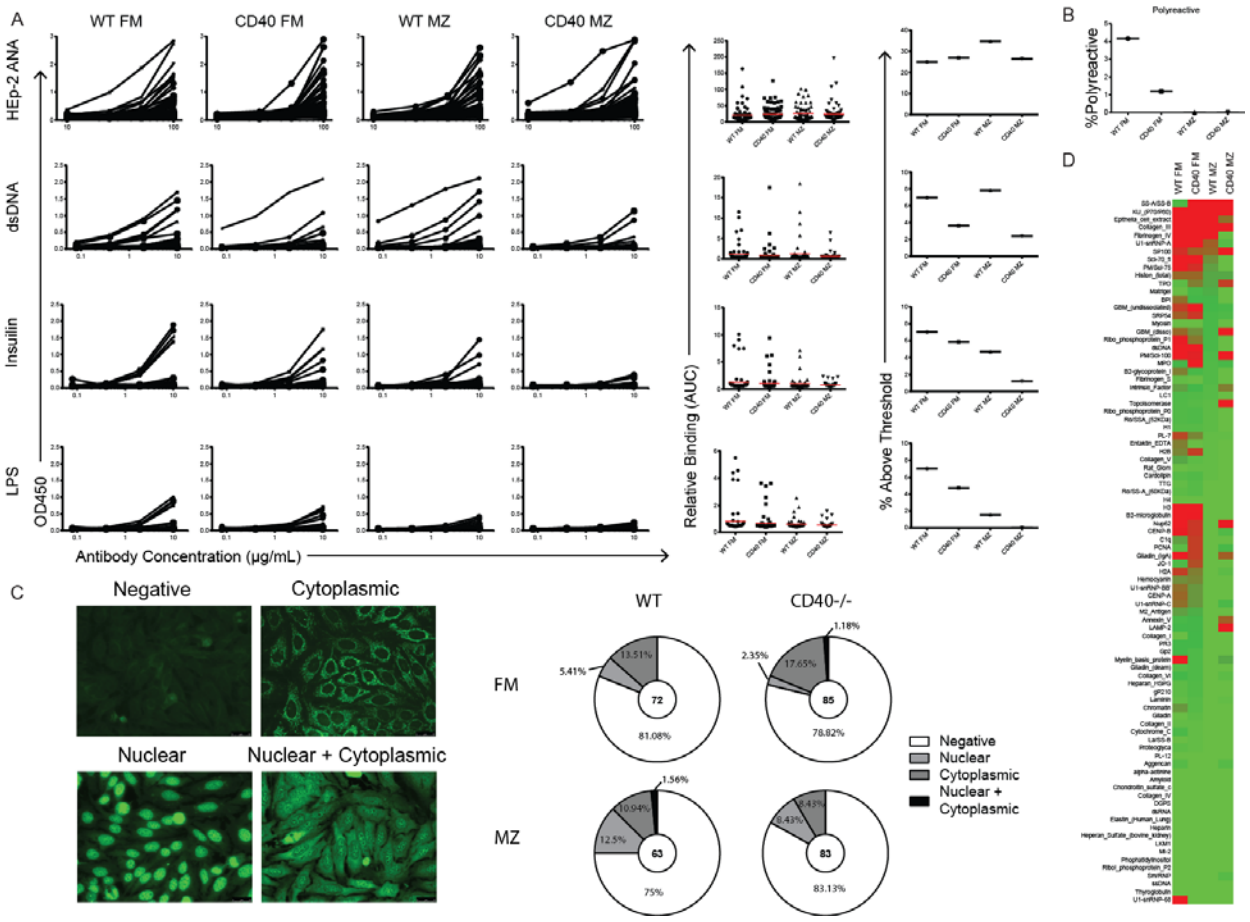

Figure 8. Single cell BCR cloning. (A) HEp-2 ANA, dsDNA, insulin, and LPS ELISA data, AUCs and % positive based on arbitrary threshold. (B) % polyreactive based on reactivity to at least 2 (dna/insulin/lps) ELISAs. (C) HEp-2 IFAs, showing negative, cytoplasmic, nuclear, and nuclear+cytoplasmic patterns, and characterizing the frequency of each pattern in cloned BCRs. (D) Autoantigen array with pooled groups of BCR antibodies.

Sequence Characteristics of WT and CD40-/- ANA-Positive Recombinant Antibodies

As part of the cloning process, BCR sequences were obtained for each individual recombinant antibody. Sequences were sorted based on genotype, B cell subset, and ANA ELISA reactivity, and subsequently analyzed to identify any distinguishing sequence characteristics; WT and CD40-/- ANA-negative antibodies were combined for both FM and MZ

subsets, as the focus of this analysis was to distinguish self-antigen specific BCRs selected in the presence or absence of CD40. We focused on the CDRH3 as this region contributes significantly to antibody specificity, and is the predominant source of CDR variability in naïve, unmutated BCR heavy chains. IMGT/VQuest was used for sequence alignment to the IgH locus, and the Immunoglobulin Analysis Tool (IgAT)[60] was used to generate further descriptive statistics. Average CDRH3 length did not differ between FM-negative and WT FM-positive BCRs, but was slightly lower in CD40-/- FM-positive BCRs, although this difference was not significant (Figure 9A). MZ CDRH3 lengths were also slightly lower in MZ-positive BCRs for both genotypes, but this was also not significant. Another CDRH3 characteristic correlated to antibody autoreactivity in previous studies is N-nucleotide addition at variable region junctions[61]. N-addition was quantified at both the V-D and D-J junctions, and while no differences were found at the D-J junction, significantly greater N-addition at the V-D junction (N1) was identified in both WT and CD40-/- FM-positives compared to FM negatives (Figure 9B). N1-addition was also significantly increased in CD40-/- MZ-positives but not WT MZ-positives. The fraction of sequences with 0 N1-nucleotides was also quantified, revealing a trend in both FM- and MZ-positives for fewer sequences with 0 N1 nucleotides (Figure 9C). Next, the number of negative and positive charges in CDRH3 amino acid sequences was quantified, demonstrating a decrease in negative charges and a corresponding increase in positive charges in ANA-positive antibodies across all genotypes and B cell subsets, although this trend was stronger in FM relative to MZ sequences (Figure 9D,E). CDRH3 hydrophobicity was calculated using the normalized Kyte-Doolittle (KD) scale, which assigns a value to each amino acid with negative numbers representing hydrophilic and positive numbers representing hydrophobic residues. Each sequence is then assigned an average index based on the individual hydrophobicities of all

CDRH3 amino acids. No significant differences were detected when comparing average KD indices for each subset. However, we further characterized the hydrophobicity distribution using established methods[62] to calculate the percentage of charged (KD < -0.7) and hydrophobic (KD > 0.6) CDRH3s. None of the ANA-positive antibodies were classified as hydrophobic, while many fell into the charged range, particularly in the CD40-/- MZ-positives (Figure 9G). Finally, amino acid usage patterns were compared across all subsets, revealing reduced tyrosine and increased arginine and tryptophan in ANA-positive CDRH3s (Figure 9H).

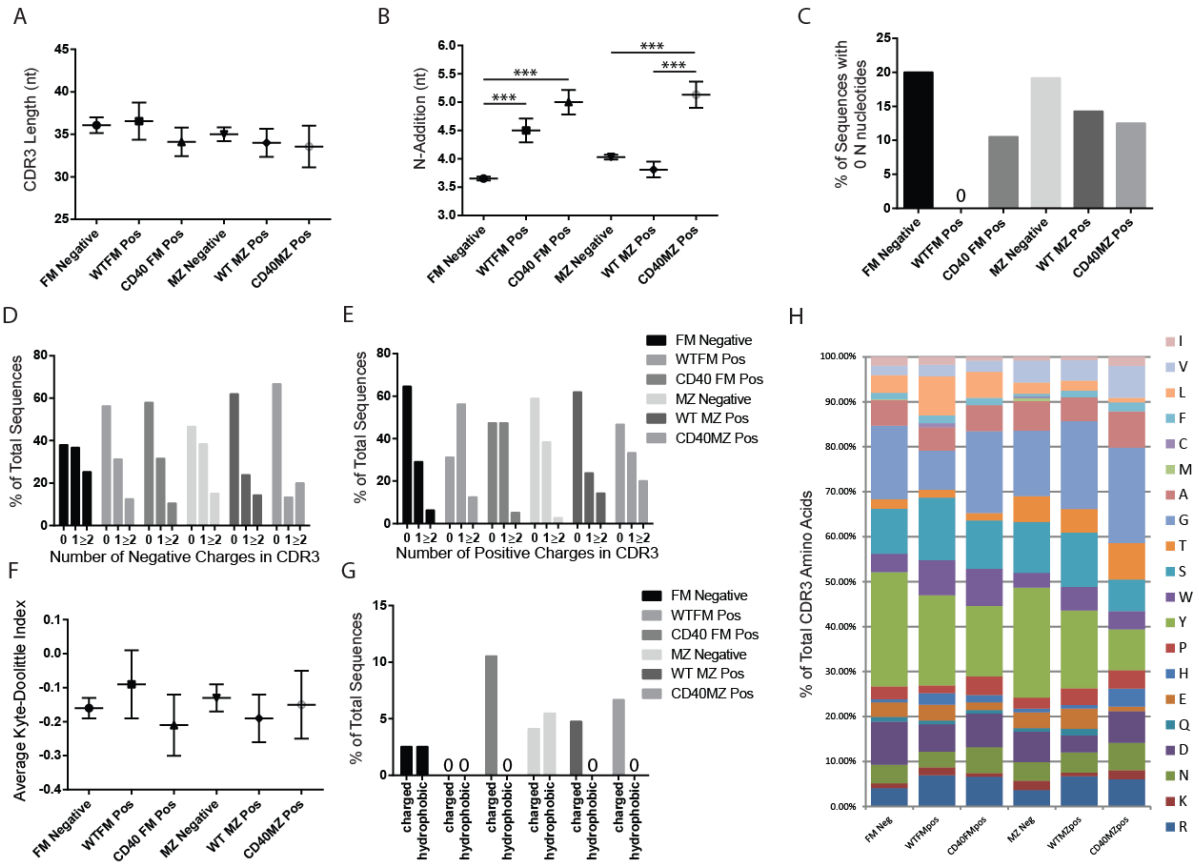

Figure 9. BCR IgH sequences from recombinant antibodies were sorted based on subset, genotype, and ANA ELISA-reactivity. They were analyzed to determine CDRH3 length (A), N1-addition (B), fraction of sequences with no N1-addition (C), negative CDRH3 charges (D), positive charges (E), average KD index (F), fractions of charged and hydrophobic CDRH3s calculated based on individual KD indices (G), and total CDRH3 amino acid usage (H).

High-throughput Sequencing of BCR Heavy Chain Genes in WT and CD40-/- Mice

To extend the scope of our repertoire analysis, high-throughput sequencing of BCR heavy chain genes was carried out by pyrosequencing 5'-RACE-generated amplicons. This method was selected to reduce bias induced by using multiple 5' V-region primers. FM and MZ subsets were sorted from WT and CD40-/- mice as well as WT/CD40-/- mixed BM chimeras; three mice were combined to generate each individual sequencing sample, and 4 independent samples were analyzed for each sorted subset, resulting in a total of between 3-5 $x10^4$ sequences per subset, and the analysis was restricted to unique clonotypes to avoid PCR amplification-induced bias (Figure 10). Both CD40-/- FM and MZ subsets, compared to their WT counterparts, displayed small but statistically significant decreases in CDRH3 length (Figure 11A). The CD40-/- MZ subset had slightly higher, although not significant, N1-addition and a corresponding decrease in the fraction of sequences with 0 N1 nucleotides (Figure 11B,C). No difference was observed in the total fractions of positive and negative CDRH3 charges (Figure 11D,E). However, comparison of average KD indices revealed a significant increase in the CD40-/- MZ subset compared to WT MZ (Figure 11F). Calculation of charged and hydrophobic fractions revealed an increase in both in WT MZ relative to WT FM sequences, and while the CD40-/- FM subset was unaffected, CD40-/- MZ sequences contained decreased fractions of both charged and hydrophobic CDRH3s (Figure 11G). Total frequency of CDRH3 amino acids was very similar among all subsets, the largest difference was a 1.5% reduction in tyrosine use in CD40-/- MZ relative to WT MZ sequences (Figure 11H).

	Total Sequences	Functional Sequences	Unique Clonotypes
WT FM	42481	20167	8102
CD40 FM	49220	22864	9060
WT MZ	43338	22216	4305
CD40 MZ	46553	24319	9368
Ly5.1 FM	36878	25612	1897
Ly5.2 FM	36803	25748	3303
Ly5.1 MZ	32267	24191	1180
Ly5.2 MZ	31182	21881	2310
Vk8	19474	16298	10083
Vk8xCD40-/-	25382	20943	8753

Figure 10. Tabulation of total sequences obtained. Sorted FM and MZ subsets are each composed of 4 independent samples from 3 pooled mice. Vk8 and Vk8CD40-/- samples are CD43-depleted splenocytes from two samples taken from 3 pooled mice.

An identical analysis was carried out in subsets sorted from WT/CD40-/- mixed BM chimeras. Overall, CDRH3 lengths were lower in chimera samples compared to the non-chimeric setting, but no significant differences were detected among sorted chimera subsets (Figure 12A). N1-addition was higher in the chimeric setting compared to non-chimeras, and significantly higher along with a reduced frequency of 0-N1 CDRH3s in CD40-/- MZ relative to WT MZ sequences (Figure 12B,C). Surprisingly, the average KD index for the chimera WT MZ subset was not significantly lower than the WT FM subset, as it was in a non-chimeric setting, suggesting mixed BM chimeras may not fully recapitulate normal specificity-based selection into the MZ (Figure 12F). However, fewer charged CDRH3s were found in CD40-/- FM and MZ sequences compared to WT, consistent with data from non-chimeras (Figure 12G). Comparison of total amino acid usage revealed lower tyrosine and higher glycine in CD40-/- FMs and higher serine in CD40-/- MZs compared to WT controls (Figure 12H).

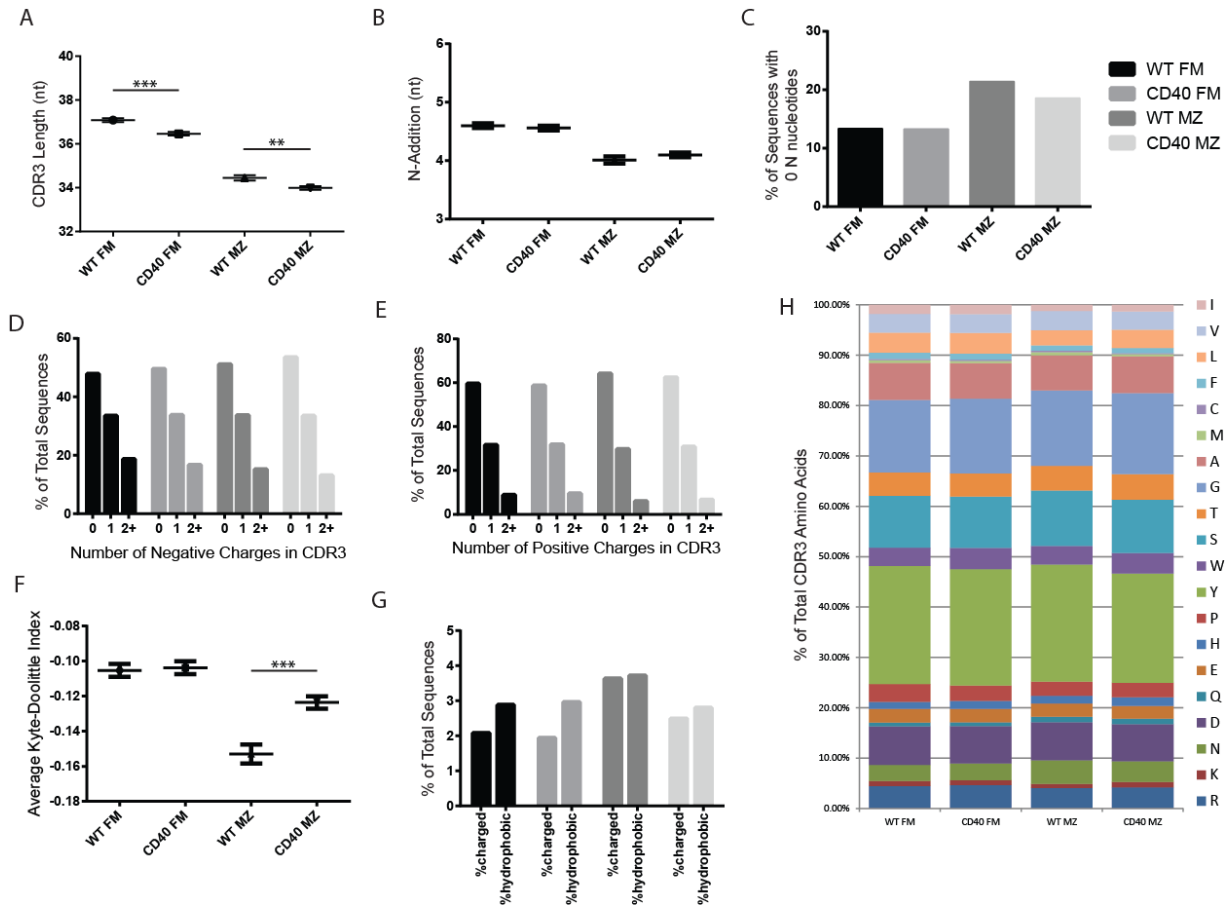

Figure 11. High throughput BCR heavy chain sequencing of FM and MZ subsets sorted from WT and CD40 KO mice. Analysis includes CDRH3 length (A), N1-addition (B), fraction of sequences with no N1-addition (C), negative CDRH3 charges (D), positive charges (E), average KD index (F), fractions of charged and hydrophobic CDRH3s calculated based on individual KD indices (G), and total CDRH3 amino acid usage (H).

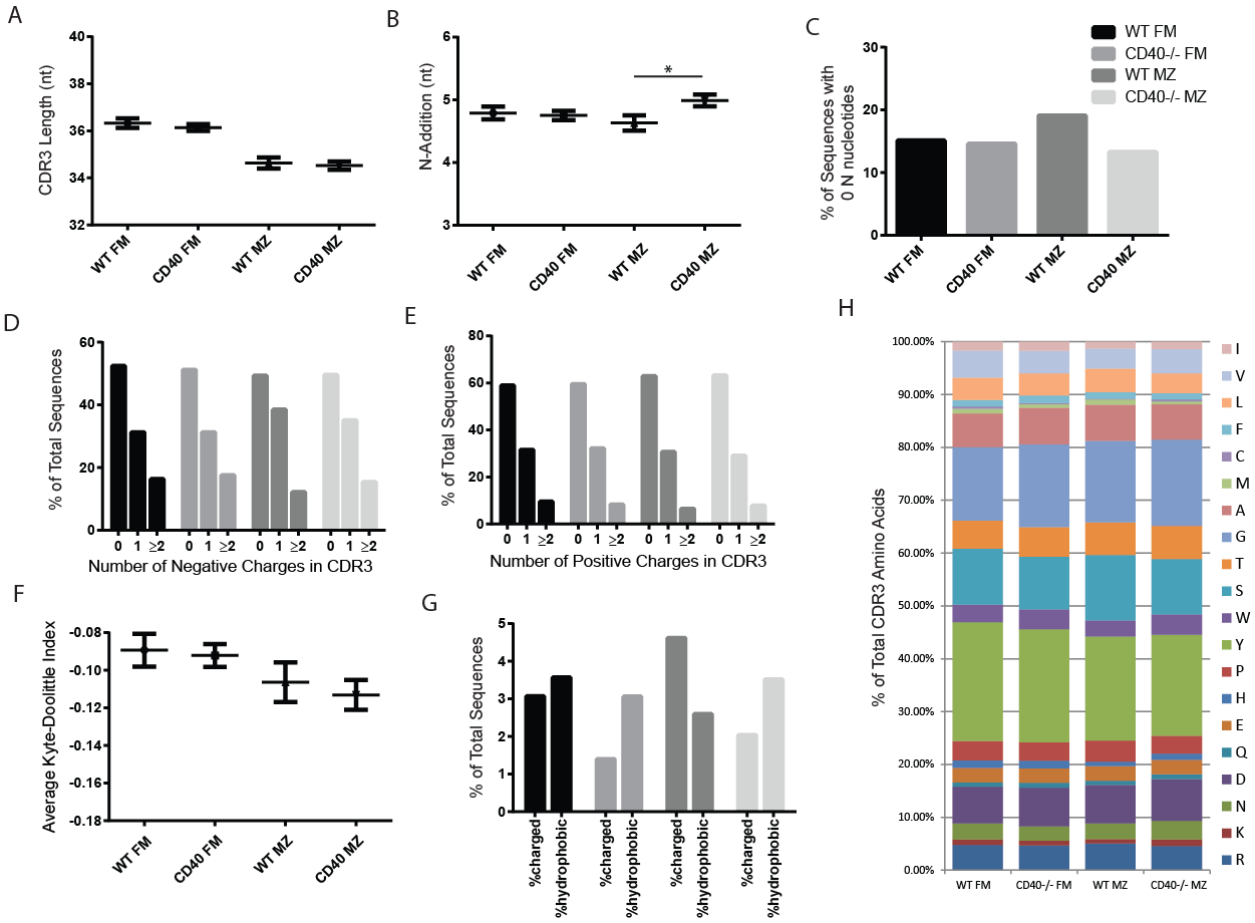

Figure 12. High throughput BCR heavy chain sequencing of FM and MZ subsets sorted from WT/CD40 KO mixed BM chimeras. Analysis includes CDRH3 length (A), N1-addition (B), fraction of sequences with no N1-addition (C), negative CDRH3 charges (D), positive charges (E), average KD index (F), fractions of charged and hydrophobic CDRH3s calculated based on individual KD indices (G), and total CDRH3 amino acid usage (H).

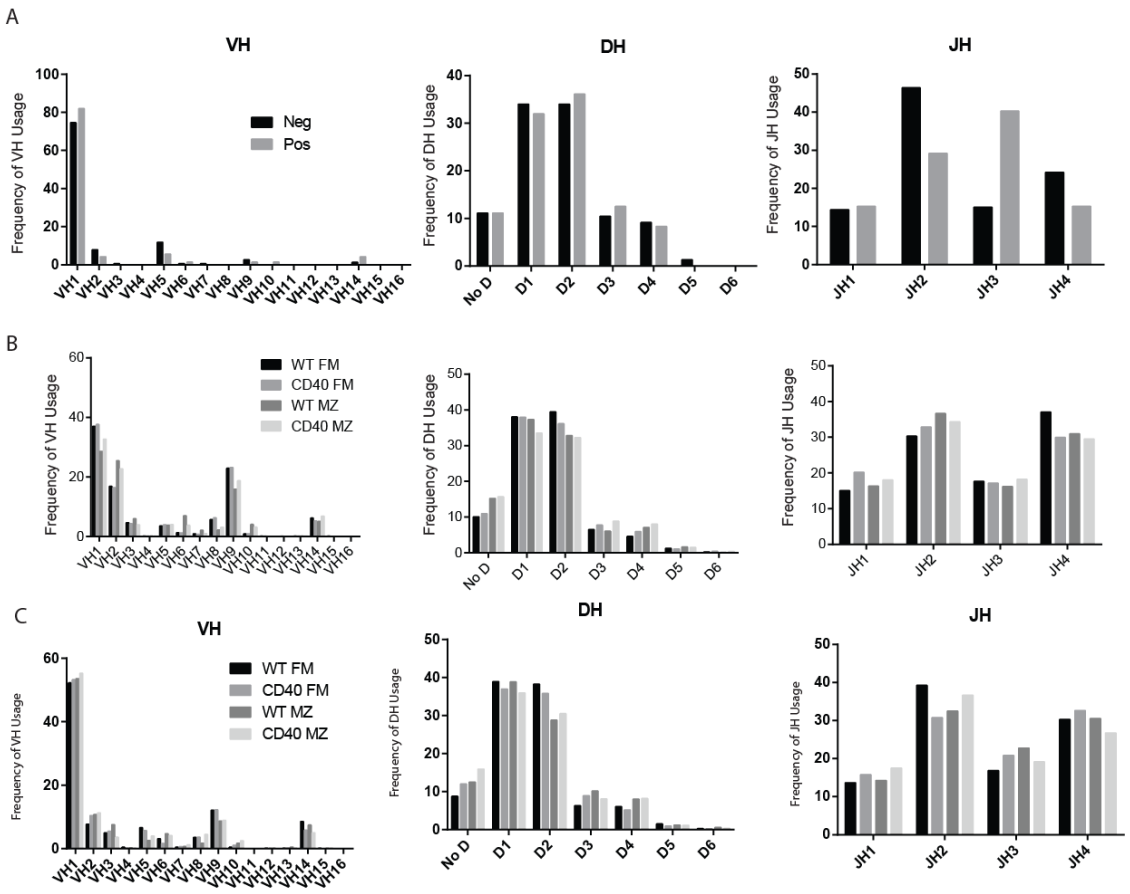

Figure 13. VDJ usage frequencies in IgH sequences from (A) recombinant BCR clones sorted based on ANA-reactivity, (B) WT and CD40-/- mice, and (C) WT/CD40-/- mixed BM chimeras.

Reduced VDJ Combinatorial Diversity in Absence of CD40

Based on the model that CD40 promotes survival and development of transitional cells, we wanted to assess total BCR sequence diversity in the absence of CD40. To accomplish this, we crossed CD40-/- mice to Vk8-transgenic mice to obtain a model with restricted light chain rearrangement so that heavy chain variability accounts for the vast majority of total BCR diversity. Total splenic B cells were isolated from Vk8-tg and Vk8xCD40-/- mice and BCR sequence data was obtained as described above. One noticeable difference was found in CDRH3

characteristics, the Vk8CD40 BCRs had a small but significant increase in N1-addition compared to Vk8 (Figure 15). To evaluate BCR diversity, we used tools developed in ecology to analyze species abundance distributions. We did not obtain sufficient sequence data to evaluate full heavy chain clonal diversity; instead, sequence data was organized based on VDJ combinations alone. An empirical cumulative distribution function depicts VDJ abundance in Vk8-tg and Vk8xCD40-/- B cells, demonstrating that most VDJ combinations are present at low abundance while very few VDJ combinations are highly abundant (Figure 14D). Compared to Vk8-tg, the Vk8xCD40-/- distribution reflects fewer rare VDJ combinations and a slightly more even distribution of most VDJ combinations. Rarefaction analysis was used to assess the accumulation of VDJ combinations with increasing depth of sequencing, demonstrating that both data sets are approaching a theoretical VDJ saturation, with the Vk8CD40-/- sample appearing to have a lower asymptote reflecting fewer total VDJ combinations (Figure 14E). Finally, the Species Prediction and Diversity Estimation (SPADE) program was used to calculate 0, 1st, and 2nd order true diversity indices for each population[63]. 0 order diversity was calculated using the Chao-1 estimator[64], and can be interpreted as the predicted total number of VDJ combinations in the sampled subsets. This value was 5,513 for Vk8-tg mice and 4,293 for Vk8xCD40-/- mice, predicting that the sampled Vk8-tg spleens contain approximately 25% of possible VDJ combinations, and that the CD40-deficienct Vk8-tg mice had about 1,000 fewer VDJ combinations (Figure 14F). The exponential of Shannon entropy and inverse of Simpson's index were used to calculate 1st and 2nd order diversity, respectively, both of which show slightly increased higher-order diversity in Vk8xCD40-/- mice, indicating a greater number of more abundant VDJ combinations when CD40 is absent. These data are consistent with the idea that

CD40 supports the survival and selection of particular B cells that, based on their BCR, would otherwise not enter mature compartments.

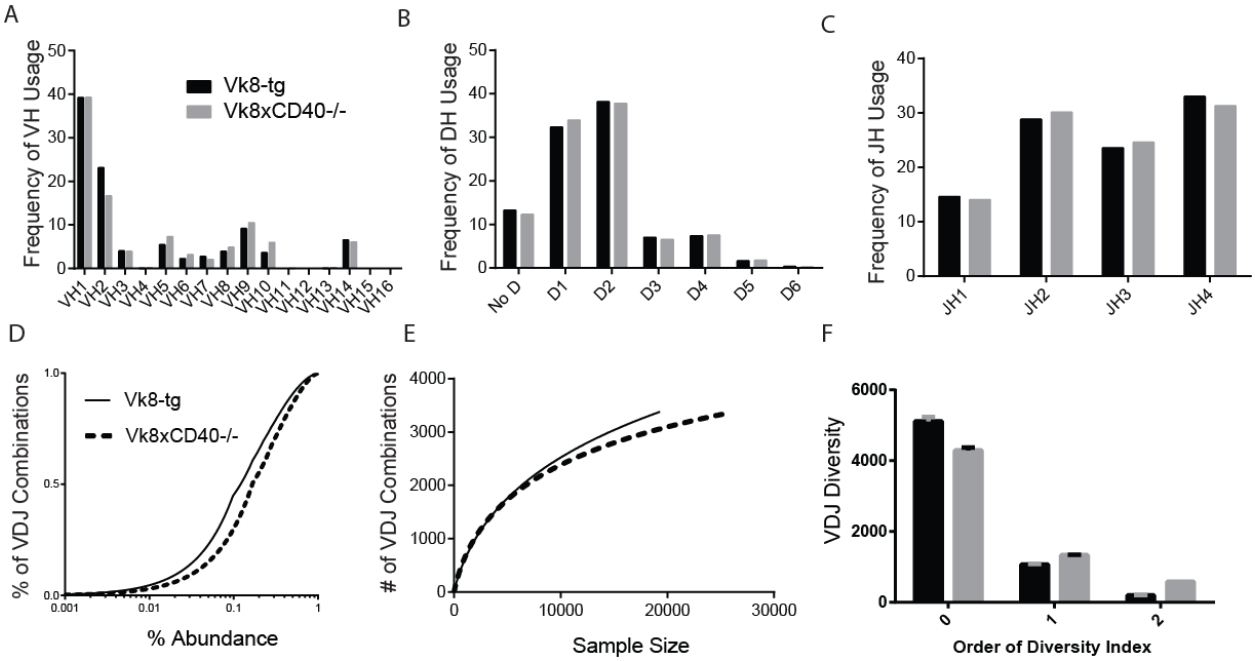

Figure 14. Reduced BCR diversity in the absence of CD40. VDJ usage frequencies in IgH sequences from Vk8 and Vk8CD40-/- mice (A-C). (D) Empirical cumulative distribution function for VDJ combination frequencies in Vk8-tg and Vk8CD40-/- B cells. (E) Individual rarefaction demonstrating the approach to saturation of VDJ combinatorial diversity as sequencing depth increases. (F) Diversity index calculations using SPADE.

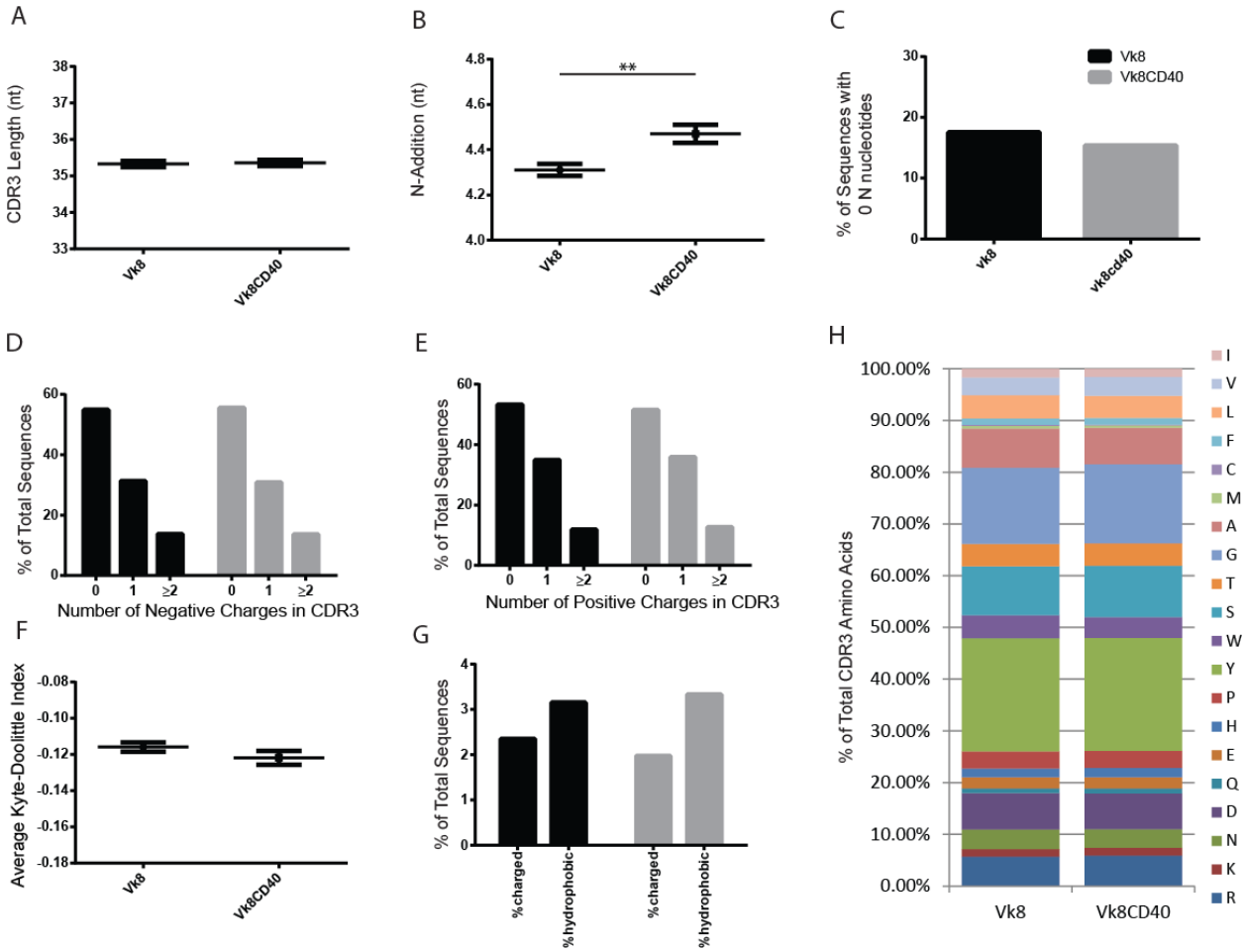

Figure 15. High throughput BCR heavy chain sequencing of Vk8-tg and Vk8xCD40-/- B cells. Analysis includes CDRH3 length (A), N1-addition (B), fraction of sequences with no N1-addition (C), negative CDRH3 charges (D), positive charges (E), average KD index (F), fractions of charged and hydrophobic CDRH3s calculated based on individual KD indices (G), and total CDRH3 amino acid usage (H).

2.3 Discussion

Peripheral selection of developing B cells is a critical step in the formation of a mature B cell repertoire that is capable of protecting from infection and mediating necessary homeostatic functions, but also presents minimal risk of autoreactivity. BCR signals and BAFF are well appreciated as critical regulators of peripheral B cell survival, although the role of antigen-

engagement remains controversial. We present data suggesting the additional involvement of CD40, through interaction with CD40L-expressing naïve CD4+ T cells, in the survival and developmental progression of transitional B cells.

Transitional B cells are particularly sensitive to the signals driving homeostatic proliferation (HP) in a lymphopenic environment, and therefore we used HP to look for novel contributors to peripheral B cell selection. Previous studies have demonstrated roles for Btk and BAFF in driving B cell HP. Here, we demonstrate that engagement of CD40 by CD40L on CD4+ T cells makes a major contribution to lymphopenia-induced B cell HP, as absence of these components results in decreased proliferation and stunted phenotypic changes common to HP. This process was proposed to be T cell independent in the past based on the demonstration of higher HP when transferring WT B cells into SCID vs. into XID recipient mice[65]. However, while XID mice have reduced B cell numbers sufficient to drive B cell HP, they still have a substantial number of mature peripheral B cells. In contrast, SCID mice lack B cells, and this likely explains the greater level of HP relative to XID recipients. We agree that T cells are not absolutely required for HP, but propose that when present they contribute significantly to the proliferative response to B cell lymphopenia. As a result, lacking naïve T cell provision of CD40L may result in a decreased rate, and altered outcome, of B cell reconstitution following any setting of B cell lymphopenia, including certain infections and post-HSC transplant. Consistent with this idea, preliminary data in our lab measuring B cell reconstitution rates in response to sublethal irradiation demonstrates fewer B cells at multiple time points when CD4+ T cells are depleted. A recent study also determined that B cell maturation in a humanized mouse model was less efficient in the absence of T cells[57].

Btk has been proposed to serve its function during HP either through BCR signaling or through possible TLR engagement. We tested these ideas by evaluating HP with MyD88-/- and TRIF-/- donor B cells, neither of which had any observable effect. As the role of Btk is thus most likely through BCR signaling, we sought to determine whether antigen-induced signals drive B cell HP. When M167 transgenic mice were used as donors, Id+ PC-specific B cells clearly divided to a greater extent than Id- cells, and, most intriguingly, removal of CD4+ T cells only impacted Id- B cells. These data suggest that either T cell help or antigen-induced BCR signaling is sufficient to drive B cell HP.

From this finding, we began to consider a model in which the BCR and CD40 could independently support peripheral B cell development. Consistent with prior studies, in the absence of lymphopenia, CD40-/- mice exhibited no alterations in the numerical composition of the peripheral B cell compartment, and no evidence for alteration in replicative history based upon the KREC assay. The only phenotypic change noticed in CD40-/- mice was a decrease in MHCII surface expression in the MZp subset (Figure 2F); further study is required to determine whether CD40 might play a role in promoting follicular shuttling and antigen presentation in this subset. We next tested the idea that alternative signaling pathways might compensate for the lack of CD40 in supporting B cell development. Serum BAFF levels were elevatied in both CD40-/- and CD40L-/- mice , a finding that mirrored the increase in serum BAFF described in humans lacking CD40L[51]. WT/CD40 mixed BM chimeras were setup to evaluate the development of WT and CD40-deficient B cells in an identical environment.

In contrast to our observations in knock out animal, analysis of WT/CD40-/- mixed BM chimeras demonstrated a robust competitive advantage for CD40-expressing B cells beginning at

the late transitional stage and, most notably, within the MZ subset. While this study focused on events in the periphery, prior work has demonstrated a role for CD40 in BM B cell development[66], and this likely explains why a slightly increased proportion of CD40-/- donor BM was required to establish chimeras with an equal proportion of early transitional cells. Depletion of CD4+ T cells markedly reduced this competitive advantage, particularly in transitional B cells. Using this approach, we observed a modest residual selective advantage for CD40+ cells within the MZ subset- findings that likely reflect either a low level of residual T cells, acquisition of CD40L-expression by non-CD4+ T cells, or the presence of CD40L-expressing myeloid cells. Additional studies are necessary to determine whether certain myeloid CD40L+ subsets support MZ development or survival.

To further investigate how CD40 might cooperate with other key transitional B cell signals, we evaluated the expression of BAFF family receptors in chimeric mice, as the upregulation of BAFFR in particular is important for transitional B cell progression[58]. A striking increase in BAFFR and TACI expression was observed in transitional B cells expressing CD40 compared to CD40-/- cells. Notably, this phenotype was *only* observed in the mixed chimera setting. We hypothesize that this finding reflects a relative increase in access of WT B cells to limited CD40L, a process that promotes competitive selection in the presence of CD40-/- transitional cells. As CD40 engagement of CD40L modulates its expression on naïve CD4+ T cells, the presence of CD40-/- cells may allow a greater level of CD40L to accumulate, resulting in stronger signals delivered to WT cells. Consistent with this idea, the BAFFR phenotype appeared to increase in magnitude as the fraction of CD40-deficient donor BM increased; in other words, as the fraction of WT, CD40-expressing cells goes down, so does competition for CD40L, allowing increased signals for WT cells that results in greater upregulation of BAFFR.

In accord with these observations, BAFFR transcripts were increased in WT T1 B cells in chimera animals, and *in vitro* CD40 stimulation promoted increased BAFFR levels in peripheral B cells. In summary, we propose that CD40 signals promote the transitional B cell developmental program by inducing increased BAFFR expression, leading to enhanced expression of survival-associated transcription factors.

To explore the idea that BCR and CD40 signals cooperate independently to support peripheral B cell development, we tried to evaluate how inhibition of one of these signals affects dependence on the other. Previous work using CD40-deficient *Xid* mice have suggested that decreased BCR signaling increases the dependence on CD40 for B cell development. Our findings extend this work by direct analysis of the role of CD4+ T cells in this process. CD4-depletion in *Xid* and *btk/tec*-deficient mice led to a severe block in developmental progression of transitional B cells. As inhibition of tec-family kinases cannot distinguish between antigen-induced vs. tonic BCR signals, CD40-deficient MD4-transgenic mice were made to evaluate this concept. HEL-specific B cells, without transgenic expression of HEL, have little to no specificity for self, but tonic BCR signaling should be intact. When CD40-deficient MD4-transgenic mice were evaluated, we found significantly decreased numbers of peripheral B cells, demonstrating that in the absence of efficient antigen-induced BCR signals, CD40 is critical for optimal peripheral B cell development.

In contrast to the MD4 model, M167-tg mice have a polyclonal B cell pool with an enriched fraction of Id+ PC-specific cells that are expanded in the late transitional and MZ subsets. The effect of CD40-deficiency on antigen-mediated selection of PC-specific cells was evaluated by creating CD40-/- x M167-tg mice and using mixed BM chimeras generated from

WT and CD40-/- M167-tg donors. An increase in PC-specific cells in both the late transitional and MZ subset when CD40 is absent demonstrates that lack of CD40 can alter antigen-mediated selection of transitional B cells. Interestingly, we also found a decreased number of total FM B cells in CD40-/- x M167-tg mice. While M167-tg mice do undergo light chain rearrangement, their BCR repertoire is still significantly limited by lack of heavy chain rearrangement, and this restriction may result in fewer B cells having a BCR-specificity able to support B cell development in the absence of CD40. These combined findings strongly support the concept that as the BCR repertoire becomes more limited, CD40 plays an increasingly important role in peripheral B cell development.

To directly test this model in a physiologic setting with unrestricted B cell populations, we utilized single-cell BCR cloning and specificity testing. Our combined findings provide the first direct comparative analysis of the specificity of naïve FM and MZ B cell subsets in WT animals and reveal distinct alterations in BCR specificy in the absence of CD40 signals. Compared to the WT FM subset, BCRs derived from WT MZ B cells were significantly enriched for ANA-positive BCRs, a finding that is consistent with previous work suggesting that the MZ subset is enriched for self-antigen specific B cells[67–69]. In CD40-/- mice, we observed an increase in ANA-reactivity in the FM subset and, most notably, we identified a substantial decrease in ANA-reactivity of the MZ subset compared to WT. Interestingly, compared to WT BCRs, dsDNA reactivity was decreased in both FM and MZ subsets from CD40-/- mice. CD40-/- BCRs also exhibited lower reactivity to LPS and insulin- consistent with an overall decrease in polyreactivity. Detailed IFA analysis confirmed the reduction in ANA-reactivity in CD40-/- clones and also demonstrated unique pattern frequencies. Specifically, while nuclear patterns were enriched in WT MZ compared to WT FM, consistent with our dsDNA ELISA data, a

decrease in nuclear pattern (and a concomitant increase in cytoplasmic reactivity) was observed in CD40-/- subsets. These observations demonstrate that WT MZ B cells are enriched for ANA-positive reactivity, but that such cells utilize a more restricted spectrum of specificities implying that a select set of autoreactive specificities directly favors MZ B cell development. In contrast, B cells that express a broader range of BCR specificities, including receptors with modest polyreactivity, enter the FM subset. Loss of CD40-CD40L interaction significantly alters these events leading to: 1) an increased frequency of autoreactive FM B cells; 2) a decreased frequency of autoreactive MZ B cells, and 3) an altered specificity profile of autoreactive B cells in both FM and MZ subsets. Taken together, our findings clearly indicate that deficiency of the CD40 signaling pathway impacts the specificity of the mature B cell repertoire.

Our findings are partially consistent with results obtained from CD40L-deficient humans, but contain several notable differences. The increase in ANA-positive ELISAs in CD40-/- FMs resembles the increase in ANA-reactivity described in mature naïve B cells from CD40L-deficient humans, although lower in magnitude. However, we found lower polyreactivity and nuclear IFA patterns in CD40-/- subsets whereas human CD40L-deficient subsets displayed the opposite, increased polyreactivity and nuclear staining patterns. These differences may be due to the vastly different environmental exposure encountered by humans compared to mice in specific pathogen free conditions, which likely impacts B cell selection. Further, we did not extend our analysis past a young age in mice, and it is likely that the effect of CD40-deficiency becomes greater as mice grow older and BM export of newly formed B cells decreases. Additional specificity tests may shed more light on how selection is altered in the CD40-deficient setting.

To build upon our findings testing the specificity of recombinant antibodies, we also analyzed BCR sequence data derived from these receptors. By sorting sequences based on ANA-reactivity, we identified an increase in positive charges, arginine use, and N-addition in the ANA-positive compared with ANA-negtive BCRs, consistent with previous analyses of other autoreactive receptors[3,61,70]. However, when WT and CD40-/- ANA-positive antibodies were evaluated separately, WT MZ ANA-positive BCRs did not exhibit increased N-addition compared to ANA-negative BCRs. In contrast, CD40-/- MZ ANA-positive BCRs had significantly higher N-addition. These sequence differences further support our observations based on specificity testing suggesting altered selection of BCRs in the absence of CD40. ANA-positive CD40-/- derived antibodies were also enriched for charged CDR3s based on KD index; of note, none of the ANA-positive antibodies were classified as hydrophobic. Because hydrophobic CDR3s are thought to be negatively selected during development[62], the lack of hydrophobic CDRH3s in ANA-positive BCRs suggests that this test does not account for certain autoreactive specificities, warranting the development of further specificity tests. Once recombinant antibodies are characterized with additional specificity tests, it will be informative to continue associating BCR sequence features with particular reactivities.

To expand our analysis of the BCR repertoire to a much larger number of candidate BCRs, we performed high-throughput sequencing of IgH genes in sorted FM and MZ subsets from WT, CD40-/-, and WT/CD40-/- mixed BM chimera mice. We restricted analysis to unique clonotypes to avoid bias from PCR amplification. Consistent with altered BCR-specificity based selection in CD40-deficient setting, we identified key differences in CDRH3 length, N-addition, and KD index values in CD40-deficient BCR sequences. Our analyses of sequences derived from chimeric mice largely resembled those from non-chimeric BCR sequences, with the notable

exception that the WT MZ subset did not have a significantly lower KD index relative to WT FM in chimeras. This may indicate a failure of mixed BM chimeras to completely recapitulate BCR-specificity based selection into the MZ subset, perhaps due to incomplete reconstitution of the full spectrum of BM precursors or altered environmental conditions such as serum BAFF levels. Alternatively, this phenotype may be unique to the situation of a relatively smaller WT transitional subset (because the 90:10 CD40-/-:WT donor BM ratio chimeras were sequenced) outcompeting CD40-/- cells for entry into the MZ. Lastly, analysis of VDJ combinatorial diversity in Vk8-tg WT mice resulted in an estimate of approximately 5,000 VDJ combinations present in splenic B cells. This represents slightly less than 25% of the total number of possible IgH VDJ combinations in C57BL/6 mice. In contrast, Vk8xCD40-/- animals were predicted to have 1,000 fewer VDJ combinations, indicating a restriction of heavy chain diversity in the absence of CD40. Collectively, we interpret data from high throughput sequencing experiments to indicate altered specificity based selection into mature compartments in the absence of CD40, resulting in a reduced BCR diversity, and supporting a model in which B cells with particular BCR specificities require CD40 to complete development in the periphery.

The data presented here argue strongly in favor of a role for T cells and CD40 in peripheral B cell development. Further, B cell reconstitution in response to B cell lymphopenia is predicted to be significantly delayed without a sufficient population of naïve CD4+ T cells providing CD40L signals. Although B cell development can proceed in the absence of CD40, we show here that this setting does not recapitulate normal selection of the BCR repertoire. Importantly, this alteration of BCR diversity may prevent efficient generation of humoral immune responses. For example, many patients have poor responses to pneumococcal vaccines following BM transplant, despite having reconstituted normal B cell numbers[71]. In fact, there is

also an association between decreased pneumococcal response and T cell depletion, which is a common practice during BM transplant to mitigate GVH disease[72]. In addition, altered BCR repertoire in the absence of CD40 signals may predispose to autoimmunity, as hyper-IgM patients lacking CD40L suffer from various autoimmune symptoms[73]. These collective effects should be taken into account when considering treatments that suppress T cells or the CD40 pathway. In addition to blocking T cell help during B cell activation, these therapies will likely perturb B cell development and BCR-specificity based selection. Modulation of CD40 signaling with inhibitors and agonists *in vivo* may also represent a strategy to regulate B cell diversity. This could prove useful in the setting of inefficient vaccines, which may elicit stronger responses if the naïve BCR repertoire can be temporarily expanded.

2.4 Methods

Mice

Ly.5.1^{+} and Ly5.2^{+} C57BL/6, μMT, RagKO, CD40-/-, CD40L-/-, *MyD88*$^{-/-}$, TRIF-/-, Xid, tec/btk DKO, MD4-transgenic, M167-transgenic, and Vk8-transgenic mice were bred and maintained in the SPF animal facility of Seattle Children's Research Institute (Seattle, WA) and handled according to IACUC approved protocols. M167 heavy chain transgenic mice (M167H Tg mice, line U243-4) were provided by J. Kenny and A. Lustig (National Institute of Aging,

Bethesda, MD) and established as a M167H Tg/Tg homozygous breeding colony in the animal facility of the Albert Einstein College of Medicine.

Reagents and Antibodies

Anti-murine antibodies used in this study include Ly5.1 (A20), Ly5.2 (RA3-6B2), AA4.1, and CD62L (MEL-14; eBioscience); CD24 (M1/69), CD21 (7G6), B220 (RA3-6B2), IgD (11-26C.2A), CD4(RM4-5) from BD Biosciences; BAFF-R (204406) and TACI (R&D Systems) BP1 (FG35.4), CD25 (PC61), CD62L (MEC-14), CD11c (N418), Gr-1 (RB6-8C5), CD23 (B3B4) from Caltag; IgM (1B4B1), Kappa (187.1), Lambda (JC5-1), goat anti mouse IgG-, IgG2b-, IgG2c-, IgG3- HRP conjugated and SA-HRP conjugated from Southern Biotechnology; CD19 (ID3), NK.1 (PK136), IgM^a (DS-1), CD8a (53-6.7) from BioLegend; and Cy5 anti-rabbit polyclonal IgG from Jackson ImmunoResearch.

Flow Cytometry and Cell Sorting

As previously described[10,74], single cell suspensions from BM, peripheral blood and spleen were incubated with fluorescently-labeled antibodies, data collected on a FACSCalibur or LSR II (BD Biosciences) and analyzed using FlowJo software (Treestar Inc). Cell sorting was done using an Aria II, sort purities were >90% in all studies.

Adoptive cell transfer.

CD43-depleted B cells or sorted B cell subsets were incubated with 0.05 μM CFSE at 37°C for 8 min, washed three times with complete media, and then washed with PBS. In experiments using "feeder" B cells, CD43-depleted splenic B cells were prepared and mixed with sorted B cells. For transfer of sorted T1 or $CD21^{int}$ T2 B cells, a total number of 15×10^6 cells in 250 μl PBS were injected by tail vein into μMT or C57BL/6 mice.

T Cell Depletion

Mice were treated weekly with ip injection of 250 μg anti-CD4 (GK1.5) or isotype control (rat IgG2b) antibody (UCSF Antibody Core).

Bone Marrow Transplantation

BM was harvested from WT, $CD40^{-/-}$, M167-tg, or CD40-/-xM167-tg mice. BM from CD40-/- and WT mice was mixed at either a 65:35 or 90:10 ratio, and 5 x 10^6 total BM cells in PBS were injected i.v. into lethally irradiated (1050 cGy) μMT recipients. BM from M167-tg and CD40-/-xM167-tg were mixed at a 50:50 ratio.

Real-time PCR.

Sorted B cell populations were pelleted and frozen at −80°C. RNA was isolated using the RNeasy Micro kit (QIAGEN) and converted into cDNA by reverse transcription (Superscript II; Invitrogen) according to the manufacturer's instructions. Real-time PCR on cDNA was performed using the iCycler real-time PCR detection system with IQ SYBR Green Supermix

(Bio-Rad Laboratories) according to the manufacturer's instructions. Ratios were calculated with mouse β2-microglobulin as housekeeping control. All real-time PCR analysis shown includes at least three independent experiments. Primer sequences used include the following: Hes1-5′GAGAAGAGGCGAAGGGCAAGAAT; Hes1-3′ GAGGTGCTTCACAGTCA; Deltex1-5′ CGGACATTTGAGACCCACTT; Deltex1-3′ CCACTTTCAAGCAGGGAGAA; CyclinD2-5′ GCCAAGATCACCCACACT; and CyclinD2-3′ GCTGCTCTTGACGGAACT. To determine the replication history of B cells, genomic DNA was isolated from sorted populations and the ratio between the κ-deleting rearrangement (IRS1 to RS) and excision circles (KREC) was determined by TaqMan-based (Applied Biosystems) real-time PCR, as previously described[28].

BrdU incorporation.

Continuous in vivo BrdU labeling was performed by feeding mice BrdU via the drinking water containing 1 μg/ml BrdU (Sigma-Aldrich) and 10% sucrose. Mice were killed at indicated time points, and splenocytes were surface stained to identify splenic B cell subsets. Cells were then fixed and permeabilized, treated with DNase, and stained with anti-BrdU FITC (BrdU kit from BD Biosciences).

In Vitro Cell Activation Studies

In vitro activation studies were performed as previously described[8,10]. Stimulating treatments included agonistic CD40 antibody (10uM) and anti-IgM (10uM).

Single-Cell BCR Cloning

cDNA was obtained using Thermo Maxima First Strand cDNA Kit, supplemented with .5% (v/v) Igepal CA-630 (Sigma-Aldrich) to a final volume of 12 ul/well. *Igh*, *Igk*, and *Igl* gene transcripts were amplified independently from cDNA with nested PCR or semi-nested PCR (*Igl*) using DreamTaq (Thermo), 2.5 ul of cDNA as template, and 400 nM of primers previously published (*Igh* from Wilson, and *Igk* and *Igk* from Tiller et al., 2009) to a final volume of 25 ul/well. First round PCR was performed at 94 C for 5 minutes, followed by 15 cycles of 94 C for 30s, 47 C(*Igk*) or 51 C(*Igh*) or 53 C(*Igl*) for 30s, 72 C for 55s, followed by 30 cycles of 94 C for 30s, 50 C(*Igk*) or 56 C(*Igh*) or 58 C(*Igl*) for 30s, 72 C for 55s, and a final incubation of 72 C for 8 min. Round 2 PCR and sequencing, gene analysis, and Ig gene-specific PCR was performed under settings previously described (Tiller et al., 2009). PCR products were cloned into expression vectors with human *IGG1*, *IGK* or *IGL* constant regions (Smith et al., 2009). Double restriction digests of Ig gene-specific PCR products were performed using 3 ul of unpurified PCR product in a 20 ul final volume using FastDigest (Thermo) enzymes of AgeI and SalI (*Igh*), BsiWI (*Igk*), or MscI (*Igl*) at the manufacturer's suggested time. Digestions were purified using GeneJET PCR Purification Kit (Thermo). Ligations were performed using Rapid Ligation Kit (Thermo) and 12.5 ng of purified digestions and 50 ng of linearized vector at a final volume of 10 ul. Transformations were completed using 5 ul of unpurified ligation reactions and competent *E. coli* DH5a bacteria, heat shocked at 42 C and plated onto LB carbenicillin plates (100ug/ml). Colonies were streaked onto a plate and then sequenced directly after placement in 6 ul of water (HyClone) and heated for five cycles of 95 C for 1.5 min and 4 C for 1 min, followed by 95 C for 3 min. Heated water colonies were used as template and sequenced. Sequences were analyzed to match original round 2 gene segment PCR sequences without mutation. Positive colonies were

grown in 3 ml LB (EMD) and .1mg/ml carbenicillin (Bioline) for 16 h at 37 C. Plasmid DNA was purified using Qiaprep Miniprep columns in a Qiacube (Qiagen). HEK293T cells in 100 mm plates at 70-80% confluency were transiently transfected with 4 ug of each heavy and light chain plasmid and 32 ug of polyethyleneimine in an 888 ul solution of 10 mM HEPES (Fisher) and 150 mM NaCl (EMD) (pH 7.05). Cells were cultured with serum-free media and supernatant extracted as previously described (Smith et al., 2009). Antibodies were purified using 400 ul Pierce Protein A Agarose beads (Thermo) in 5 ml polypropylene gravity columns (Thermo). Antibodies were washed with 1M NaCl (EMD) and 1X PBS (HyClone) before being eluted with .1M Glycine-HCl (pH 2.7, EMD) and neutralized with 1M TrisHCl (EMD) to a pH of 7-7.4 and preserved with 0.05% wt/v NaN_3 (Sigma-Aldrich). Purified antibodies were quantified four times and averaged using the Nanodrop2000 Spectrophotometer (Thermo).

ELISA and ANA Screen

Antibodies were tested for ANA reactivity (Biorad) per manufacturer's protocol at 100 ug/ml and serially diluted 1:2, 1:4, and 1:10. Reactivity with insulin, LPS, PC-12, and dsDNA (Sigma-Aldrich) at 100ug/ml ug, were tested by ELISA with antibodies at 10 ug/ml and serially diluted 1:5, 1:25, and 1:125. For ELISAs, 96 well Immuno plates (Nunc) were pre-coated (10mg/ml) overnight at 4ºC with dsDNA, insulin, LPS, MDA-BSA, or MDA-LDL (Academy Bio-Medical; 20P-MD L-105). After blocking with 0.5% BSA/PBS, recombinant antibodies were added, and plates were incubated with mouse anti-human IgG-HRP (Southern Biotechnology Associates) (1:2,000 dilution). Peroxidase reactions were developed using OptEIA TMB substrate (BD Biosciences). OD450 was determined using a Victor 3 plate reader (PerkinElmer) and displayed

as average value of 3 wells. To identify high affinity anti-dsDNA antibodies, following sera addition, plates were incubated with 0.3M NaCl for 5 min. prior to performing the remainder of the above protocol. ANA screens were performed using BD EIA kit according to manufacturer instructions.

HEp-2 IFA Tests

BD IFA slides were used according to manufacturer instructions. Briefly, slides were incubated with antibodies for 30 minutes, followed by a 10 minute wash in PBS. Next, slides were incubated with FITC-conjugated anti-human IgG for 30 minutes, followed by a second 10 minute wash. Coverslips were then added with mounting media, and images were acquired using a Leica DM6000B microscope, Leica DFL300 FX camera, and Leica Application Suite Advanced Fluorescence software.

High Throughput BCR Sequencing

Total RNA was obtained from purified B cells using RNeasy reagents (Qiagen). Heavy chain cDNAs from each sample were synthesized using a 5′-RACE kit (Ambion), according to the manufacturer's protocol. For reverse transcriptase and PCR, Transcriptor High Fidelity (Roche) and Phusion Hot Start (New England Biolabs) was used, respectively. A triple nested primer strategy was used to amplify heavy chain IgM and IgD genes. An outer IgM and IgD constant region-specific primer was used for the RT reaction, a middle constant region IgM and IgD primer was used for the first round of PCR, and an innermost constant-region IgM and IgD

primer (adjacent to the J segment of the variable region) was used for the second PCR round. 454 adapters were included in the primers during second round PCR, and a bar-code strategy was used to run multiple samples simultaneously. Sequencing was done at Mycroarray on a GS Junior. Barcoded sequence data was separated using Geneious software, and IMGT/HighVQuest was used for alignment to germline IgH VDJ regions. IgAT software was used to generate descriptive statistics and calculation of CDR3 characteristics. Software from Ramit Mehr's lab was used for clonal analysis and combination of clones from various samples. SPADE software was used for calculation of diversity indices and PAST software used for individual sample rarefaction.

Statistical Evaluation

P-values were calculated using the two-tailed Student's t-test, ANOVA, or Fisher's exact test, where appropriate.

Chapter III: WASp-deficient B cells play a critical, cell intrinsic role in triggering autoimmunity

3.1 Introduction

Wiskott-Aldrich syndrome (WAS) is an X-linked immunodeficiency characterized by recurrent infections, abnormal lymphocyte function, thrombocytopenia and eczema, as well as a significantly increased risk for systemic autoimmunity[75]. The affected gene, Wiskott-Aldrich syndrome protein (*WASp)*, encodes a multidomain protein, WASp, exclusively expressed in hematopoietic cells where it is involved in signal transduction to the actin cytoskeleton[76]. Signaling defects resulting from WASp deficiency have been analyzed most extensively in T lymphocytes. Following TCR ligation, *WASp*$^{-/-}$ T cells show decreased Ca^{2+} flux, reduced actin polymerization, diminished antigen receptor (AR) endocytosis, and abnormal proliferation due to deficient IL-2 secretion[77]. WASp deficiency impacts additional lineages including B cells, NKT cells, neutrophils, dendritic cells (DCs), monocytes, and platelets. These defects may contribute independently or in combination to mediate the complex clinical features of WAS.

The functional defect that promotes autoimmunity in WAS is of great interest. Prevalence of autoimmune symptoms in WAS is high; in one study over 70% of patients had at least one autoimmune episode including autoimmune cytopenias, arthritis, vasculitis, or renal disease, and many of these patients suffered from recurrent or multiple autoimmune features[75,78]. Autoimmunity typically presents early in life, is often refractory to therapy and is associated with a worse clinical prognosis[48]. Consistent with these observations in patients, *WASp*$^{-/-}$ mice develop high titer anti-double-stranded (ds) DNA antibodies early in life[79]. However, only

minimal autoantibody-mediated disease features have been reported in this strain[47,79], suggesting such antibodies are relatively non-pathogenic.

Interestingly, a significant proportion of WAS patients treated using stem cell transplantation develop systemic autoimmunity not predicted by pre-transplant disease features[80]. This complication is strongly associated with mixed/split chimerism, indicating that residual WAS mutant lymphocytes can mediate autoimmune disease despite the coexistence of normal donor cells. These data imply that, in a chimeric setting, dysregulated function within a candidate lymphoid population is unmasked by restoration of functional activity within another hematopoietic lineage(s).

Notably, several recent studies including work from our laboratory demonstrated defects in both homeostasis and function of *WASp*$^{-/-}$ regulatory T cells (Tregs). These observations suggested that altered Treg activity might predispose to autoantibody production in *WASp*$^{-/-}$ mice[79,81,82]. In the current study, we made the surprising observation that female *WASp*$^{+/-}$ mice generate anti-nuclear antibodies at rates and titers equivalent to *WASp*$^{-/-}$ mice, even though carrier animals have an essentially normal Treg compartment due to a strong selective advantage for WASp+ Tregs. Based upon this observation, we tested the alternative hypothesis that autoantibody production in *WASp*$^{-/-}$ mice results from a B cell intrinsic defect. Consistent with this idea, we show that in the setting of WT T cells, DCs and other hematopoietic lineages, *WASp*$^{-/-}$ B cells are necessary and sufficient for development of autoantibodies. Collectively, our results suggest that BCR/TLR co-engagement on *WASp*$^{-/-}$ B cells mediates loss of tolerance which, in the presence of WT T cells, drives development of severe autoimmune disease.

3.2 Results

WASp+/- carrier females develop high titer anti-dsDNA antibodies

We previously reported that WASp is essential for normal Treg homeostasis [79], leading to the hypothesis that autoantibody production in *WASp*$^{-/-}$ mice results from a lack of Treg-mediated immunosuppression. To address this idea, we analyzed WASp+/- female mice in which more than 90% of peripheral Tregs are WASp^{+} due to a selective advantage over Tregs expressing the mutated X-linked WASp allele [79]. Surprisingly, we found no difference in the amount of anti-dsDNA autoantibodies between *WASp*$^{-/-}$ and *WASp*$^{+/-}$ mice (Figure 16A). Tregs isolated from WASp+/- mice were functionally indistinguishable from WT Tregs in suppressing T cell proliferation (Figure 17A). Collectively, these data imply that impaired Treg function is unlikely to explain the development of autoantibodies in *WASp*$^{-/-}$ mice.

WASp$^{-/-}$ B cells are sufficient for high affinity, class-switched autoantibody production

We next sought to determine if autoantibody production in *WASp*$^{-/-}$ mice is a B cell intrinsic phenomenon using a mixed bone marrow (BM) chimera model. Of the multiple strategies we tested, optimal B cell reconstitution with minimal mixed chimerism in other hematopoietic lineages was achieved by transplanting a mix of 20% *WASp*$^{-/-}$ or WT BM with 80% μMT BM into lethally (1050 cGy) irradiated μMT recipients. To eliminate transfer of previously activated B cell populations, we utilized BM from very young donors (4-5 wk) depleted of plasma B cells. Donor sera were also prescreened to verify absence of dsDNA antibodies. Following reconstitution, B cells were entirely donor derived (*WASp*$^{-/-}$ or WT), greater than 95% of CD3^{+} T cells and CD4^{+} Foxp3^{+} Treg cells were WASp^{+}, and >85% of both NK and myeloid cells were WASp^{+} (Supplementary Figure 16B). Consistent with a B cell intrinsic role for WASp,

recipients of *WASp*$^{-/-}$ BM cells (hereafter referred to as *WASp*$^{-/-}$ chimeras) developed high titers of anti-dsDNA autoantibodies whereas WT recipients did not (Figure 16B). A proportion of *WASp*$^{-/-}$ chimeras did not have high anti-dsDNA antibody titers at 16 weeks post-transplant, but this proportion decreased when mice were analyzed at later time points (data not shown), suggesting that *WASp*$^{-/-}$ chimeras experience a progressive loss in B cell tolerance as they age. Because *WASp*$^{-/-}$ T cells are functionally abnormal we predicted that the presence of WT T cells in *WASp*$^{-/-}$ chimeras may drive more efficient germinal center (GC) responses, resulting in class switch recombination (CSR) and affinity maturation. To test this idea,

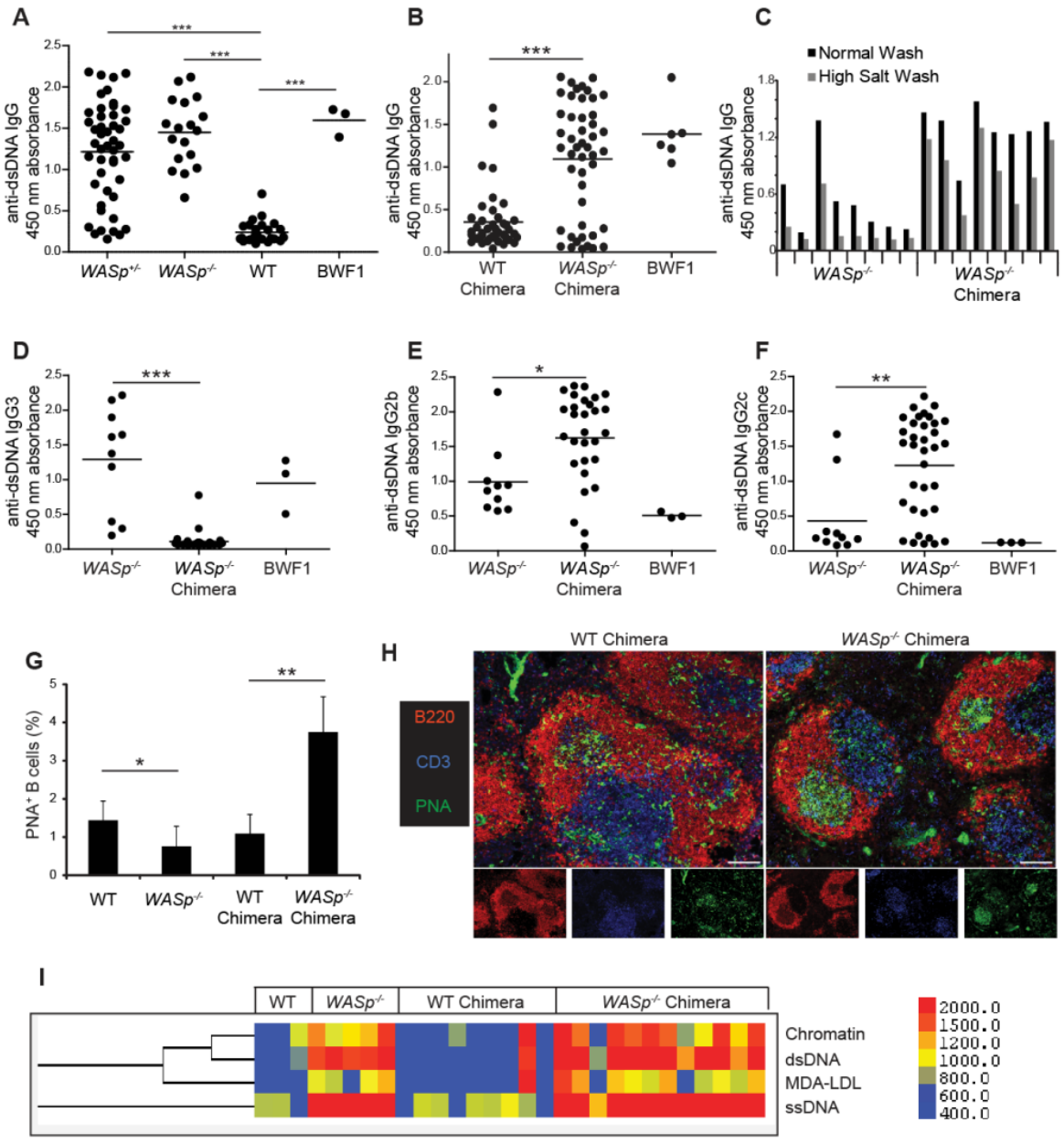

Figure 16. *WASp*$^{-/-}$ B cells are sufficient for high affinity, class-switched autoantibody production and spontaneous germinal center formation. IgG anti-dsDNA autoantibody ELISAs in (A) 6.5-12 mo old female *WASp*$^{+/-}$, *WASp*$^{-/-}$ and WT mice; and (B) WT and *WASp*$^{-/-}$ chimeras at 16 wk post-transplant. BWF1: lupus prone positive control, NZB/NZW- F1, 8 mo old. Sera diluted 1:200; each dot represents an individual animal. (C) ELISAs with low vs. high stringency washing conditions used to detect high affinity IgG anti-dsDNA antibodies in *WASp*$^{-/-}$ and *WASp*$^{-/-}$ chimeric mice (12 week old or 12 weeks post-transplant). Each pair of bars represents an individual animal. (D-F) ELISAs to detect IgG subclass-specific anti-dsDNA antibodies. (*WASp*$^{-/-}$ chimeras (n=29), *WASp*$^{-/-}$ mice (n=10); 4 mo after transplant or 4 mo old, respectively). (G) Percentage of splenic B cells staining positive for PNA by flow cytometry in

6-8 mo old WT (n=7) and *WASp*$^{-/-}$ (n=7) mice as well as WT (n=5) and *WASp*$^{-/-}$ (n=4) BM chimeras 6-8 mo post-transplant. (H) Immunofluorescent staining of splenic sections from BM chimeras showing representative follicles using B220 (red) CD3 (blue) and PNA (green); 10x objective used for image capture, scale bars = 100 μm. (I) Antigen microarray showing IgG reactivity of WT, *WASp*$^{-/-}$, WT chimera, and *WASp*$^{-/-}$ chimera sera with ssDNA, dsDNA, chromatin and malondialdehyde substituted low-density lipoprotein (MDA-LDL). Sera from WT and *WASp*$^{-/-}$ mice (1 yo) and chimeric mice (6 mo post-transplant). Scale shows digital fluorescence intensity units; 600 represents threshold for reactivity as described in methods. These data are representative of 4 independent experiments with 20-30 mice per experiment. *$P < 0.05$, **$P < 0.005$, ***$P < 0.0005$.

we evaluated anti-dsDNA autoantibody affinity using high and low stringency ELISA washing conditions. Anti-dsDNA autoantibodies were detected after high-stringency washing in *WASp*$^{-/-}$ chimeras as early as 12 weeks post-transplant, compared to a lack of consistent high-titer anti-dsDNA autoantibody production in 12 week old *WASp*$^{-/-}$ mice (Figure 16C). Next, we analyzed the subclass of anti-dsDNA autoantibodies. Strikingly, *WASp*$^{-/-}$ mice generated primarily IgG3 autoantibodies, whereas *WASp*$^{-/-}$ chimeras generated IgG2b and IgG2c, but little or no IgG3, anti-dsDNA autoantibodies (Figure 16D-F). Consistent with our hypothesis that WT T cells drive GC formation in *WASp*$^{-/-}$ chimeras, we found greater numbers of B220+PNA+ splenocytes in *WASp*$^{-/-}$ compared to WT chimeras (Figure 16G). Additionally, histological analysis of splenic sections revealed consistently larger and more frequent PNA+ GCs in *WASp*$^{-/-}$ versus WT chimeras (Figure 16H). Widespread spontaneous GC formation, as detected in *WASp*$^{-/-}$ chimeras, is a characteristic feature of several previously described autoimmune-susceptible mouse strains [83].

To determine whether other autoantibody specificities produced by *WASp*$^{-/-}$ mice are recapitulated in *WASp*$^{-/-}$ chimeras, custom microarray slides were prepared with various DNA-associated antigens as well as apoptotic cell epitopes and screened using sera from WT, *WASp*$^{-/-}$, WT chimera, and *WASp*$^{-/-}$ chimera mice. IgG antibody reactivity to chromatin, dsDNA, ssDNA,

and the apoptosis associated neo-determinant, malondialdehyde (MDA) as a conjugate with low density lipoprotein (MDA-LDL), was detected in both *WASp*$^{-/-}$ and *WASp*$^{-/-}$ chimera sera, but not in WT mice or WT chimeras (Figure 16I). ELISAs confirmed the presence of anti-MDA-LDL antibodies in *WASp*$^{-/-}$ mice and chimeras, and further subclass analysis revealed that, in a similar pattern to anti-dsDNA antibodies, *WASp*$^{-/-}$ mice produced primarily IgG3 antibodies whereas *WASp*$^{-/-}$ chimeras produced IgG2b and IgG2c anti-MDA-LDL antibodies (Figure 18).

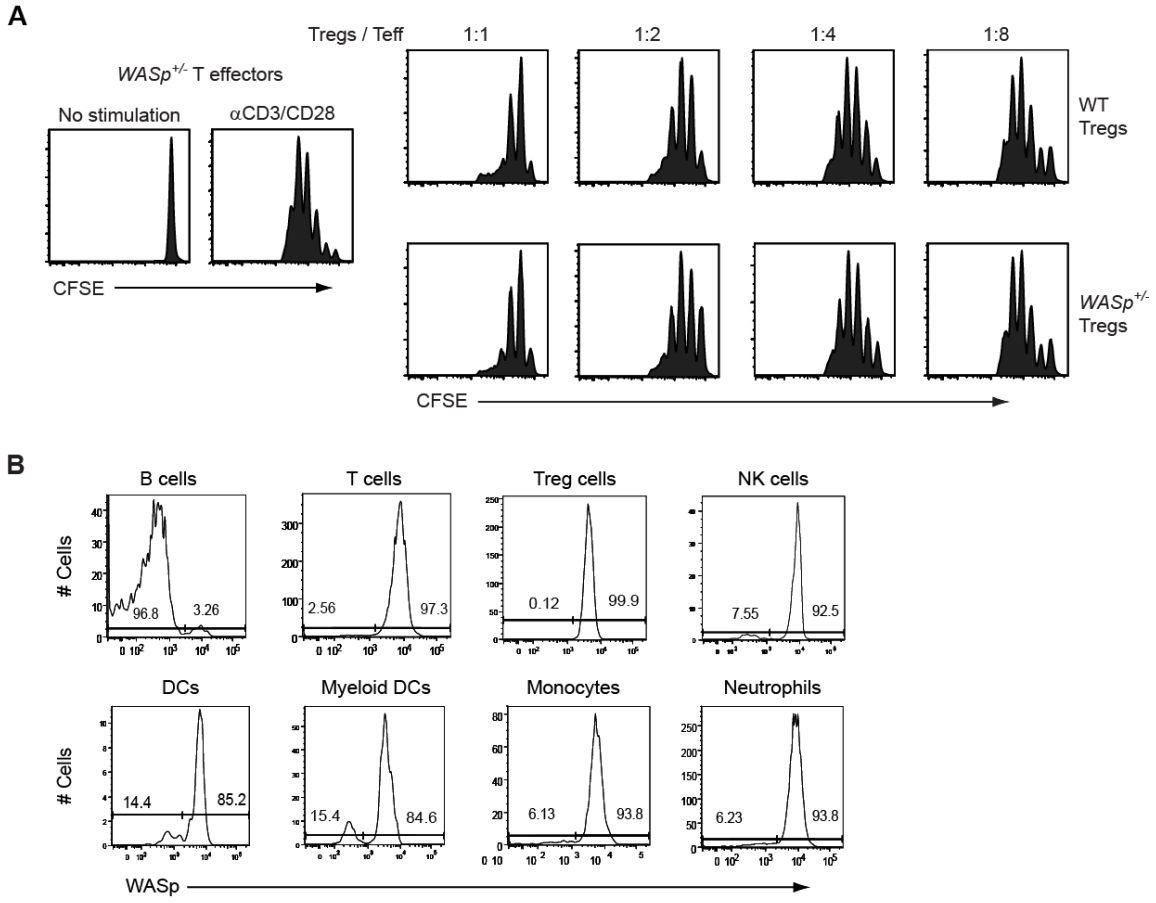

Figure 17. Functional analysis of WASp+/- Tregs and relative chimerism of splenic populations in transplanted mice. (A) Treg suppression assay. $CD4^{+}CD25^{-}$ effector T cells (Teff) were isolated from WASp+/- mice, labeled with CFSE and cultured with WT or WASp+/- Tregs at Treg/Teff ratios noted in the presence of irradiated APCs. Cultures were stimulated with anti-CD3 (3mg/ml) and anti-CD28 (1mg/ml) for 110 hr. Data are representative of two experiments. (B) Representative data showing relative WASp intracellular staining in hematopoietic-derived lineages in BM chimeras generated following transplantation of 20:80 cell

mixtures of *WASp*$^{-/-}$ and μMT BM into lethally irradiated μMT recipients. Data are representative of 4 independent experiments. Markers used for gating: B cells: B220^{+}CD19^{+}, T cells: CD3^{+}, Treg cells: CD4^{+}Foxp3^{+}, NK cells: CD3^{-}NK1.1^{+}, DCs: CD3^{-}CD11c^{+}CD11b$^{low/neg}$, Myeloid DCs: CD3^{-}CD11c^{+}CD11b^{+}, Monocytes: CD11b^{+}GR1$^{low/neg}$ and Neutrophils: CD11b^{+}Gr1^{+}.

These combined experiments support the conclusion that WASp deficiency in B cells is sufficient for development of high affinity, class-switched DNA and apoptotic antigen specific autoantibodies in the presence of WT-derived hematopoietic cells.

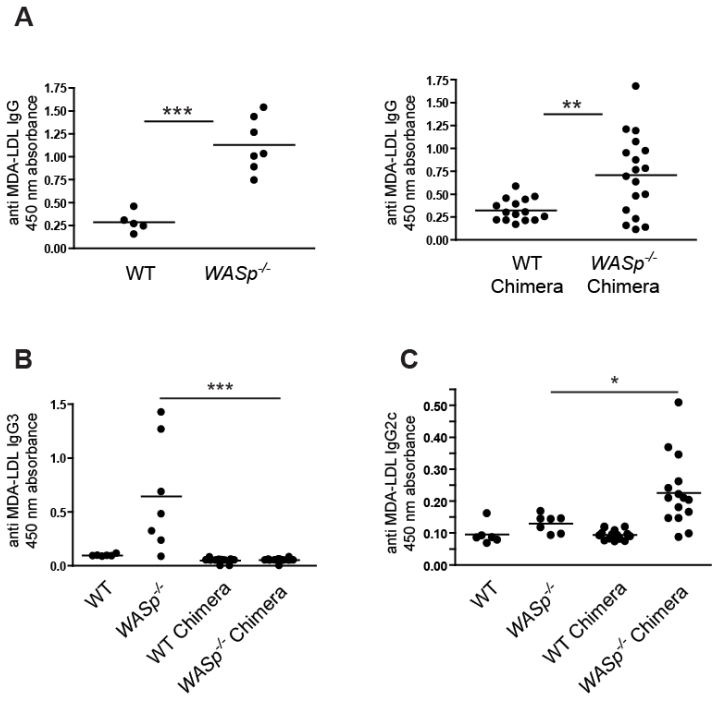

Figure 18. ELISA analysis of MDA-LDL reactivity.

Sera from WT, *WASp*$^{-/-}$, WT chimeric, and *WASp*$^{-/-}$ chimeric mice were tested for reactivity to MDA-LDL using ELISAs specific for IgG (A), IgG3 (B), and IgG2c (C). Data are representative of 2 independent experiments.

***WASp*$^{-/-}$ chimeras develop systemic autoimmunity and exhibit early mortality**

Despite the presence of high titer anti-dsDNA autoantibodies, *WASp*$^{-/-}$ mice on a C57BL/6 background do not develop systemic autoimmune features or increased mortality (data not shown). To assess the longer-term consequences of B cell-specific WASp-deficiency, cohorts of *WASp*$^{-/-}$ vs. WT chimeras were followed for >1yr. Strikingly, *WASp*$^{-/-}$ chimeras exhibited increased mortality beginning at ~7 mo post-transplant with only 50% survival at 12 mo compared with 97% in WT recipients (Figure 19A).

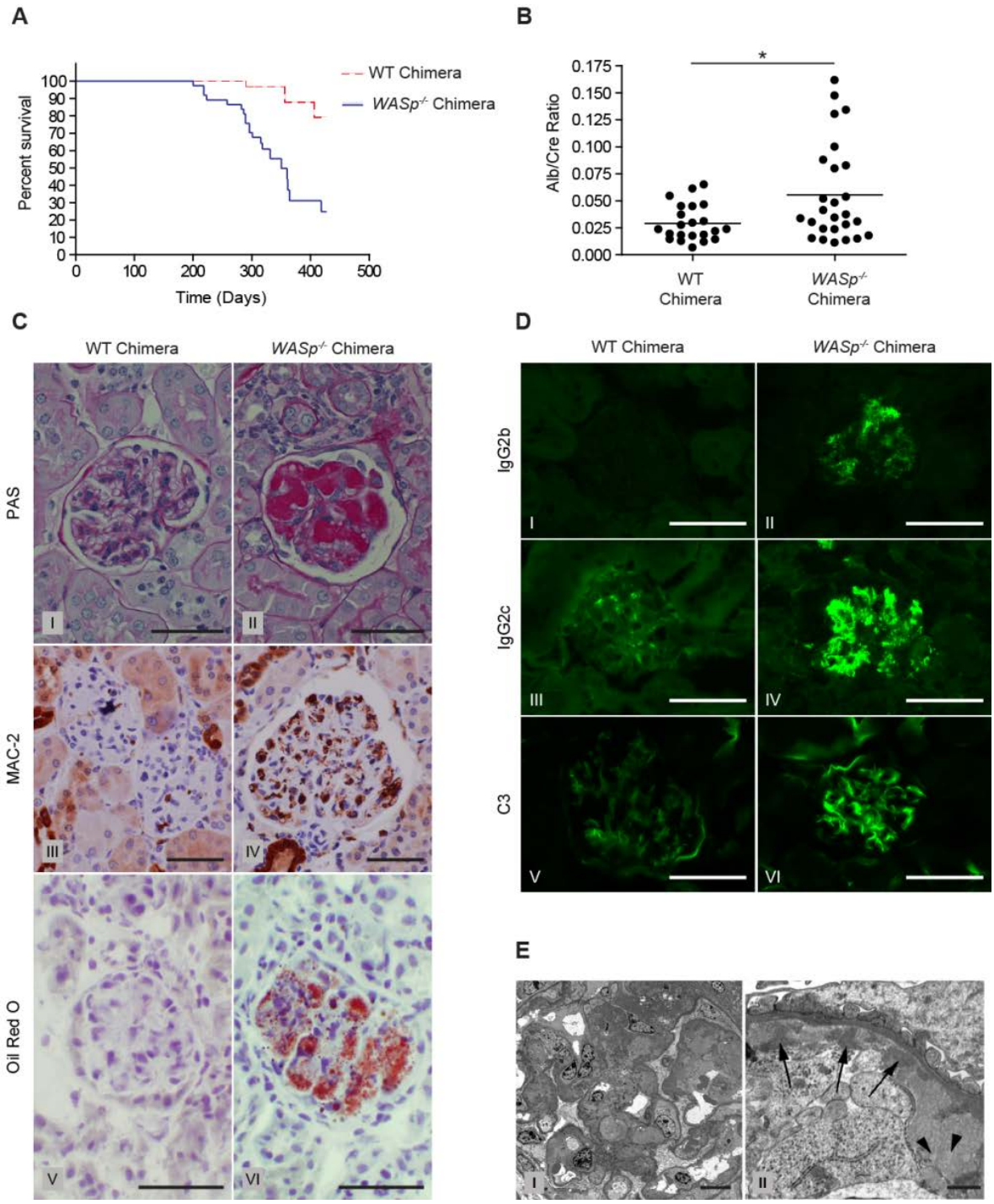

Figure 19. *WASp*$^{-/-}$ chimeras develop systemic autoimmunity and exhibit early mortality. (A) Kaplan-Meier survival curve of WT chimeras (n=37) and *WASp*$^{-/-}$ chimeras (n=31), $P < 0.0005$. (B) Urine albumin:creatinine ratio in BM chimeras at 7-12 months post-transplant, WT chimeras (n=22), *WASp*$^{-/-}$ chimeras (n=26), *$P < 0.05$. (C) Representative glomeruli from WT and *WASp*$^{-/-}$ BM chimeras. PAS, Periodic acid-Schiff stain. Scale bars = 50 μm. (D) Immunofluorescence showing IgG2b and IgG2c subclass antibodies and complement C3

deposited in *WASp*$^{-/-}$ chimera glomeruli. Data in c-d are representative of mice 7 months post-transplant. Scale bars = 50 μm. (E) Electron micrographs of glomeruli of *WASp*$^{-/-}$ chimeras. Left panel (low power; 1600x, scale bar = 10 μm). Right panel (high power; 16,900x, scale bar = 1 μm) shows confluent deposition of large amounts of electron dense material (arrows) characteristic of immune complexes in subendothelial portions of glomerular capillary walls, admixed with aggregates of vesiculated material characteristic of lipoproteins, corresponding to the lipid deposits confirmed by Oil red O staining (arrowheads), (representative of 4 *WASp*$^{-/-}$ chimeras). Data are representative of 4 independent experiments, electron micrographs taken from only one experiment.

To better characterize disease features we monitored renal function and performed extensive histopathological analyses in several cohorts. To screen for renal disease, we measured urine protein/creatinine ratio. *WASp*$^{-/-}$ chimeras developed progressive proteinuria beginning 5-6 mo after transplant (Figure 19B). Next, we analyzed the kidneys of *WASp*$^{-/-}$ chimeras for histological abnormalities and identified widespread glomerular lesions exhibiting prominent accumulations of eosinophilic thrombus-like material within glomerular capillaries, as well as increases in mesangial matrix accumulation, focal mesangiolysis and glomerular basement membrane splitting (Figure 19C II). In contrast, WT chimeras were normal in appearance (Figure 19C I). MAC-2 staining of kidney sections revealed macrophage infiltration of glomeruli from *WASp*$^{-/-}$ but not WT chimeras (Figure 19C III, IV). Notably, oil red O staining of frozen sections identified the presence of neutral lipids within glomeruli of *WASp*$^{-/-}$ chimeras, but not in WT chimeras (Figure 19C V, VI) that appeared to correlate with the intracapillary accumulations of eosinophilic material. Immunofluorescent staining demonstrated deposition of IgG2b, IgG2c, and complement C3 in *WASp*$^{-/-}$ chimera glomeruli (Figure 19D II,IV,VI), whereas less C3 deposition and little to no IgG2b and IgG2c deposition was detected in WT chimeras (Figure 19D I,III,V). However, there were no differences in deposition of IgG, IgA and IgM. Glomerular thrombi appeared moderately electron dense by electron microscopy (Figure 19E, left panel) and

higher magnification analysis revealed focal regions of fibrillar organization, consistent with co-deposited immune complexes (Figure 19E, right panel, arrows). Many of the thrombi had vacuoles of differing sizes that appeared to be lipid or lipoprotein accumulations (Figure 19E, arrowheads). In contrast, liver, lungs, joints, and gastrointestinal tract appeared unaffected in *WASp*$^{-/-}$ chimeras (data not shown). These results demonstrate that *WASp*$^{-/-}$ chimeras develop systemic autoimmune disease characterized by generation of autoantibodies, severe renal histopathology, and early mortality.

WASp -/- B cells are hyper-responsive to key activation signals in vitro and in vivo

We next sought to determine whether *WASp*$^{-/-}$ B cells exhibit an altered response to BCR engagement. *WASp*$^{-/-}$ splenic follicular mature (FM) B cells consistently exhibited a higher peak Ca^{2+} flux in comparison with WT FM B cells after BCR stimulation, a difference most pronounced using lower dose anti-IgM (Figure 20A). IgM surface expression was equivalent or slightly lower in *WASp*$^{-/-}$ B cells, indicating that altered BCR density could not account for our findings (Figure 20A). Experiments using Ca^{2+}-free media and/or the Ca^{2+} ATPase-inhibitor thapsigargin indicated *WASp*$^{-/-}$ FM B cells exhibit enhanced extracellular Ca^{2+} influx after BCR engagement (Figure 20D, Figure 21A).

Next, we evaluated proliferation downstream of BCR engagement by measuring CFSE dilution. We observed increased proliferation in *WASp*$^{-/-}$ FM B cells as compared to WT controls in response to anti-IgM stimulation (Figure 20B). Intriguingly, both LPS and CpG stimulation also lead to increased cell cycling (Figure 20B), indicating that hyper-responsiveness was not limited to BCR engagement. *WASp*$^{-/-}$ B cells also displayed slightly increased CD25 and reduced

CD62L expression compared to WT B cells, consistent with a more activated state post-stimulation (Supplementary Figure 20B). To exclude that these observations were due to altered lymphoid environments, we generated BM chimeras consisting of 50% $Ly5.1^{+}$ WT and 50% $Ly5.2^{+}$ *WASp*$^{-/-}$ cells. Ca^{2+} flux and proliferation experiments using cells isolated from transplanted mice led to findings that mirrored the above results (Figure 20 D,E).

WASp plays an important role in cytoskeletal rearrangement, leading us to hypothesize that a defect in BCR internalization might explain the observed increase in AR responsiveness. While down-regulation in BCR surface expression was detected in *WASp*$^{-/-}$ B cells after BCR stimulation, this decrease was much less pronounced over the first 10 min compared to WT cells (Figure 20C). Together, these data indicate that *WASp*$^{-/-}$ B cells are hyper-responsive to BCR stimulation, possibly due to decreased receptor internalization.

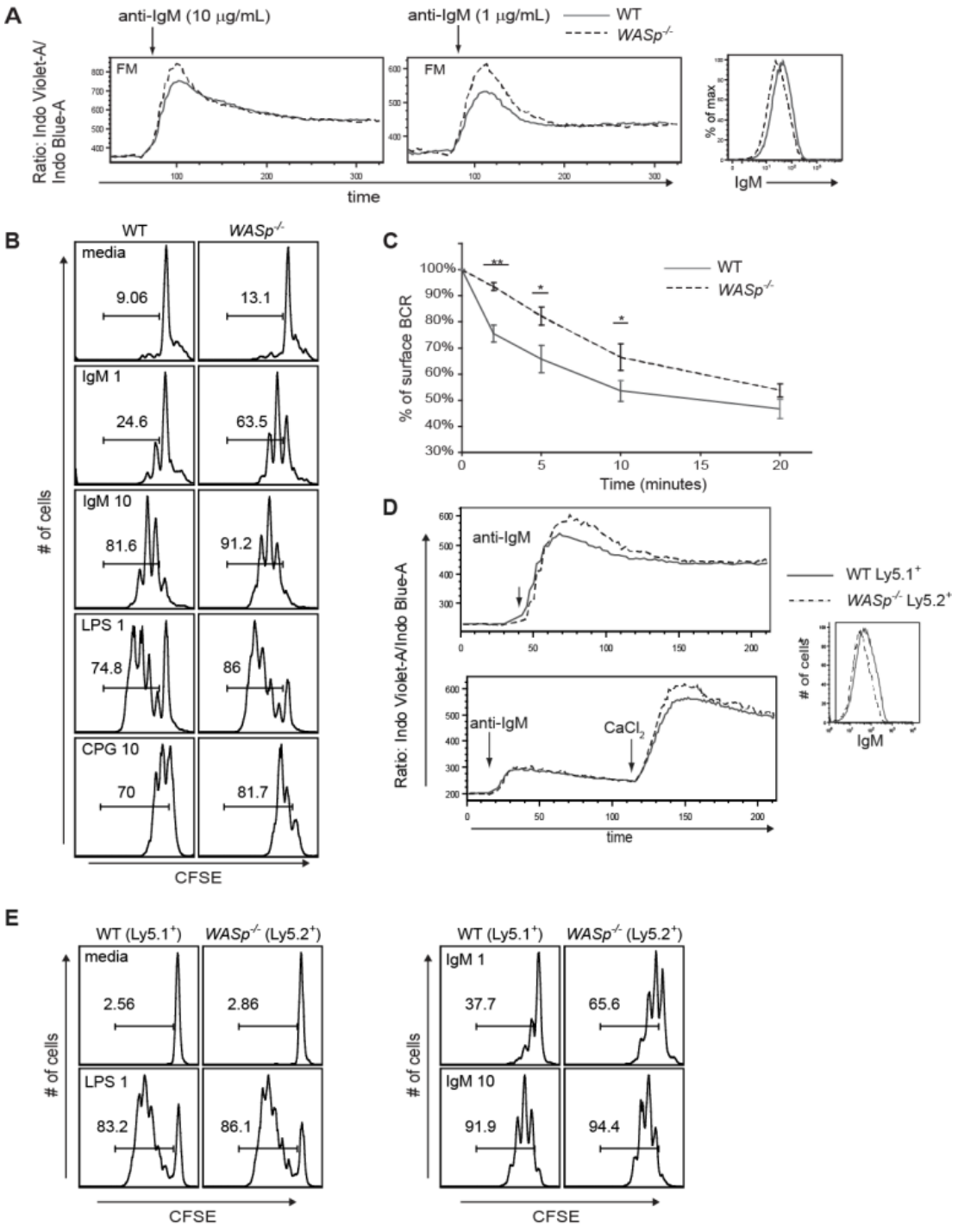

Figure 20. *WASp*$^{-/-}$ B cells are mildly hyper-responsive and display reduced BCR internalization. (A) Left and middle panel, Ca^{2+} flux in FM B cells stimulated with 10 or 1 μg/ml anti-IgM. Right panel, sIgM expression in WT vs. *WASp*$^{-/-}$ FM B cells. Data are representative of 4 independent experiments (n=8). (B) CFSE proliferation assay of sorted WT vs. *WASp*$^{-/-}$ FM B cells on day 3 post stimulation (1=1μg/mL; 10=10μg/mL). Data are representative of 3 experiments (n=10). (C) BCR internalization assay. WT and *WASp*$^{-/-}$ splenic

B cells were incubated with biotinylated F(ab')$_2$ fragments to bind the BCR and chased for the indicated time points. Data are displayed as % surface BCR relative to 0 time point. Data are representative of two independent experiments (n=6 per experiment). (D-E) To assess the BCR signaling response in WT and *WASp*$^{-/-}$ B cells derived from the same environment, BM from WT (Ly5.1+) and *WASp*$^{-/-}$ (Ly5.2+) mice was mixed at a 50:50 ratio and transplanted into lethally irradiated μMT recipient mice; recipients were sacrificed at 6-8 wk post-transplant. (D) Ca^{2+} flux in stimulated FM B cells in the presence (upper panel) or absence (lower panel) of extracellular Ca^{2+} showing response in WT (Ly5.1+) vs. *WASp*$^{-/-}$ (Ly5.2+) gated FM populations stimulated with 10μg/mL anti-IgM. Right panel shows relative sIgM expression in WT vs. *WASp*$^{-/-}$ FM B cells. (E) Proliferation of sort-purified, WT (Ly5.1+) vs. *WASp*$^{-/-}$ (Ly5.2+) FM B cells isolated from BM chimeras at day 3 post-stimulation with the indicated mitogens. Data are representative of 2 independent experiments (n= 4 per experiment). FM B cells were sorted as CD19+CD24^{int}CD21^{int} cells as previously described [10].

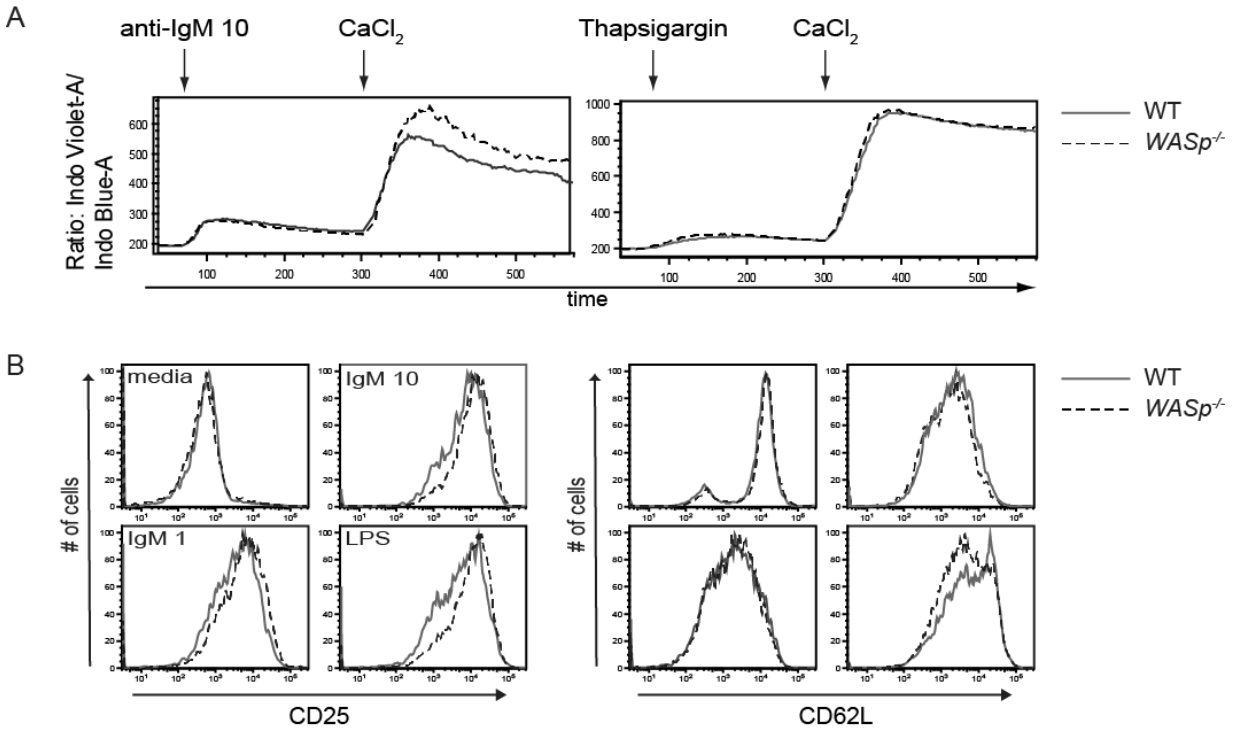

Figure 21. ***WASp*$^{-/-}$ B cells exhibit a specific enhancement in BCR triggered extracellular calcium influx and altered activation marker expression.** (A) Ca^{2+} flux in WT or *WASp*$^{-/-}$ FM B cells in Ca^{2+}-free media stimulated with anti-IgM (10mg/ml) or treated with Thapsigargin; followed by addition of $CaCl_2$ to the media. Data are representative of 2 independent experiments (n=4). (B) Expression of CD25 and CD62L on WT vs. *WASp*$^{-/-}$ FM B cells 48hr after stimulation using the indicated mitogens. Data are representative of 2 independent experiments (n=4 of each strain).

CD4 T cell depletion reduces autoantibody production and prevents disease in *WASp*$^{-/-}$ chimeras

We hypothesized that the presence of WT T cells was critical for the formation of GCs, IgG2 subclass CSR, and development of systemic autoimmune disease in *WASp*$^{-/-}$ chimeras. To test this hypothesis, we treated a new cohort of WT and *WASp*$^{-/-}$ chimeras weekly with monoclonal CD4 depleting antibody (Figure 22). While *WASp*$^{-/-}$ chimeras depleted of CD4 T cells still produced IgG anti-dsDNA antibodies, albeit at lower levels than in untreated *WASp*$^{-/-}$ chimeras, CD4 depletion completely prevented IgG2c anti-dsDNA production (Figure 23A). In contrast, IgG3 autoantibodies were not eliminated by CD4 depletion (Figure 23A). In addition, although lower in titer than untreated *WASp*$^{-/-}$ chimeras, IgG2b autoantibodies were significantly higher in CD4-depleted *WASp*$^{-/-}$ chimeras than in WT chimeras (Figure 23A). As expected, *WASp*$^{-/-}$ chimeras depleted of CD4 T cells did not exhibit an increase in GC phenotype ($B220^{+}PNA^{+}FAS^{+}$) splenocytes (Figure 23B) and lacked spontaneous GC formation in splenic sections (Figure 23C). Finally, CD4 depletion prevented the glomerular pathology, IgG2b/c and C3 deposition that were observed in untreated or isotype antibody-treated *WASp*$^{-/-}$ chimeras (Figure 23D). These data support our hypothesis that WT T cells in *WASp*$^{-/-}$ chimeras drive CSR and affinity maturation of autoreactive *WASp*$^{-/-}$ B cells, leading to production of pathologic autoantibodies and systemic autoimmune disease.

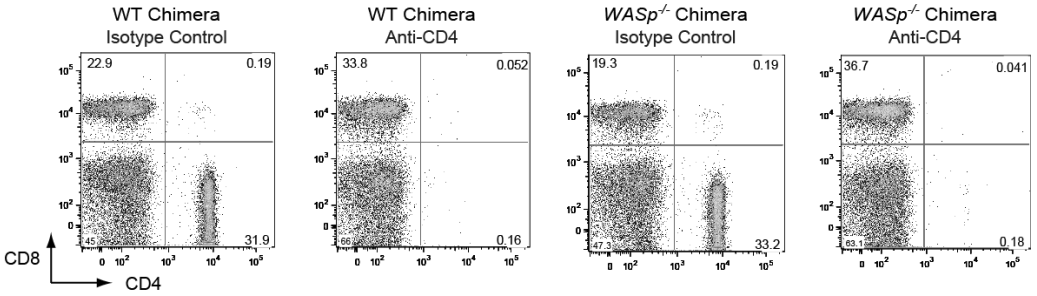

Figure 22. FACS analysis of peripheral blood in anti-CD4 vs. isotype control treated mice. WT or *WASp*$^{-/-}$ chimeric mice were treated weekly using anti-CD4 depleting or isotype control mAbs. Peripheral blood was collected at wk 12 post-transplant and analyzed by FACS to assess efficacy of CD4 T cell depletion. Representative data from 4 animals are shown. Animals exhibiting sustained CD4 depletion were analyzed for anti-dsDNA antibody production as shown in Figure 16A.

B cell MyD88 signaling is required for autoimmunity in *WASp*$^{-/-}$ BM chimeras

Because we observed enhanced proliferation of *WASp*$^{-/-}$ B cells in response to *in vitro* TLR engagement, we asked whether B cell intrinsic TLR signaling is required for autoantibody production in *WASp*$^{-/-}$ BM chimeras. *WASp*$^{-/-}$*MyD88*$^{-/-}$ double-deficient mice were generated and used as donors to generate cohorts of BM chimeras in which all B cells lacked both WASp and MyD88 while all other hematopoietic lineages were WT-derived. *WASp*$^{-/-}$*MyD88*$^{-/-}$ chimeras did not produce IgG (or IgG subclass) anti-dsDNA antibodies (Figure 23A), demonstrated no increase in PNA^{+}FAS^{+} B cells (Figure 23B), and did not develop spontaneous GC formation on splenic sections (Figure 23C). In addition, *WASp*$^{-/-}$*MyD88*$^{-/-}$ chimeras were completely protected from developing renal pathology and glomerular IgG2b/c and C3 deposition (Figure 23D). These results indicate that B cell intrinsic MyD88 signaling is essential for production of anti-dsDNA antibodies, GC formation, and development of systemic autoimmune disease in *WASp*$^{-/-}$ chimeras.

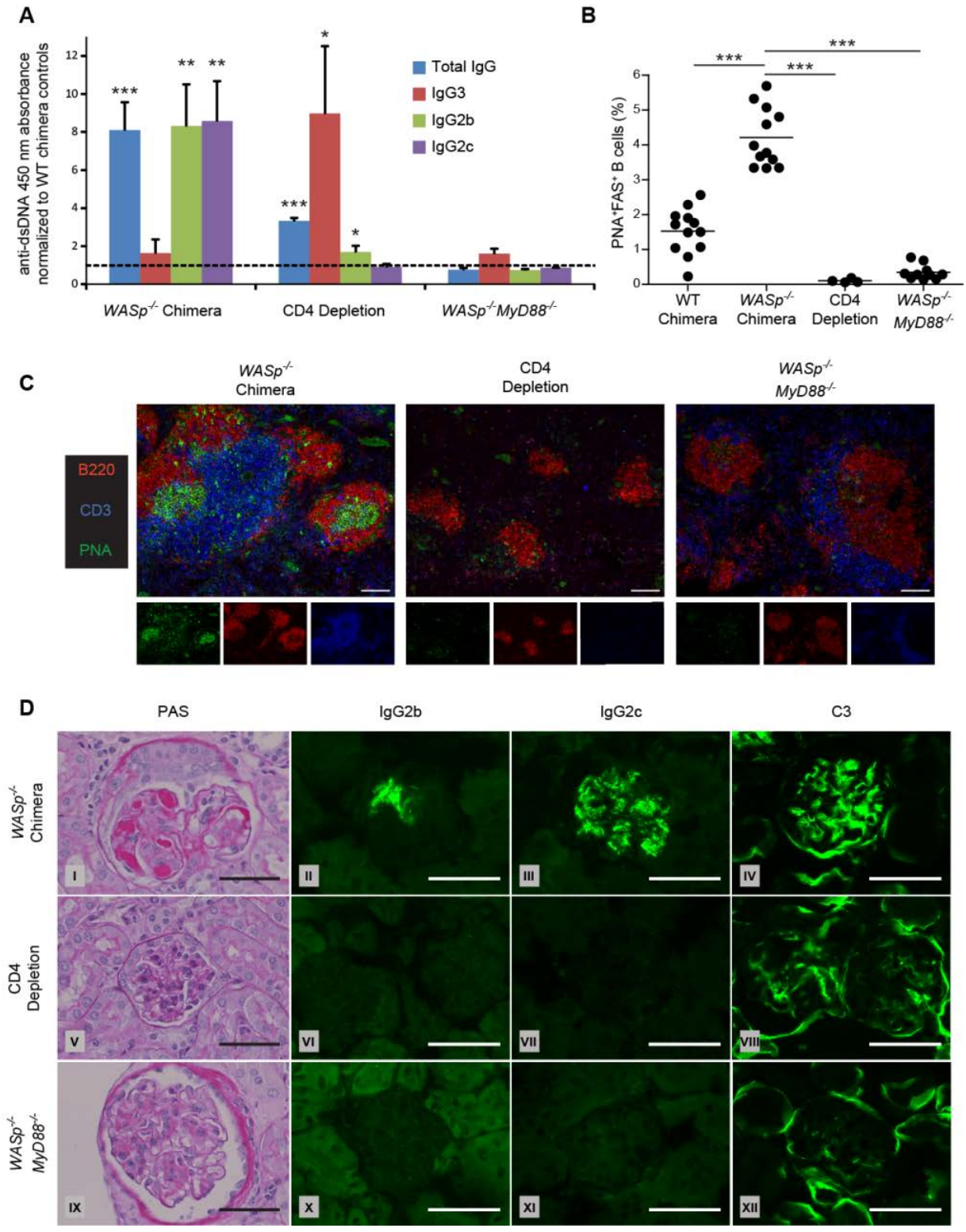

Figure 23. CD4 T cell depletion or B cell intrinsic MyD88-deficiency prevents disease development in *WASp*$^{-/-}$ chimeras. (A) ELISAs were used to measure dsDNA-specific total

IgG, IgG3, IgG2b, and IgG2c serum antibodies (18 weeks post-transplant) in *WASp*$^{-/-}$ chimeras, *WASp*$^{-/-}$ chimeras treated weekly with CD4-depleting antibody (labeled 'CD4 Depletion') and from *WASp*$^{-/-}$*MyD88*$^{-/-}$ chimeras (labeled '*WASp*$^{-/-}$*MyD88*$^{-/-}$'). Data is normalized to values obtained from WT chimera controls run alongside each experimental group, and significance tests demonstrate whether experimental values are statistically greater than control values for each ELISA. Dotted line is at normalized value 1, representing autoantibody levels in WT chimeras. (B) Percentage of splenic PNA^{+} FAS^{+} B cells in WT chimeras, *WASp*$^{-/-}$ chimeras, CD4-depleted *WASp*$^{-/-}$ chimeras and *WASp*$^{-/-}$*MyD88*$^{-/-}$ chimeras (6 mo post-transplant). (C) Immunofluorescent staining of splenic sections from *WASp*$^{-/-}$ chimeras (6 mo post-transplant) to measure GC formation in *WASp*$^{-/-}$ chimeras, CD4-depleted *WASp*$^{-/-}$ chimeras, and *WASp*$^{-/-}$ *MyD88*$^{-/-}$ chimeras. Representative follicles (10x objective) are shown using B220 (red) CD3 (blue) and PNA (green). Scale bars = 100 μm. (D) Glomeruli of indicated chimeras were stained with indicated reagents. PAS, Periodic acid-Schiff. Scale bars = 50 μm. *$P < 0.05$, **$P < 0.005$, ***$P < 0.0005$. Isotype treated WT and *WASp*$^{-/-}$ chimeras showed no differences from untreated animals, respectively, and therefore data from isotype-treated mice are not shown as a separate group. Data are representative of two independent experiments with *WASp*$^{-/-}$*MyD88*$^{-/-}$ chimeras (n=30 and n=15), and one independent CD4-depletion experiment (n=24).

3.3 Discussion

Autoimmunity is a hallmark of WAS, typically manifesting as humoral autoimmunity in up to 70% of WAS patients[75,78]. Additionally, a large number of patients develop systemic autoimmunity following stem cell transplantation and this complication strongly correlates with mixed chimerism[80]. Here we demonstrate that autoantibody production in *WASp*$^{-/-}$ mice does not result from a lack of Treg-mediated immunosuppression. We next addressed whether *WASp*$^{-/-}$ B cells might trigger autoimmunity using mixed BM chimeras where only B cells lacked expression of WASp. Our data indicate that *WASp*$^{-/-}$ B cells play a primary role in driving autoimmunity; indicating that a single gene defect in B cells, yielding a modest increase in BCR and TLR signaling, is sufficient to trigger a cell intrinsic loss in tolerance, culminating in pathogenic autoantibody production and lethal autoimmune disease in the setting of intact T cell

function. We further show that B cell intrinsic MyD88 signaling is essential for spontaneous GC formation, autoantibody production and development of renal pathology.

Consistent with a B cell intrinsic model, we show for the first time that *WASp*$^{-/-}$ B cells are modestly hyper-responsive to both anti-IgM and TLR stimulation, as measured by Ca^{2+} flux, proliferative responses, and modulation of activation markers. Additionally, we show that *WASp*$^{-/-}$ B cells exhibit decreased BCR internalization, possibly accounting for at least a subset of these increased responses. Despite delayed BCR internalization, *WASp*$^{-/-}$ mice do not have increased surface IgM levels on naïve B cells. This may be because delayed internalization does not affect steady-state surface IgM levels, or, alternatively, *WASp*$^{-/-}$ mice may have more autoreactive B cells in the pre-immune repertoire, resulting in increased BCR engagement and subsequent downregulation. Increased responsiveness to TLR ligands may also be due to altered receptor processing, but this has not yet been tested. Contrary to our findings in B cells, multiple reports have shown decreased AR responsiveness in *WASp*$^{-/-}$ T cells. Although the precise mechanisms remain to be determined, the opposing effect of WASp deficiency in B vs. T cell AR signals likely reflects differing roles for the actin cytoskeleton in initiating and sustaining such responses. Of note, our findings are consistent with previous data in WASp-interacting protein (WIP) deficient mice[84]. While WIP-/- B cells exhibited increased proliferation and CD69 expression in response to BCR and TLR4 engagement, WIP-/- T cells failed to proliferate or produce IL2 after TCR stimulation; findings consistent with the role for WIP in stabilizing WASp expression[85]. In concert with our findings, autoimmune glomerulonephritis has also been described in WIP-/- mice[86].

Importantly, despite being intrinsically autoreactive, our data clearly show that *WASp*$^{-/-}$ B cells alone are not sufficient to initiate severe autoimmune disease. *WASp*$^{-/-}$ mice develop anti-dsDNA autoantibodies but, in contrast to *WASp*$^{-/-}$ chimeras, show minimal organ pathology and have normal lifespans. Strikingly, *WASp*$^{-/-}$ mice primarily generated IgG3 anti-dsDNA antibodies, as might be expected as a result of a T-independent process, whereas autoantibodies in *WASp*$^{-/-}$ chimeras were comprised of IgG2 isotypes, previously shown to be associated with C3 deposition and nephritis in SLE animal models[87]. This suggests that in *WASp*$^{-/-}$ mice, *WASp*$^{-/-}$ T cells provided suboptimal cognate T cell help, an idea consistent with defective activation of *WASp*$^{-/-}$ T cells in response to CD3 ligation or antigen specific target cells[77]. In contrast, WT T cells present in *WASp*$^{-/-}$ chimeras appear to be essential to drive CSR and affinity maturation of pathogenic autoantibodies. Consistent with this view, CD4 T cell depletion abrogated the generation of IgG2c anti-dsDNA antibodies despite intact production of IgG3 autoantibodies, and prevented formation of renal pathology. However, although at lower levels than in *WASp*$^{-/-}$ chimeras treated with isotype antibodies, *WASp*$^{-/-}$ chimeras depleted of CD4 T cells still produced IgG2b anti-dsDNA antibodies, indicating T-independent activation and CSR can explain some of the IgG2b autoantibodies in *WASp*$^{-/-}$ chimeras. The presence of IgG2b subclass autoantibodies in CD4-depleted chimeras, but not *WASp*$^{-/-}$ mice, suggests that hematopoietic cells other than CD4 T cells may provide activating signals that contribute to CSR, dependent on the expression of WASp. *WASp*$^{-/-}$ DCs have an impaired ability to prime T cells[88], and may also lack the ability of WT DCs to promote B cell activation, possibly via impaired antigen presentation or secretion of soluble factors.

TLR signaling and MyD88 play a prominent role in B cell activation in various autoimmune models (reviewed in[89]) and DNA-specific B cells are capable of activation and

antibody production *in vitro* after only BCR and TLR engagement[90,91]. Therefore, we evaluated the contribution of TLR signaling in our model by generating chimeras lacking both WASp and MyD88 only in the B cell compartment. Deficiency of MyD88 prevented development of IgG anti-dsDNA antibodies, spontaneous GCs, and renal pathology, confirming its importance in the autoimmune disease observed in *WASp*$^{-/-}$ chimeras. Antigen-specific IgG2c, but not IgG2b, IgG3, or IgG1, in response to T-dependent antigen immunization has been shown in other studies to completely depend on B cell MyD88 signaling, possibly due to the failure of MyD88-deficient B cells to activate IFN-gamma producing effector T cells[92]. In our model, the lack of any IgG DNA-specific antibodies in the absence of B cell MyD88 signals suggests that initial activation of DNA-specific B cells requires simultaneous BCR and TLR engagement, perhaps by cell death derived nuclear autoantigens. Experiments are underway to determine whether specific TLRs, such as TLR9, are responsible for the effect of MyD88 deficiency. Additionally, based upon the requirement for MyD88 in TACI dependent CSR, it will be of interest to determine the potential role for TACI engagement by BAFF or APRIL in this process[93].

In summary, we provide insight into the pathogenesis of autoimmunity in *WASp*$^{-/-}$ mice, suggesting that hyper-responsive B cells play a primary role in initiating loss of tolerance and producing anti-DNA autoantibodies. Several mouse models have been described in which alterations in B cell signaling molecules contribute to development of autoimmune disease[94–96]. In mice lacking the inhibitory receptor FcγRIIB, development of autoimmunity also appears to be B cell intrinsic and MyD88/TLR9-dependent[87]. Recent data on this model suggests this is primarily due to failure of GC cell negative selection, and not a defect in selection of the pre-immune repertoire[59]. While further experimentation is required to define how increased antigen responsiveness in *WASp*$^{-/-}$ B cells first impacts BCR specificities within the mature repertoire,

according to our model, DNA-reactive *WASp*$^{-/-}$ naive B cells are initially activated by combined BCR and TLR engagement, to which *WASp*$^{-/-}$ B cells are hyper-responsive. In *WASp*$^{-/-}$ chimeras, these activated, autoantigen-specific B cells then recruit T cell help leading to GC formation and production of high-affinity, class-switched autoantibodies. This idea is consistent with recent evidence from models using transgenic BCRs in autoimmune-prone mice suggesting that B cells can play a primary role initiating systemic autoimmunity through dual BCR/TLR activation[42]. While not directly evaluated here, we predict that these combined events are exaggerated by, and may require, increased levels of BAFF in recipient μMT mice; an idea consistent with the role for T-independent, MyD88-dependent generation of autoantibodies in BAFF transgenic mice [13]. Notably, elevated BAFF is also observed in WAS (and other immune deficient) patients undergoing stem cell transplantation and may similarly amplify alterations in B cell tolerance in that setting (DJ Rawlings, AM Scharenberg, unpublished observations). Ultimately, autoantibody-containing IgG2b/c immune complexes deposit in tissues such as kidney glomeruli, initiating end-organ pathology via their preferential binding to activating IgG Fc receptors[97].

Our findings appear to provide a compelling mechanistic explanation for clinical observations wherein a large proportion of WAS transplant recipients with mixed chimerism develop severe, humoral autoimmunity, and suggest that these events should be considered in the design of future strategies for stem cell transplantation and viral-based gene replacement in WAS. Moreover, our data lend strong support to an emerging model (reviewed in[40]) whereby BCR/TLR mediated activation of autoreactive B cells can function as the primary driver leading to subsequent break in T cell tolerance and systemic autoimmunity.

3.4 Methods

Mice

Ly.5.1^{+} and Ly5.2^{+} C57BL/6, μMT, *WASp*$^{-/-}$ (F10 on a C57BL/6 background), and *MyD88*$^{-/-}$ mice were bred and maintained in the SPF animal facility of Seattle Children's Research Institute (Seattle, WA) and handled according to IACUC approved protocols.

Reagents and Antibodies

Anti-murine antibodies used in this study include CD24 (M1/69), CD21 (7G6), B220 (RA3-6B2), IgD (11-26C.2A), CD11 (9M1/70), IgD^{a} (AMS 9.1), CD3e (145 2C11), CD4(RM4-5) from BD Biosciences; BP1 (FG35.4), CD25 (PC61), CD62L (MEC-14), CD11c (N418), Gr-1 (RB6-8C5), Foxp3 (FJK-16S) from EMD Bioscience; CD23 (B3B4) from Caltag; IgM (1B4B1), Kappa (187.1), Lambda (JC5-1), goat anti mouse IgG-, IgG2b-, IgG2c-, IgG3- HRP conjugated and SA-HRP conjugated from Southern Biotechnology; CD19 (ID3), NK.1 (PK136), IgM^{a} (DS-1), CD8a (53-6.7) from BioLegend; and Cy5 anti-rabbit polyclonal IgG from Jackson ImmunoResearch. Purified polyclonal rabbit anti-WASp was provided by Dr. Hans Ochs (UW, Seattle).

Flow Cytometry and Cell Sorting

As previously described[10,74], single cell suspensions from BM, peripheral blood and spleen were incubated with fluorescently-labeled antibodies, data collected on a FACSCalibur or LSR II (BD

Biosciences) and analyzed using FlowJo software (Treestar Inc). Intracellular WASp staining, cell sorting and, gating strategies were also performed as previously described. Sort purities were >90% in all studies.

Bone Marrow Transplantation

BM was harvested from *WASp*$^{-/-}$ or WT mice, and plasma cells were depleted using anti-CD138 microbeads (Miltenyi Biotech). BM from *WASp*$^{-/-}$ or WT mice was mixed at a 20:80 ratio with μMT BM, and 5 x 10^6 total BM cells in PBS were injected i.v. into lethally irradiated (1050 cGy) μMT recipients. To generate 50:50 *WASp*$^{-/-}$:WT mixed BM chimeras, *WASp*$^{-/-}$ and C57BL/6 Ly5.1+ BM cells were mixed equally and injected into lethally irradiated μMT mice.

Immunofluorescence of Spleen Sections

Mouse spleens were embedded in OCT compound and frozen over dry ice and isopropyl alcohol. 5 μm sections were cut on a cryostat, mounted on Superfrost plus slides, dried, fixed in -20º C acetone for 20 minutes, dried at RT and stored at -80º C. For immunofluorescence staining sections were rehydrated in staining buffer (PBS, 1% goat serum, 1% BSA, 0.1% Tween-20), washed, and stained for 30 minutes at RT with B220-PE, PNA-FITC, and CD3-AlexaFluor 647. Slides were washed and fixed with mounting media, and images were acquired using a Leica DM6000B microscope, Leica DFL300 FX camera, and Leica Application Suite Advanced Fluorescence software.

In Vitro Cell Activation Studies

In vitro activation studies were performed as previously described[8,10]. Ca^{2+} flux was measured by flow cytometry using splenic B cells incubated with Indo-1 (Molecular Probes), surface stained, and then washed and stimulated with a stimulatory anti-IgM $F(ab)_2$. Thapsigargin (10 μg) or $CaCl_2$ was added as indicated. Treg suppression assays were performed as described[79].

ELISA

96 well Immuno plates (Nunc) were pre-coated (10mg/ml) overnight at 4ºC with dsDNA or MDA-LDL (Academy Bio-Medical; 20P-MD L-105). After blocking with 0.5% BSA/PBS, diluted sera were added, and plates were incubated with goat anti-mouse IgG-, IgG3-, IgG2b-, or IgG2c-HRP (Southern Biotechnology Associates) (1:2,000 dilution). Peroxidase reactions were developed using OptEIA TMB substrate (BD Biosciences). OD450 was determined using a Victor 3 plate reader (PerkinElmer) and displayed as average value of 3 wells. To identify high affinity anti-dsDNA antibodies, following sera addition, plates were incubated with 0.3M NaCl for 5 min. prior to performing the remainder of the above protocol.

Renal Histopathology and Urine Analysis

Kidney tissue was fixed in neutral buffered formalin, processed and embedded in paraffin according to standard practices. Tissue sections were stained with hematoxylin and eosin (H&E), periodic acid-Schiff (PAS) and silver methenamine. Portions of kidney in OCT were snap-frozen and frozen sections were used for immunofluorescence and Oil red O staining. Portions of formalin fixed tissue were processed for EM as previously described[98]. For immunofluorescence,

acetone-fixed frozen sections were air-dried, washed in PBS, and incubated with fluorescein-conjugated antibodies against mouse IgG, IgM, IgA, and complement C3 from Cappel Pharmaceuticals; IgG3, IgG2b, and IgG2c from Southern Biotechnology; and MAC2 from Cedarlane. After washing, slides were mounted with Vectashield mounting media (Vector) and viewed using a Nikon OptiPhot-2. Images were acquired using a Canon Eos 5D Mark II and the corresponding product software, and Adobe Photoshop was used for gamma adjustments. Alb:Cr ratios were determined according to manufacturer's instructions using Albuwell M and Creatinine Companion kits from Exocell.

BCR-Internalization Assay

Internalization assay was performed as described[99]. Anti- CD19 was used for gating splenic B cells.

Antigen Microarrays

Microarray studies were performed with nitrocellulose coated slides as described [100]. Background correction used a Matlab script, and the mean values for replicate spots were determined with JMP 7.0 software (www.jmp.com). Cluster analysis diagrams from comparisons of replicate arrays, after processing with monoclonal IgM or sera, were generated with Cluster 3.0 (Stanford University) and Java TreeView (rana.lbl.gov/EisenSoftware.htm). Background levels were confirmed based on replicate slides developed without sera (not shown). In these studies, a level of 600 digital fluorescence intensity units was set as a threshold for significant reactivity, which was the mean background ±3 SD.

T Cell Depletion

Mice were treated weekly with ip injection of 250 μg anti-CD4 (GK1.5) or isotype control (rat IgG2b) antibody (UCSF Antibody Core) beginning 5 weeks post-transplant.

Statistical Evaluation

P-values were calculated using the two-tailed Student's t-test. For analysis of survival, Kaplan-Meier analyses' were used.

Conclusions

Together, the studies presented here extend our understanding of development and function of B cells in the periphery. First, I sought to identify additional signals controlling selection of transitional B cells. CD4 T cells and CD40 were shown to contribute significantly to B cell HP in response to lymphopenia. CD40 expressing B cells also outcompete CD40-deficient B cells in mixed BM chimeras, beginning at the late transitional stage and most notably in the MZ subset. In these chimeras, CD40 drives increased expression of BAFFR on early transitional cells, which likely mediates a pro-survival effect. The use of transgenic BCR models, single-cell BCR cloning, and high throughput BCR heavy chain sequencing demonstrates an altered BCR repertoire in mature B cell subsets when CD40 is absent. Data on CD40, detailed in Chapter II, suggests that acquisition of T cell help and CD40 signaling supports transitional B cell development in addition to its well-established role in supporting humoral immune responses. Second, I helped determine the B cell intrinsic role of WASp in driving autoimmunity. WASp-/- B cells were demonstrated to be sufficient for the generation of autoantibodies and development of end-organ autoimmune tissue damage. Deficiency of WASp alters signaling thresholds downstream of the BCR, TLRs, and possibly other receptors, increasing responsiveness to ligand engagement. Finally, autoimmunity in the setting of WASp-/- B cells critically depends on B cell-specific expression of MyD88, demonstrating a requirement for TLR signaling in autoreactive B cell activation and autoantibody production. These results demonstrate that tuning of immune receptors specifically on B cells is sufficient to drive autoimmunity, and also provide further evidence of the pathogenic potential of dual BCR and TLR engagement on autoreactive B cells.

My proposed model of peripheral B cell development posits that as immature B cells enter the spleen, their progression through transitional stages is critically dependent on reception of external survival signals. The preliminary signal can come from CD40L on naïve CD4+ T cells and/or ligand-engagement of the BCR. At the early transitional stage, a specific threshold of BCR signaling affinity allows survival of T1 cells. At affinities above this threshold, apoptosis is rapidly induced in T1 B cells, whereas B cells with very low BCR signaling fail to upregulate critical survival factors and are strongly outcompeted. Engagement of CD40L on naïve CD4+ T cells can support survival of B cells on both ends of the BCR signaling threshold. B cells below this threshold can receive survival signals and upregulate BAFFR in response to CD40 engagement. CD40 can also rescue transitional B cells from apoptosis induced by BCR signaling, and thereby also supports survival of cells that, without CD40, would undergo apoptosis due to 'above-threshold' BCR signaling. In summary, CD40 is required for development of transitional B cells at both ends of the BCR signaling threshold, and the absence of CD40 results in a narrowing of the available naïve BCR repertoire.

Control of BCR signaling as well as other active immune receptors on peripheral B cells is required for proper orchestration of repertoire selection and mature B cell activation. Our studies on WASp clearly demonstrate that tuning the responsiveness of these key receptors leads to impaired B cell function and can drive development of autoimmunity. Specialized B cell subsets, such as the MZ compartment, are composed of conserved BCR specificities designed to mediate rapid responses to infection and homeostatic clearance of apoptotic cells. FM B cells are poised to respond to persistent infections by entering germinal center reactions, undergoing affinity maturation, and differentiating into class-switched, antibody-secreting plasma cells. As additional tolerance mechanisms are in place during affinity maturation in GCs, FM B cells can

tolerate modest levels of autoreactivity in preimmune B cells. MZ cells, on the other hand, secrete antibody more readily, although most commonly this is restricted to the IgM subclass. Failure of proper BCR-specificity based selection into these different compartments has been thought to contribute to pathogenic humoral responses, especially autoimmunity. Distinguishing between altered selection of the BCR repertoire and heightened activation of mature B cells selected normally has been a particular challenge in determining the etiology of autoimmune disease.

To address this issue, I have employed multiple molecular technologies to allow the thorough analysis of BCR repertoire in polyclonal, unrestricted systems. The use of single-cell cloning and specificity testing in tandem with high throughput BCR sequencing offers an unprecedented method to address selection of B cells. Most of the data on which current theories of B cell selection are built upon data derived from experiment utilizing transgenic BCRs or very limited sequence data. Now, using approaches described in my studies, one can more rigorously test existing or new models via assessing the specificity and sequence characteristics of B cells at key stages of peripheral development. Models of autoimmunity, such as WASp-deficiency, can be examined with these technologies to allow more precise identification of activated B cells, and to determine whether the naïve B cell compartment demonstrates altered specificity-based selection that predisposes to B intrinsic dysregulation as observed in Chapter III.

With the ability to accurately analyze BCR specificity in naïve B cell compartments, the precise role(s) for antigen-driven clonal expansion vs. tonic signaling, co-receptor signaling, and other means for positive selection of naïve B cells can now be more comprehensively addressed. There is growing appreciation for positive selection in B cells; a recent study using an *in vivo*

reporter of antigen-mediated BCR signaling demonstrated that most mature B cells appear to have received some level of antigen-induced BCR signal[101]. The spectrum of BCR specificities and signal strength permissive of B cell development into various mature subsets is likely critical for both homeostatic functions and the proper orchestration of humoral immunity. Such signals appear to be particularly important for innate-like B cell populations including MZ and B1 B cells. Alterations in normal B cell selection have been proposed to drive several autoimmune conditions, and could also be involved in the setting of immunodeficiency; while it has remained difficult to accurately assess alterations in selection in the past, the strategy presented here will serve to remedy this deficit.

Our studies demonstrate that a major challenge to specificity testing of recombinant antibodies derived from naïve BCRs is that current methods are most effective for evaluating high affinity antibodies generated from an immune response. Selection of B cells in the periphery likely operates at a much lower affinity threshold[102], and this concept is important in interpreting data derived from transgenic models in which only high affinity BCR-antigen interactions were evaluated. ELISA and autoantigen array tests currently available are not optimized for the accurate assessment of low affinity antibody specificity, and this area needs to be developed to increase our ability to use BCR cloning to study the naïve B cell repertoire. One promising method is the development of antigen tetramer reagents that can be used to purify B cells with particular BCR specificities[102]. The affinity of isolated B cells was calculated by determining the concentration of monomeric antigen necessary to outcompete tetrameric antigen during magnetic bead-based purification. This method could be expanded to analyze additional BCR-specificities of particular interest, but a higher throughput version of this technique would be ideal for the analysis of large numbers of BCRs.

With a greater understanding of how B cell selection operates, and the signals that control this process, it will become possible to develop new approaches to modulating B cell function. This could be utilized in the setting of autoimmunity or immunodeficiency where selection thresholds might need to be shifted back in to the 'normal' range. Alterations in B cell selection should also be avoided following BM transplant, where prevention of GVHD should involve inhibition of activation-specific pathways instead of pan T cell suppression. Additionally, the control of B cell selection may prove useful in the setting of vaccines. In particular for pathogens with rare antigens, such as HIV, there are sometimes no or too few naïve B cells with the proper specificity to mount an efficient response. Expansion of the available naïve BCR repertoire could drastically improve the success of certain vaccines. Based on data presented here, the provision of CD40 signals in conjunction with vaccination would be a candidate intervention that we would predict to temporarily expand the available BCR repertoire, increasing the likelihood of achieving a robust, protective humoral response. In fact, this may be a strategy that the immune system already employs during times of infection, as CD4+ T cells express more CD40L in the setting of an immune response. In addition to driving activation of mature B cells, this phenotype may promote a temporary increase in transitional B cell survival and selection, allowing an expanded BCR repertoire during times of infection.

References

1. Murphy, Kenneth, Travers, Paul, Walport, M. *Janeway's Immunobiology*. 885 (Garland Science, Taylor & Francis Group, LLC: 2008).

2. Burnet, F. M. The Clonal Selection Theory of Acquired Immunity. *Cambridge University Press* (1959).

3. Wardemann, H. *et al.* Predominant autoantibody production by early human B cell precursors. *Science (New York, N.Y.)* **301**, 1374–7 (2003).

4. Loder, F. *et al.* B cell development in the spleen takes place in discrete steps and is determined by the quality of B cell receptor-derived signals. *The Journal of experimental medicine* **190**, 75–89 (1999).

5. Allman, D. & Pillai, S. Peripheral B cell subsets. *Current opinion in immunology* **20**, 149–57 (2008).

6. Lindsley, R. C., Thomas, M., Srivastava, B. & Allman, D. Generation of peripheral B cells occurs via two spatially and temporally distinct pathways Generation of peripheral B cells occurs via two spatially and temporally distinct pathways. *Hematology* 2521–2528 (2009).doi:10.1182/blood-2006-04-018085

7. Norvell, A., Mandik, L. & Monroe, J. Engagement of the antigen-receptor on immature murine B lymphocytes results in death by apoptosis. *The Journal of Immunology* (1995).

8. Andrews, S. F. & Rawlings, D. J. Transitional B cells exhibit a B cell receptor-specific nuclear defect in gene transcription. *Journal of immunology (Baltimore, Md. : 1950)* **182**, 2868–78 (2009).

9. Allman, D. *et al.* Resolution of three nonproliferative immature splenic B cell subsets reveals multiple selection points during peripheral B cell maturation. *Journal of immunology (Baltimore, Md. : 1950)* **167**, 6834–40 (2001).

10. Meyer-Bahlburg, A., Andrews, S. F., Yu, K. O., Porcelli, S. A. & Rawlings, D. J. Characterization of a late transitional B cell population highly sensitive to BAFF-mediated homeostatic proliferation. *J Exp Med* **205**, 155–168 (2008).

11. Mackay, F. & Schneider, P. Cracking the BAFF code. *Nat. Rev. Immunol.* **9**, 491–502 (2009).

12. Schiemann, B. *et al.* An essential role for BAFF in the normal development of B cells through a BCMA-independent pathway. *Science (New York, N.Y.)* **293**, 2111–4 (2001).

13. Groom, J. R. *et al.* BAFF and MyD88 signals promote a lupuslike disease independent of T cells. *J. Exp. Med.* **204**, 1959–71 (2007).

14. Shulga-Morskaya, S. & Dobles, M. B cell-activating factor belonging to the TNF family acts through separate receptors to support B cell survival and T cell-independent antibody formation. *The Journal of ...* (2004).

15. Mackay, F., Figgett, W. A., Saulep, D., Lepage, M. & Hibbs, M. L. B-cell stage and context-dependent requirements for survival signals from BAFF and the B-cell receptor. *Immunol. Rev.* **237**, 205–225 (2010).

16. Stadanlick, J. E. *et al.* Tonic B cell antigen receptor signals supply an NF-kappaB substrate for prosurvival BLyS signaling. *Nature immunology* **9**, 1379–87 (2008).

17. Smith, S. & Cancro, M. Cutting edge: B cell receptor signals regulate BLyS receptor levels in mature B cells and their immediate progenitors. *The Journal of Immunology* (2003).

18. Rolink, a G., Andersson, J. & Melchers, F. Characterization of immature B cells by a novel monoclonal antibody, by turnover and by mitogen reactivity. *European journal of immunology* **28**, 3738–48 (1998).

19. Allman, D., Ferguson, S., Lentz, V. & Cancro, M. Peripheral B cell maturation. II. Heat-stable antigen (hi) splenic B cells are an immature developmental intermediate in the production of long-lived marrow-derived B cells. *The Journal of Immunology* **151**, 4431 (1993).

20. Sater, R. a, Sandel, P. C. & Monroe, J. G. B cell receptor-induced apoptosis in primary transitional murine B cells: signaling requirements and modulation by T cell help. *International immunology* **10**, 1673–82 (1998).

21. Stadanlick, J. E. & Cancro, M. P. BAFF and the plasticity of peripheral B cell tolerance. *Current opinion in immunology* **20**, 158–61 (2008).

22. Cancro, M. P. & Kearney, J. F. B cell positive selection: road map to the primary repertoire? *J Immunol* **173**, 15–19 (2004).

23. Lam, K. P., Kühn, R. & Rajewsky, K. In vivo ablation of surface immunoglobulin on mature B cells by inducible gene targeting results in rapid cell death. *Cell* **90**, 1073–83 (1997).

24. Levine, M. H. *et al.* A B-cell receptor-specific selection step governs immature to mature B cell differentiation. *Proceedings of the National Academy of Sciences of the United States of America* **97**, 2743–8 (2000).

25. Gaudin, E. *et al.* Positive selection of B cells expressing low densities of self-reactive BCRs. *The Journal of experimental medicine* **199**, 843–53 (2004).

26. Hayakawa, K. *et al.* Positive Selection of Anti-Thy-1 Autoreactive B-1 Cells and Natural Serum Autoantibody Production Independent from Bone Marrow B Cell Development. *Journal of Experimental Medicine* **197**, 87–99 (2002).

27. Kenny, J. J., O'Connell, C., Sieckmann, D. G., Fischer, R. T. & Longo, D. L. Selection of antigen-specific, idiotype-positive B cells in transgenic mice expressing a rearranged M167-mu heavy chain gene. *J Exp Med* **174**, 1189–1201 (1991).

28. Van Zelm, M. C., Szczepanski, T., Van der Burg, M. & Van Dongen, J. J. M. Replication history of B lymphocytes reveals homeostatic proliferation and extensive antigen-induced B cell expansion. *The Journal of experimental medicine* **204**, 645–55 (2007).

29. Cyster, J. G. B cell follicles and antigen encounters of the third kind. *Nature immunology* **11**, 989–96 (2010).

30. Lund, F. E. Cytokine-producing B lymphocytes-key regulators of immunity. *Curr. Opin. Immunol.* **20**, 332–338 (2008).

31. Harris, D. P. *et al.* Reciprocal regulation of polarized cytokine production by effector B and T cells. *Nature immunology* **1**, 475–82 (2000).

32. Mauri, C. & Bosma, A. Immune regulatory function of B cells. *Annual review of immunology* **30**, 221–41 (2012).

33. Martin, F., Oliver, A. M. & Kearney, J. F. Marginal zone and B1 B cells unite in the early response against T-independent blood-borne particulate antigens. *Immunity* **14**, 617–629 (2001).

34. Cerutti, A., Cols, M. & Puga, I. Marginal zone B cells: virtues of innate-like antibody-producing lymphocytes. *Nature Reviews Immunology* **13**, 118–132 (2013).

35. Chen, Y., Park, Y. B., Patel, E. & Silverman, G. J. IgM antibodies to apoptosis-associated determinants recruit C1q and enhance dendritic cell phagocytosis of apoptotic cells. *J Immunol* **182**, 6031–6043 (2009).

36. Peng, Y., Kowalewski, R., Kim, S. & Elkon, K. B. The role of IgM antibodies in the recognition and clearance of apoptotic cells. *Mol Immunol* **42**, 781–787 (2005).

37. Meyer-Bahlburg, A., Bandaranayake, A. D., Andrews, S. F. & Rawlings, D. J. Reduced c-myc expression levels limit follicular mature B cell cycling in response to TLR signals. *J. Immunol.* **182**, 4065–75 (2009).

38. Rawlings, D. J., Schwartz, M. A., Jackson, S. W. & Meyer-Bahlburg, A. Integration of B cell responses through Toll-like receptors and antigen receptors. *Nature reviews. Immunology* **12**, 282–94 (2012).

39. Hou, B. *et al.* Selective utilization of Toll-like receptor and MyD88 signaling in B cells for enhancement of the antiviral germinal center response. *Immunity* **34**, 375–84 (2011).

40. Shlomchik, M. J. Activating systemic autoimmunity: B's, T's, and tolls. *Curr. Opin. Immunol.* **21**, 626–33 (2009).

41. Celhar, T., Magalhães, R. & Fairhurst, a-M. TLR7 and TLR9 in SLE: when sensing self goes wrong. *Immunologic research* **53**, 58–77 (2012).

42. Herlands, R. A., Christensen, S. R., Sweet, R. A., Hershberg, U. & Shlomchik, M. J. T cell-independent and toll-like receptor-dependent antigen-driven activation of autoreactive B cells. *Immunity* **29**, 249–260 (2008).

43. Gregersen, P. K., Diamond, B. & Plenge, R. M. GWAS implicates a role for quantitative immune traits and threshold effects in risk for human autoimmune disorders. *Current opinion in immunology* **24**, 538–43 (2012).

44. Dai, X. *et al.* A disease-associated PTPN22 variant promotes systemic autoimmunity in murine models. *The Journal of clinical …* **123**, (2013).

45. Bottini, N., Vang, T., Cucca, F. & Mustelin, T. Role of PTPN22 in type 1 diabetes and other autoimmune diseases. *Seminars in Immunology* **18**, 207–213 (2006).

46. Cambier, J. Autoimmunity risk alleles: hotspots in B cell regulatory signaling pathways. *The Journal of clinical investigation* 16–19 (2013).doi:10.1172/JCI69289.1928

47. Nikolov, N. P. *et al.* Systemic autoimmunity and defective Fas ligand secretion in the absence of the Wiskott-Aldrich syndrome protein. *Blood* **116**, 740–7 (2010).

48. Imai, K. *et al.* Clinical course of patients with WASP gene mutations. *Blood* **103**, 456–464 (2004).

49. Westerberg, L. S. *et al.* WASP confers selective advantage for specific hematopoietic cell populations and serves a unique role in marginal zone B-cell homeostasis and function. *Blood* **112**, 4139–4147 (2008).

50. Freitas, A. A., Lembezat, M. P. & Rocha, B. Selection of antibody repertoires: transfer of mature T lymphocytes modifies VH gene family usage in the actual and available B cell repertoires of athymic mice. *International immunology* **1**, 398–408 (1989).

51. Hervé, M. *et al.* CD40 ligand and MHC class II expression are essential for human peripheral B cell tolerance. *The Journal of experimental medicine* **204**, 1583–93 (2007).

52. Oka, Y. *et al.* Profound reduction of mature B cell numbers, reactivities and serum Ig levels in mice which simultaneously carry the XID and CD40 deficiency genes. *International immunology* **8**, 1675–85 (1996).

53. Khan, W. N. *et al.* Impaired B cell maturation in mice lacking Bruton's tyrosine kinase (Btk) and CD40. *International Immunology* **9**, 395–405 (1997).

54. Lesley, R., Kelly, L. M., Xu, Y. & Cyster, J. G. Naive CD4 T cells constitutively express CD40L and augment autoreactive B cell survival. *Proceedings of the National Academy of Sciences of the United States of America* **103**, 10717–22 (2006).

55. Choudhury, A., Cohen, P. L. & Eisenberg, R. a B cells require "nurturing" by CD4 T cells during development in order to respond in chronic graft-versus-host model of systemic lupus erythematosus. *Clinical immunology (Orlando, Fla.)* **136**, 105–15 (2010).

56. Milićević, N. M., Nohroudi, K., Milićević, Z., Hedrich, H.-J. & Westermann, J. T cells are required for the peripheral phase of B-cell maturation. *Immunology* **116**, 308–17 (2005).

57. Lang, J. *et al.* Studies of Lymphocyte Reconstitution in a Humanized Mouse Model Reveal a Requirement of T Cells for Human B Cell Maturation. *Journal of immunology (Baltimore, Md. : 1950)* (2013).doi:10.4049/jimmunol.1202810

58. Rowland, S. L., Leahy, K. F., Halverson, R., Torres, R. M. & Pelanda, R. BAFF Receptor Signaling Aids the Differentiation of Immature B Cells into Transitional B Cells following Tonic BCR Signaling. *Journal of immunology (Baltimore, Md. : 1950)* (2010).doi:10.4049/jimmunol.1001708

59. Tiller, T. *et al.* Development of self-reactive germinal center B cells and plasma cells in autoimmune Fc gammaRIIB-deficient mice. *The Journal of experimental medicine* **207**, 2767–78 (2010).

60. Rogosch, T. *et al.* Immunoglobulin analysis tool: a novel tool for the analysis of human and mouse heavy and light chain transcripts. *Frontiers in immunology* **3**, 176 (2012).

61. Volpe, J. M. & Kepler, T. B. Genetic correlates of autoreactivity and autoreactive potential in human Ig heavy chains. *Immunome research* **5**, 1 (2009).

62. Schelonka, R. L. *et al.* Categorical selection of the antibody repertoire in splenic B cells. *European journal of immunology* **37**, 1010–21 (2007).

63. Chao, A. and Shen, T.-J. Program SPADE (Species Prediction And Diversity Estimation). at <http://chao.stat.nthu.edu.tw>

64. Chao, A. Nonparametric estimation of the number of classes in a population. *Scandinavian J. Stat.* **11**, 265–270 (1984).

65. Cabatingan, M. S., Schmidt, M. R., Sen, R. & Woodland, R. T. Naive B lymphocytes undergo homeostatic proliferation in response to B cell deficit. *Journal of immunology (Baltimore, Md. : 1950)* **169**, 6795–805 (2002).

66. Seijkens, T., Engel, D., Tjwa, M. & Lutgens, E. The role of CD154 in haematopoietic development. *Thrombosis and haemostasis* **104**, 693–701 (2010).

67. Li, Y., Li, H. & Weigert, M. Autoreactive B cells in the marginal zone that express dual receptors. *The Journal of experimental medicine* **195**, 181–8 (2002).

68. Julien, S., Soulas, P., Garaud, J.-C., Martin, T. & Pasquali, J.-L. B cell positive selection by soluble self-antigen. *Journal of immunology (Baltimore, Md. : 1950)* **169**, 4198–204 (2002).

69. Wang, H. & Clarke, S. H. Regulation of B-cell development by antibody specificity. *Current opinion in immunology* **16**, 246–50 (2004).

70. Krishnan, M., Jou, N. & Marion, T. Correlation between the amino acid position of arginine in VH-CDR3 and specificity for native DNA among autoimmune antibodies. *The Journal of Immunology* (1996).

71. Jain, N. *et al.* Immune reconstitution after combined haploidentical and umbilical cord blood transplant. *Leukemia & lymphoma* **54**, 1242–1249 (2013).

72. Slatter, M. a *et al.* Polysaccharide antibody responses are impaired post bone marrow transplantation for severe combined immunodeficiency, but not other primary immunodeficiencies. *Bone marrow transplantation* **32**, 225–9 (2003).

73. Jesus, A. a, Duarte, A. J. S. & Oliveira, J. B. Autoimmunity in hyper-IgM syndrome. *Journal of clinical immunology* **28 Suppl 1**, S62–6 (2008).

74. Meyer-Bahlburg, A. *et al.* Wiskott-Aldrich syndrome protein deficiency in B cells results in impaired peripheral homeostasis. *Blood* **112**, 4158–4169 (2008).

75. Sullivan, K. E., Mullen, C. A., Blaese, R. M. & Winkelstein, J. A. A multiinstitutional survey of the Wiskott-Aldrich syndrome. *J Pediatr* **125**, 876–885 (1994).

76. Thrasher, A. J. WASp in immune-system organization and function. *Nat Rev Immunol* **2**, 635–646 (2002).

77. Bouma, G., Burns, S. O. & Thrasher, A. J. Wiskott-Aldrich Syndrome: Immunodeficiency resulting from defective cell migration and impaired immunostimulatory activation. *Immunobiology* **214**, 778–790 (2009).

78. Dupuis-Girod, S. *et al.* Autoimmunity in Wiskott-Aldrich syndrome: risk factors, clinical features, and outcome in a single-center cohort of 55 patients. *Pediatrics* **111**, e622–7 (2003).

79. Humblet-Baron, S. *et al.* Wiskott-Aldrich syndrome protein is required for regulatory T cell homeostasis. *J Clin Invest* **117**, 407–418 (2007).

80. Ozsahin, H. *et al.* Long-term outcome following hematopoietic stem-cell transplantation in Wiskott-Aldrich syndrome: collaborative study of the European Society for Immunodeficiencies and European Group for Blood and Marrow Transplantation. *Blood* **111**, 439–445 (2008).

81. Maillard, M. H. *et al.* The Wiskott-Aldrich syndrome protein is required for the function of CD4(+)CD25(+)Foxp3(+) regulatory T cells. *J Exp Med* **204**, 381–391 (2007).

82. Marangoni, F. *et al.* WASP regulates suppressor activity of human and murine CD4(+)CD25(+)FOXP3(+) natural regulatory T cells. *J Exp Med* **204**, 369–380 (2007).

83. Luzina, I. G. *et al.* Spontaneous formation of germinal centers in autoimmune mice. *J Leukoc Biol* **70**, 578–584 (2001).

84. Anton, I. M. *et al.* WIP deficiency reveals a differential role for WIP and the actin cytoskeleton in T and B cell activation. *Immunity* **16**, 193–204 (2002).

85. Ramesh, N. & Geha, R. Recent advances in the biology of WASP and WIP. *Immunol Res* **44**, 99–111 (2009).

86. Curcio, C. *et al.* WIP null mice display a progressive immunological disorder that resembles Wiskott-Aldrich syndrome. *J Pathol* **211**, 67–75 (2007).

87. Ehlers, M., Fukuyama, H., McGaha, T. L., Aderem, A. & Ravetch, J. V TLR9/MyD88 signaling is required for class switching to pathogenic IgG2a and 2b autoantibodies in SLE. *J. Exp. Med.* **203**, 553–561 (2006).

88. Bouma, G., Burns, S. & Thrasher, A. J. Impaired T-cell priming in vivo resulting from dysfunction of WASp-deficient dendritic cells. *Blood* **110**, 4278–4284 (2007).

89. Marshak-Rothstein, A. & Rifkin, I. R. Immunologically active autoantigens: the role of toll-like receptors in the development of chronic inflammatory disease. *Annual review of immunology* **25**, 419–41 (2007).

90. Fields, M. L. *et al.* Exogenous and endogenous TLR ligands activate anti-chromatin and polyreactive B cells. *Journal of immunology (Baltimore, Md. : 1950)* **176**, 6491–502 (2006).

91. Viglianti, G. a *et al.* Activation of autoreactive B cells by CpG dsDNA. *Immunity* **19**, 837–47 (2003).

92. Barr, T. a, Brown, S., Mastroeni, P. & Gray, D. B cell intrinsic MyD88 signals drive IFN-gamma production from T cells and control switching to IgG2c. *J. Immunol.* **183**, 1005–12 (2009).

93. He, B. *et al.* The transmembrane activator TACI triggers immunoglobulin class switching by activating B cells through the adaptor MyD88. *Nat. Immunol.* **11**, 836–845 (2010).

94. Bolland, S. & Ravetch, J. V Spontaneous autoimmune disease in Fc RIIB-deficient mice results from strain-specific epistasis. *Immunity* **13**, 277–285 (2000).

95. Cornall, R. J. *et al.* Polygenic autoimmune traits: Lyn, CD22, and SHP-1 are limiting elements of a biochemical pathway regulating BCR signaling and selection. *Immunity* **8**, 497–508 (1998).

96. Grimaldi, C. M., Hicks, R. & Diamond, B. B cell selection and susceptibility to autoimmunity. *Journal of immunology (Baltimore, Md. : 1950)* **174**, 1775–81 (2005).

97. Nimmerjahn, F. & Ravetch, J. V Divergent immunoglobulin g subclass activity through selective Fc receptor binding. *Science (New York, N.Y.)* **310**, 1510–2 (2005).

98. Taneda, S. *et al.* Cryoglobulinemic glomerulonephritis in thymic stromal lymphopoietin transgenic mice. *American Journal of Pathology* **159**, 2355 (2001).

99. Sharma, S., Orlowski, G. & Song, W. Btk regulates B cell receptor-mediated antigen processing and presentation by controlling actin cytoskeleton dynamics in B cells. *J Immunol* **182**, 329–339 (2009).

100. Silverman, G. J. *et al.* Genetic imprinting of autoantibody repertoires in systemic lupus erythematosus patients. *Clin Exp Immunol* **153**, 102–116 (2008).

101. Zikherman, J., Parameswaran, R. & Weiss, A. Endogenous antigen tunes the responsiveness of naive B cells but not T cells. *Nature* **489**, 160–4 (2012).

102. Taylor, J. J. *et al.* Deletion and anergy of polyclonal B cells specific for ubiquitous membrane-bound self-antigen. *The Journal of experimental medicine* **209**, 2065–77 (2012).